universität wien

MASTERARBEIT / MASTER'S THESIS

Titel der Masterarbeit / Title of the Master's Thesis

„Serum antibody-mediated binding inhibition of the human cytomegalovirus trimeric gH/gL/gO glycoprotein complex to platelet-derived growth factor receptor alpha arises with high IgG avidity“

verfasst von / submitted by

Lukas Eisler, BSc

angestrebter akademischer Grad / in partial fulfilment of the requirements for the degree of

Master of Science (MSc)

Wien, 2024 / Vienna, 2024

Studienkennzahl lt. Studienblatt / degree programme code as it appears on the student record sheet:	UA 066 834
Studienrichtung lt. Studienblatt / degree programme as it appears on the student record sheet:	Masterstudium Molekulare Biologie
Betreut von / Supervisor:	Priv.-Doz. Dr. Irene Görzer

Abstract

Human Cytomegalovirus (HCMV) cell entry into fibroblasts is initiated by binding of the trimeric glycoprotein complex gH/gL/gO to the host cells platelet-derived growth factor receptor alpha (PDGFRα). Despite their important role in the prevention of viral spread, little is known about the humoral immune response in form of serum antibodies particularly inhibiting this interaction and their capability to provide strain overlapping immunity in regard to the polymorphic gO subunit. To approach this matter, we aimed for the expression and purification of soluble trimeric complex, utilizing the gO1c (TB40/E) and gO4 (Towne) variants, and the development of a receptor-binding assay, to detect such inhibitory antibodies as well as determine their emergence after primary infection. In contrast to the expression of trimeric gH/gL/gO utilizing the gO4 subunit, the co-expression with the gO1c subunit led to low protein yield, implicating a subtle expression mechanism with dependence on the gO genotypes and maybe other cofactors. Serum analysis exhibited that high IgG titer HCMV seropositive individuals and Cytotect®CP, a hyperimmunoglobulin preparation, inhibit receptor-binding in a dose-dependent manner. The comparison between HCMV seropositive individuals with different IgG avidity and a follow-up on IgG avidity maturation within individual patients revealed that inhibitory antibodies were only present upon high IgG avidity. Our current data indicates that trimer-specific IgG serum antibodies blocking PDGFRα receptor binding are indeed generated after primary infection but emerge late during IgG avidity maturation.

Human Cytomegalovirus; Envelope glycoprotein complex; Platelet-derived growth factor receptor alpha; Humoral immune response; IgG avidity; Protein purification; Enzyme-linked immunosorbent assay;

Table of Contents

I have made every effort to locate all owners of the image rights and have obtained their consent to use the images in this work. Should a copyright infringement nevertheless become known, please contact me.

1 Introduction

1.1 The Human Cytomegalovirus

The *Herpesviridae* describe a large family of double-stranded DNA viruses that are distinguished into the three subfamilies of alpha-, beta- and gamma-herpesviruses. Among these, the most famous members in reference to human pathogens are the *Herpes simplex virus 1*, *Herpes Simplex virus 2*, *Varicella Zoster virus*, *Epstein-Barr virus*, *Cytomegalovirus*, *Roseolovirus* and *Kaposi's Sarcoma-associated herpes virus*, which cause cutaneous lesions and potentially cancer. (Roizman, Knipe and Whitley, 2001; Herbein, 2022) The Genus *Cytomegalovirus* (CMV) belongs to the subfamily of the beta herpesviruses and mainly refers to the Human Cytomegalovirus (HCMV), also described as *human herpes virus 5 (HHV-5),* due to its adaption to the human host. Following a primary infection, the active immune response in combination with viral immune evasion leads to the development of a latent infection state, during which the virus persists within restricted sites of the body and potentially reactivates. Due to the genetic variability of certain gene loci within the HCMV genome, re-infection of already infected individuals with a different strain is possible. Resulting mixed infections with multiple strains provide opportunities for viral recombination leading to the generation of novel strains with unpredictable pathogenicity (Meyer-König *et al.*, 1998; Puchhammer-Stöckl *et al.*, 2006; Sijmons *et al.*, 2015).

1.2 Prevalence and Risk of Infection

First isolated in 1956, HCMV is yet known to be an ubiquitous pathogen with a global estimated IgG seroprevalence of 83% across the general population. Thereby, the prevalence significantly differs between developing and developed countries, showing values up to 90% or higher in the Eastern Mediterranean, Africa, Asia and South America. (Zuhair *et al.*, 2019) Intraregional, the socioeconomic status, educational level and the ethnicity have a major impact on the seroprevalence of the residential populations. (Krech, 1973; Cannon, Schmid and Hyde, 2010; Fowler *et al.*, 2022) Generally, the HCMV IgG seroprevalence is observed to increase with age, as approximately a third of all children born in the USA are already infected by the age of 5 years and over 50% of adults past the age of 40 are infected according to the Centers for Disease Control and Prevention (CDC). (CDC., 2023) (Cannon, Schmid and Hyde, 2010; Fowler *et al.*, 2022) Upon an active infection, HCMV is shed through most body fluids, providing for several transmission pathways upon close and intimate contact. (CDC., 2023) In developing countries HCMV infections are usually acquired early in life, due to breastfeeding and crowded living conditions. Children up to 5 years of age

are a primary reservoir for the virus, which they shed primarily through their saliva and urine, infecting other children, childcare workers, parents, and grandparents. (Adler, 1991; Cannon, Hyde and Schmid, 2011; van Zuylen *et al.*, 2017; Kabani *et al.*, 2023) From the early adolescence, kissing and sexual contact provide further ways for viral transmission. (Sohn *et al.*, 1991; Fowler and Pass, 2006; Staras *et al.*, 2008)

After infection of naive, immunocompetent individuals, HCMV infection usually proceeds asymptomatically and thus remains undetected. However, in some cases infection takes up an incubation period of three to twelve weeks, causing mononucleosis-like illness and indirect long-term effects that are yet not fully understood. (Griffiths, 2020) Groups that are majorly affected by HCMV infections are congenitally infected infants and immunocompromised individuals, like transplant patients or people suffering from HIV infection. Although the numbers are likely underestimated, HCMV still represents the most frequently detected congenital infection with a worldwide live birth prevalence of 0.6% in developed countries and up to 5% in developing countries. Out of all congenitally infected children born, only 10% show symptoms at birth and thus leave the majority of the infections undetected and untreated. (Dollard, Grosse and Ross, 2007; Fowler and Boppana, 2018) Congenital HCMV infection can cause long-term cognitive and developmental impairments, most commonly sensorineural hearing loss, and is also associated with an increased mortality rate in infants. (Boppana *et al.*, 1992; Fowler and Boppana, 2006; Kenneson and Cannon, 2007) Since women of childbearing age show a global average seroprevalence of 86%, the increased awareness regarding vertical HCMV transmission is a major concern. (Cannon, Schmid and Hyde, 2010; Zuhair *et al.*, 2019)

For individuals with compromised immunity HCMV proposes a major threat as opportunistic pathogen. The lack of immunosurveillance allows for uncontrolled lytic replication of the virus, leading to high viremia which again causes end organ disease (EOD) in form of retinitis, pneumonitis, hepatitis, gastrointestinal ulceration, nephritis or pancreatitis, depending on the affected tissue. (Griffiths, 2020) Particularly recipients of solid organ or hematopoietic stem cell transplants (SOT/SCT), are at lethal risk of graft-versus-host disease, due to reactivation of persistent HCMV infections, reinfection with a donor-derived strain and hence mixed infections. (Lamberson and Dock, 1992; Bowden, 1995; Contreras and Ho, 2022) Especially lung transplants are major contributors for mixed HCMV infections derived from the donor allograft. (Külekci *et al.*, 2022) The latest update on the HCMV-specific IgG seroprevalence showed that about 86% of blood and organ donors around the globe have antibodies and thus can potentially transmit the virus. (Zuhair *et al.*, 2019)

1.3 Virion structure

HCMV shows the typical features of the Herpesvirus structure and represents the largest member of the herpesvirus family with approximately 200 nm in diameter. The fully functional virus particle adopts the architecture of a sphere, containing the viral genome within the nucleocapsid, which again is coated by the tegument layer and the viral envelope (Figure 1). (Murphy and Shenk, 2008)

With 235 kilobases in size, HCMV carries one of largest genomes among human-related viruses and the largest genome within the family of the *Herpesviridae*. It consists of a linear double-stranded desoxyribonucleic acid (DNA) molecule resembling the architecture of a type E structured genome, consisting of two unique domains, being referred as the unique long (UL) and the unique short (US) domain. According to the genome structure, the HCMV gene nomenclature is referred to the position of the gene loci in the respective domain, for example *UL74*. Each of the domains is flanked by one inverted repeat sequence at the terminal end (TR_L/ TR_S) and the intersectional end (IR_L/ IR_S) between the domains. Due to possible recombination events between the repetitive regions, the genome can be found as an equimolar mix of four different isomeric forms, which differ in the orientation of the unique long and unique short domains, respectively. (Weststrate, Geelen and Van Der Noordaa, 1980; Roizman *et al.*, 1981) The coding capacity of the HCMV genome is estimated between 164 – 192 unique open reading frames (ORFs), but remains elusive because of the genomic alterations among different HCMV strains. (Davison *et al.*, 2003; Murphy *et al.*, 2003; Dolan *et al.*, 2004; Sijmons, Van Ranst and Maes, 2014)

The genome is densely packed within an icosahedral nucleocapsid (T=16) built out of 162 capsomers, which again assemble from pentameric, hexameric and triplex structures formed by the major capsid proteins. (Zhou *et al.*, 2000; Yuan *et al.*, 2018) It serves the transport and protection of the viral DNA during cell entry and egress from the nucleus. (Newcomb *et al.*, 1996)

The tegument layer consists of an inner and outer sub-compartment that surround and fill the space between the nucleocapsid and the viral envelope. It contains structural and non-structural regulatory proteins that facilitate capsid stabilization, immune evasion, protein transport, control of the host cell metabolism as well as the viral gene expression, egress and virion assembly. (Chen *et al.*, 1999; Yu *et al.*, 2011) Although tegument proteins make up about 50% of the virion-associated proteome and play an important functional role across the viral replication cycle, most of them remain poorly characterized in their function and structure. (Roby and Gibson, 1986; Baldick and Shenk, 1996; Varnum *et al.*, 2004; Yu *et al.*, 2011; Bogdanow *et al.*, 2023)

The outer layer of the virion is the viral envelope, which is formed by a lipid bilayer derived from the cellular membrane system of the Golgi apparatus. Embedded within the viral envelope are several glycoprotein-complexes that interact with cell-associated components and receptors to facilitate the entry into several host cells (Figure 1). The best-known components of the complexes in the viral envelope are the glycoproteins gM (UL100), gN (UL73), gB (UL55), gH (UL75), gL (UL115), gO (UL74), gpUL128, gpUL130 and gpUL131A. These combine in different manners to build the gM/gN, the gB, the trimeric gH/gL/gO and the pentameric gH/gL/UL128-UL131A glycoprotein complexes. (Kari *et al.*, 1990; Kaye, Gompels and Minson, 1992; Li, Nelson and Britt, 1997; Mach *et al.*, 2000; Ryckman *et al.*, 2008) Thereby, gM and gB are shown to be the most abundant glycoproteins within the envelope. (Varnum *et al.*, 2004) The abundance of the trimeric and pentameric gH/gL-complexes differs between the different HCMV strains, which is shown to have an impact on the HCMV cell tropism and spread patterns. (Zhou *et al.*, 2013; Zhang *et al.*, 2018; Fornara *et al.*, 2023)

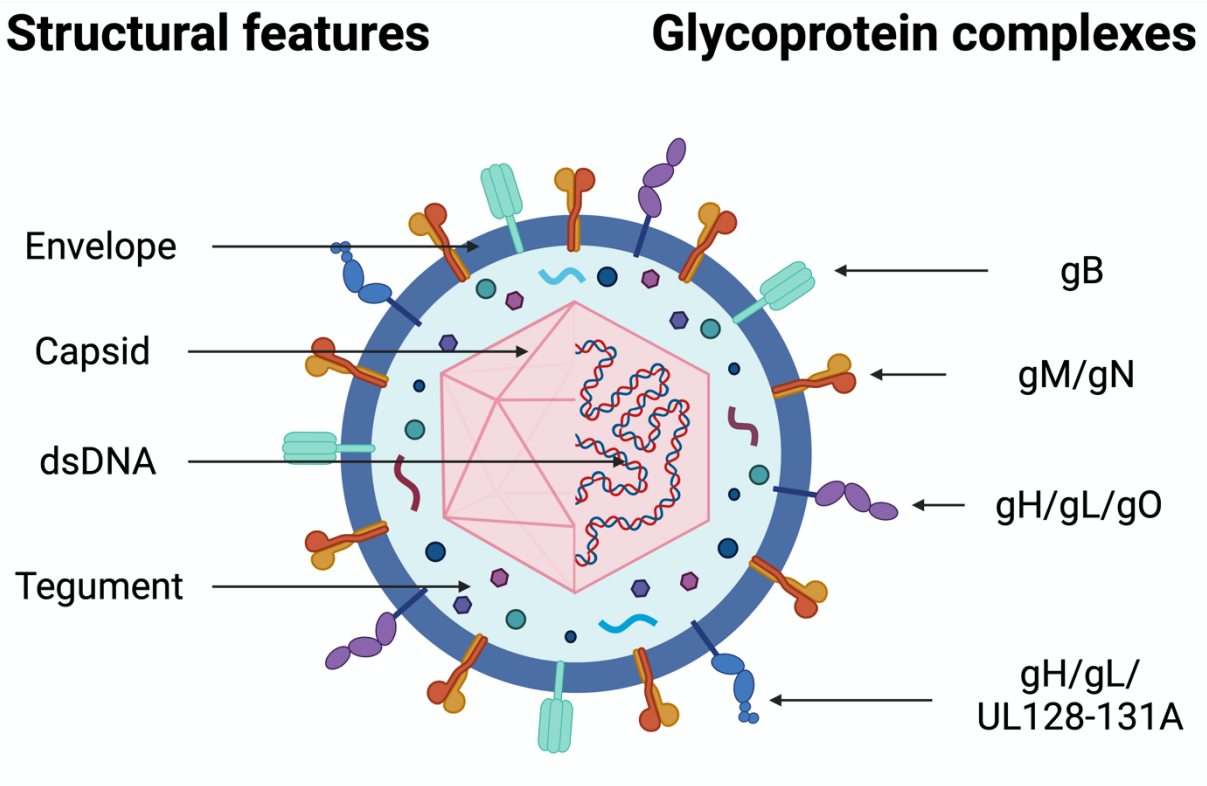

Figure 1: HCMV virion structure. *Simplified illustration of a HCMV virus particle highlighting the structural features (left) and the HCMV-related glycoprotein complexes gM/gN, gB, gH/gL/gO and gH/gL/UL128-131 embedded within the viral envelope (right).*

1.4 Lytic replication and viral spread

Upon infection, HCMV enters the body through the mucosal epithelium of the mouth, nose or genitalia. From there the virus infects specific target cells in order to amplify through lytic replication or disseminate throughout different tissues and organs upon latent infection. (Crough and Khanna, 2009). The viral life cycle describes the active replication and generation of viral progeny upon lytic infection of a permissive cell and involves the stages of cell entry, genome replication, virion assembly and the egress. Each structural component of the virus thereby plays its own essential role during this process.

1.4.1 Cell entry

Although the core entry machinery, consisting of the glycoproteins gH, gL and gB, is conserved among herpesviruses, HCMV cell entry is a highly complex mechanism that is yet not completely resolved. (Sathiyamoorthy *et al.*, 2017) Additionally to the core machinery, different herpes viruses have developed individual accessory glycoproteins and thus evolved a specific cell tropism. In the case of HCMV, the glycoproteins gO and UL128/UL130/UL131A represent the extending subunits to the gH/gL heterodimeric core complex. (Ciferri, Chandramouli, Donnarumma, *et al.*, 2015)

The initial attachment between the virus and the target cell is created by the gM/gN complex, which binds to heparin-like structures on the cell surface. (Kari and Gehrz, 1992, 1993; Mach *et al.*, 2005) In the next step, receptor binding is mediated by either the pentameric gH/gL/UL128-131A or the trimeric gH/gL/gO complex. Through their specificity to different cell receptors, they enable the infection of different cell types (Figure 2). (Liu *et al.*, 2018; Nguyen and Kamil, 2018) The pH-dependent pathway is triggered by binding of the pentameric gH/gL/UL128-131A complex to neuropilin-2 receptor protein (Nrp2). (Martinez-Martin *et al.*, 2018) This pathway leads to the endosomal uptake of the receptor-bound virion and is needed for entry into epithelial cells, endothelial cells and myeloid cells. (Ryckman *et al.*, 2006; Ryckman, Chase and Johnson, 2008; Nogalski *et al.*, 2013; Liu *et al.*, 2018) Upon binding of the trimeric gH/gL/gO complex to the platelet-derived growth factor receptor alpha (PDGFRα), the pH-independent pathway gets activated, promoting the direct entry at the cell surface either via membrane fusion or a form of rapid macropinocytosis. (Compton, Nepomuceno and Nowlin, 1992; Hetzenecker, Helenius and Krzyzaniak, 2016; Kabanova *et al.*, 2016; Wu *et al.*, 2017) Although this specific interaction in particular is sufficient for the entry into fibroblasts and dendritic cells (Langerhans cells), it has already been shown that the trimeric complex is also required for the infection of epithelial and endothelial cells, implicating a co-dependent function of the pentameric and trimeric complex for those cell types.

(Wille *et al.*, 2010; Lauron *et al.*, 2014; Stegmann *et al.*, 2017; Liu *et al.*, 2018) The trimer-associated receptor repertoire has further been demonstrated to include the transforming growth factor beta receptor 3 (TGFßR3). (Martinez-Martin *et al.*, 2018) Both, PDGFRα and TGFßR3 bind the trimeric complex with affinity and in a mutually exclusive manner, indicating them as independent entry receptors. (Kschonsak *et al.*, 2021) In consideration to this, it is not completely clear which entry receptor the trimeric gH/gL/gO complex uses for the entry of epithelial and endothelial cells. Apart from the described permissive cell types, the panel of HCMV further includes smooth muscle cells and also CD34+ bone marrow cells. (Maciejewski *et al.*, 1992; Sinzger *et al.*, 1995; Von Laer *et al.*, 1995; Haspot *et al.*, 2012)

After receptor binding, membrane fusion is mediated by the gB complex, a viral class III fusogen. The complex undergoes an irreversible transition from its metastable pre-fusion to a stable post-fusion state, upon which the viral and cellular membrane systems are pulled together until they merge. (Wille *et al.*, 2013) While the structural mechanisms are largely understood, the trigger for the conformational change remains unclear. (Y. Liu *et al.*, 2021) Similar to the HSV-1/2 and EBV models, it is speculated that interaction with the gH/gL-complexes, as well as the pH change within the endosome, suffice to activate the conformational change that leads to membrane fusion. (Ryckman *et al.*, 2006; Patrone *et al.*, 2007; Chowdary *et al.*, 2010; Stampfer and Heldwein, 2013; Nicola, 2016; Vanarsdall *et al.*, 2016) In 2015, Zhou *et al.* reconstituted the infectivity of virions rich on pentameric gH/gL/UL128-131A, but poor on trimeric gH/gL/gO, by the use of a chemical fusogen and argued that the gB-mediated membrane fusion is likely to be triggered by distinct mechanisms throughout the entry pathways mediated by the different gH/gL-complexes. (Zhou, Lanchy and Ryckman, 2015)

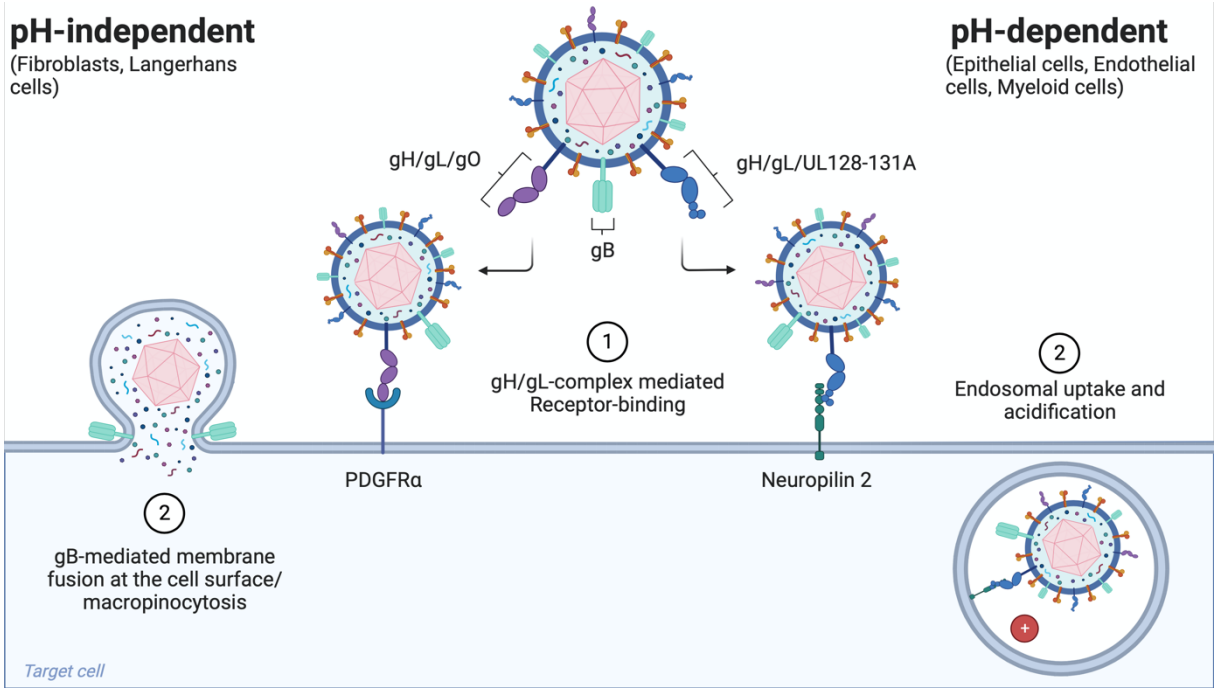

Figure 2: HCMV cell entry pathways. *Simplified illustration of the HCMV cell entry mediated by the pH-independent or pH-dependent pathway, which in turn are activated by binding of the trimeric gH/gL/gO (left) and pentameric gH/gL/UL128-131A complexes (right), respectively.*

1.4.2 Genome replication, virion assembly and egress

Upon membrane fusion, the nucleocapsid and the tegument layer are released into the cytoplasm. Since most tegument proteins have not been characterized yet, the total extent of their functions remains elusive. Nevertheless, some of them are known to promote capsid transportation, DNA release, viral gene expression, immune evasion and in the end also the egress of formed nucleocapsids and virion assembly. (Kalejta, 2008) The capsid-bound fraction of tegument proteins hitchhikes the cellular microtubule network in order to transport the capsid to the nucleus and later introduce the double-stranded DNA through a nuclear pore complex. (Ogawa-Goto *et al.*, 2003) Within the nucleus, an interplay of cellular and viral regulatory proteins and transcription factors initiate a fine-tuned sequence of viral gene expression consisting of immediate early genes (IE/ 2 to 4 hours post infection), early genes (E/ up to 24 hours post infection) and late genes (L/ from 24 hours post infection). (Demarchi, Schmidt and Kaplan, 1980) Within the nucleus, these gene cascades regulate viral protein expression, genome replication and its integration into newly formed nucleocapsids. Upon disruption of the nuclear lamina and formation of the nuclear egress complex, the assembled capsids exit the nucleus and hitchhike the cellular secretory pathway. (Hamirally *et al.*, 2009) The capsids wander through the endoplasmic reticulum (ER) into the cytosol and then through the virion assembly complex (VAC), formed by the Golgi apparatus and endosomal

vesicles. There they acquire the proteins of the tegument layer and the viral envelope, containing the viral glycoprotein complexes. (Moorman *et al.*, 2010) In the end, the infectious particles, but also some non-infectious particles, so-called dense bodies lacking a nucleocapsid and the viral DNA, are transported to the cell membrane and released into the extracellular space. (Mettenleiter, 2002; Alwine, 2012)

1.4.3 Viral spread

Upon the release, viral particles can either spread in a cell-associated manner within the initial site of infection or also in a cell-free manner carrying the infection into other tissues and organs. Fibroblast-adapted laboratory strains apparently change their spread pattern from cell-associated to cell-free, whereas upon restoration of the RL13 and UL128 gene loci, the cell-associated spread is re-established. This further implicates an associated function of the trimeric gH/gL/gO and pentameric gH/gL/UL128-131 complex abundancies in the cell-free and cell-associated spread dynamics, respectively. (Sinzger *et al.*, 1999; Adler *et al.*, 2006; Stanton *et al.*, 2010; Sampaio *et al.*, 2016) Following this, the cell-free and cell-associated spread patterns are shown to depend on the increased abundance of either trimeric gH/gL/gO or pentameric gH/gL/UL128-131 complex, respectively. (Wille *et al.*, 2010; Lemmermann *et al.*, 2015; Podlech *et al.*, 2015; Murrell *et al.*, 2017; Day *et al.*, 2020)

Among the broad collective of permissive cells, the major cell types, including fibroblasts, endothelial cells, epithelial cells and smooth muscle cell, are used as sites of active replication. (Plachter, Sinzger and Jahn, 1996) Apart from those, certain cell types infected by HCMV cause the virus to undergo into persistent infection, serving as latent reservoirs that allow for intra-host dissemination throughout different tissues. Although not definitely determined, cells permissive for persistent infections carry low loads of viral DNA and show only limited viral gene expression. So far identified cell types of latency are $CD34^+$ bone marrow cells, cells of the myeloid cell line like monocytes and probably also macrophages, immature dendritic cells (iDCs) and endothelial cells. (Schrier, Nelson and Oldstone, 1985; Grefte *et al.*, 1993; Fish *et al.*, 1996; Mendelson *et al.*, 1996; Jarvis and Nelson, 2002a; Sénéchal *et al.*, 2004; Sinclair and Sissons, 2006) This allows for the evasion of the immune response, the intra-host dissemination and multiorgan involvement upon acute infection and the inter-host transmission through transplants and blood transfusion. (Plachter, Sinzger and Jahn, 1996) In contrast to active replication, it is suggested that the IE gene cascade is downregulated during persistent infection and represses the replication cycle until external factors like stress signals, inflammation or cell differentiation, reactivate viral gene expression and restart the cycle. (Jarvis and Nelson, 2002b; Rozman *et al.*, 2022)

1.5 Trimeric gH/gL/gO complex

Since the trimeric gH/gL/gO complex plays an essential role in the infection of multiple cell types, there is a high interest to understand the structure and thus the mechanisms that rely upon it, to exploit them for possible therapeutic approaches. It has already been shown that the respective subunits of the trimeric complex are covalently linked to each other by disulfide bonds and can be detected via SDS-PAGE either as trimeric gH/gL/gO (>200 kDa) or gH/gL-core complex (~130 kDa) in form of a single band and as monomeric gH (~100 kDa), gL (~30 kDa), gO (~130 kDa) subunits in form of three bands upon reducing conditions (Kaye, Gompels and Minson, 1992; Huber and Compton, 1997; Li, Nelson and Britt, 1997; Ciferri, Chandramouli, Donnarumma, *et al.*, 2015).

1.5.1 Structure and formation

Recently performed high resolution electron microscopy in combination with 3D-reconstruction analysis of the gH/gL/gO trimer itself and as complex with PDGFRα has further revealed the structure and the binding dynamics between the gL and gO subunits and the PDGFRα cell receptor (Figure 3). (J. Liu *et al.*, 2021; Kschonsak *et al.*, 2021) The trimeric complex exhibits a boot-like architecture with the subunits arranged in a linear order and connected through disulfide bonds between highly conserved cysteine residues. The gH subunit contains a single-spanning transmembrane helix at the C-terminus that anchors the complex within the viral membrane. Upon binding of gH C-95 and gL C-47, the dimeric gH/gL-core complex is formed. (Gonzalez-Del Pino and Heldwein, 2022) The highly conserved gL C-144 further represents the connecting link for the pentamer-associated UL128 C-162 and the trimer-associated gO C-351 (strain Merlin). Notably, the gL C-144 residue can serve as binding site for another gL C-144 and promote the formation of a homodimeric gH/gL-complex (>200 kDa). (Ciferri, Chandramouli, Donnarumma, *et al.*, 2015) Although the gO variants exhibit high sequence variability, the gL-gO binding interface comprises certain regions of high conservation, so that the formation of the trimeric complex is hardly affected. (J. Liu *et al.*, 2021) Comparison of the gH/gL-core structure between the trimeric or pentameric state, shows no significant structural differences. However, the gO binding site covers the gL surface in a crown-shaped manner (~2.400 Å^2) with the residues of the binding interface adopting a loop-like structure, whereas upon binding of UL128-131 they form an alpha-helix. (Kschonsak *et al.*, 2021)

The elongated structure of the formed trimeric complex is flexible and contains multiple glycosylation sites distributed among the subunits. Thereby, the gH and gL subunit with four and one glycosylation sites, respectively, mainly carry N-linked glycans of the high mannose

form. (Bogner *et al.*, 1992; Kaye, Gompels and Minson, 1992; Ciferri, Chandramouli, Donnarumma, *et al.*, 2015) The gO subunit on the other hand, with more than ten glycosylation sites, carries most of the posttranslational modifications within the trimeric complex, with most of them being N-glycans of the high mannose form. These posttranslational modifications highly contribute to the size of the fully modified subunit, shifting the molecular weight of the polypeptide backbone from 54 kDa to approximately 130 kDa. However, removal of the N-linked glycans shifts the molecular weight of the gO subunit from 130 kDa down to only 60 kDa, indicating the presence of another posttranslational modification, most likely O-linked glycans. (Li, Nelson and Britt, 1997; Huber and Compton, 1999; Bagdonaite *et al.*, 2016) Based on the type of posttranslational modifications on the respective subunits, Huber and Compton were also able to generate a model of the formation and modification of the trimeric complex. Due to the compartment-dependent sensitivity of high-mannose N-Glycans to Endo H digestion, they concluded that during the formation of the trimeric complex, gH, gL and a precursor form of gO (~100 kDa) already assemble within the ER. After further processing within the Golgi Apparatus, Endo H sensitivity of the mature gO (~130 kDa) and also the gH subunit strongly decreased, indicating the presence of complex, Endo H-resistant glycans and a mature gH/gL/gO complex. (Huber and Compton, 1999)

The electrostatic surface charge analyzed by Kschonsak *et al.* corresponds to the presence of 19 N-linked glycosylation sites on the trimeric complex, whereby the distribution of glycosylated residues resembles enrichment at particular sites across the complex. Of those glycosylation sites, 5 were detected on gH, a single one on gL and 13 on the gO subunit. (Kschonsak *et al.*, 2021)

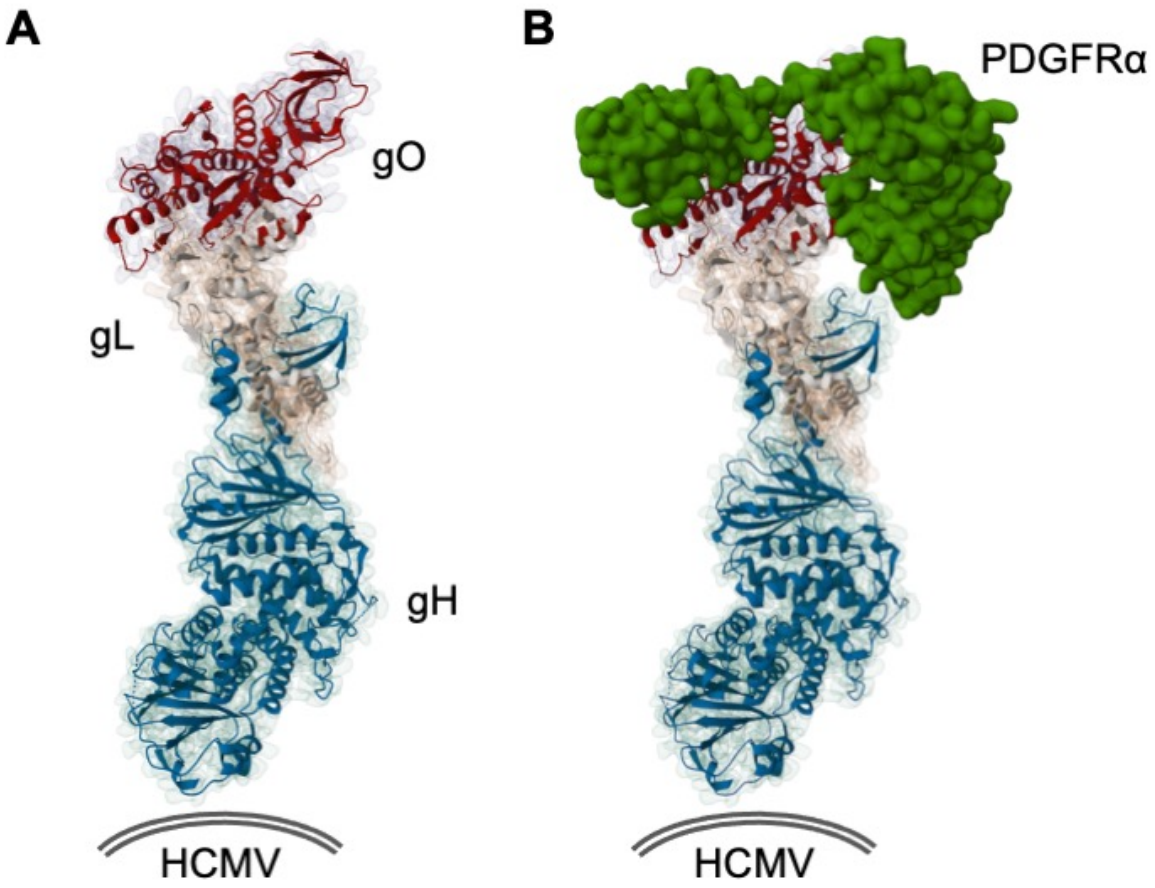

Figure 3: Electron-microscopic structure of the trimeric gH/gL/gO complex. *Image from the RCSB PDB (RCSB.org) of PDB ID 7LBF* (Kschonsak *et al.*, 2021) ***(A)*** *Front view of HCMV gH/gL/gO trimeric complex (shown in ribbon).* ***(B)*** *Front view of HCMV gH/gL/gO Trimer complex (shown in ribbon) bound to PDGFRα.*

1.5.2 PDGFRα receptor binding

The trimeric complex binds selectively and with high affinity to PDGFRα. In 2019, Stegmann et al. showed that the gO N-terminus provides the essential binding site required for receptor binding. (Kabanova *et al.*, 2016; Wu *et al.*, 2017; Stegmann *et al.*, 2019) The N-terminal ß-sheet domain and the C-terminal helical domain are linked by disulfide bonds between highly conserved cysteine residues, which forms a socket-like architecture on the gO surface. Despite the low overall conservation of the gO amino acid sequence, especially in the N-terminus, there are large unmodified areas within the surface of both domains that show high conservation.

The extracellular domain of the PDGFRα receptor consists of five immunoglobulin-domain segments (D1-D5), which are connected to an intracellular kinase domain through a single transmembrane-domain (Lemmon and Schlessinger, 2010) Upon receptor binding, PDGFRα wraps around the gO subunit of the trimeric gH/gL/gO complex. (J. Liu *et al.*, 2021) Thereby

PDGFRα Ig-domains D1 - D3 are the main contributors for binding, establishing four major connections with conserved regions across the gO surface and the gH N-terminus. Two binding sites on the gO surface are represented by a hydrophobic groove on the N-terminal domain and the basic groove between the N- and C-terminal domain, interacting with residues of PDGFRα D1 and D2. The other two binding sites comprise interactions between the gH N-terminus with PDGFRα D1 and the gO subunit with PDGFRα D3. (J. Liu *et al.*, 2021; Kschonsak *et al.*, 2021) Deletion of two heavily glycosylated loops distant to the gO binding interface could not disrupt the ability of the trimeric complex to bind to PDGFRα, indicating that the posttranslational modifications do not play a role in protein formation, protein folding or receptor binding, but rather support immune evasion. (J. Liu *et al.*, 2021) Further mutational analysis led to a loss of PDGFRα binding, only if present within all four binding sites simultaneously. (J. Liu *et al.*, 2021; Kschonsak *et al.*, 2021)

1.5.3 Polymorphisms and strain variability

Although the majority of the HCMV genome exhibits about 80 - 90% inter-strain sequence similarity, individual gene loci contain polymorphic regions that lead to the distinction of protein variants and thus different HCMV strains. (Pignatelli *et al.*, 2004) These strains are further categorized into high-passaged laboratory strains (e.g. AD169 and Towne), low-passaged laboratory strains (e.g. Merlin, TB40/E and Toledo) and clinical isolates, due to the genome alterations obtained upon fibroblast-cultivation and their differences to the wild-type genome. (Prichard *et al.*, 2001; Wilkinson *et al.*, 2015; Martí-Carreras and Maes, 2019)
Some of those multiallelic loci encode for viral glycoproteins of the viral envelope. (Vankova, Brusnigina and Novikova, 2023) This also concerns the gH and the gO subunit of the trimeric gH/gL/gO complex. The UL75 gene locus, encoding for the gH subunit, contains little sequence variability within the N-terminus that leads to distinction into the variants gH1 and gH2, that are present in the HCMV strains AD169, TB40E, VR1814, Toledo and Towne, Merlin, respectively. (Chou, 1992; Wang *et al.*, 2021) The UL74 gene locus encoding for the gO subunit, on the other hand, accounts for one of the least conserved proteins among the HCMV proteome, showing high variability within the first 100 N-terminal amino acids and minor variability between amino acids 270 to 313. Hence, five phylogenetic groups, which comprise eight different genotypes have been determined for the glycoprotein gO: gO1a (AD169), gO1b (TR), gO1c (TB40E/ Toledo/ VR1814), gO2a (PH), gO2b, gO3, gO4 (Towne) and gO5 (Merlin). While genotypes within the same groups show a sequence similarity of up to 98 – 100%, the inter-genotypic sequence diversity between genotypes of different groups ranges between 10 – 30%. (Rasmussen *et al.*, 2002; Mattick *et al.*, 2004; Stanton *et al.*, 2005) It has already been demonstrated that the genotypic diversity of the gO subunit has an

impact on the formation and abundance of trimeric complex in the viral envelope as well as the viral spread patterns and the strain-specific immunity mediated by antibodies. (Klein *et al.*, 1999; Jiang *et al.*, 2011; Zhou *et al.*, 2013; Day *et al.*, 2020; Wang *et al.*, 2021)

So far, the intra-structural binding dynamics as well as the gO-mediated receptor binding dynamics have been resolved for the gO1b and the gO1c variants of the strains TR and the VR1814. Although both, the gL- and PDGFRα-binding site mainly involve highly conserved sequence regions, the variant-specific influence on the trimer-formation and receptor-binding dynamics remain to be investigated for the other gO genotypes, in order to better understand the functional and immune evasive aspects as well as the potential and importance of the trimeric complex as therapeutic target. (J. Liu *et al.*, 2021; Kschonsak *et al.*, 2021).

1.5.4 Antigenic properties

While T-cells actively contribute to the elimination and silencing of HCMV infection, the humoral immune response is assumed to predominantly affect the dissemination within the host. (Jonjić *et al.*, 1994) Antibodies can directly bind to pathogens and either inhibit protein interactions or mark the pathogen for other immune cells. Former are referred to as inhibitory antibodies (iAbs) or even neutralizing antibodies (nAbs), given that a single antibody in particular can prevent the viral infection. (Lu *et al.*, 2018) Studies show that naturally occurring HCMV infection pre-dominantly leads to the generation of nAbs that prevent the infection of endothelial and epithelial cells, rather than the infection of fibroblast. Interestingly, fibroblast-protecting nAbs can also protect endothelial cells with at least equal efficiency. (Wang *et al.*, 2011; Falk *et al.*, 2017).

Similarly to CD4+ T-cells, glycoprotein gB represents the predominant antigenic target also for the humoral immune response, making up for approximately 50% of the total HCMV-specific antibody response in infected individuals (Britt *et al.*, 1990; Marshall *et al.*, 1992; Pötzsch *et al.*, 2011) The humoral immune response against the trimeric and pentameric gH/gL-complexes is distinguished into nAbs that target the dimeric gH/gL-core complex or the accessory proteins, which mediate receptor binding (gO/ UL128-131A). (Ai *et al.*, 2022; Gonzalez-Del Pino and Heldwein, 2022) nAbs that bind to the gH/gL core dimer usually can do this in both, the trimeric and pentameric form, whereby neutralizing epitopes are mainly found within the gH subunit. (Boppana and Britt, 1995; Urban *et al.*, 1996; Ciferri, Chandramouli, Leitner, *et al.*, 2015) Since gH-specific neutralizing epitopes, like those of the nAbs MSL-109, 13H11 and 3G16, are distant from the receptor binding site, they are described to mediate neutralization through the hampered interaction with the gB complex needed for membrane fusion (Figure 4A). (Macagno *et al.*, 2010; Fouts *et al.*, 2014; Kschonsak *et al.*, 2021) Although gH/gL-specific nAbs can inhibit entry into epithelial cells,

endothelial cells and fibroblasts, they only provide a tenth to a hundredth of the neutralizing efficiency of nAbs targeting the receptor-accessory subunits UL128, UL130 and UL131 of the pentameric complex. (Rasmussen *et al.*, 1991; Urban *et al.*, 1996) However, pentamer-specific nAbs targeting the UL128-131 subunits, in turn exclusively protect from the infection of endothelial, epithelial and myeloid cells, but not fibroblasts. (Macagno *et al.*, 2010; Ciferri, Chandramouli, Leitner, *et al.*, 2015; Ai *et al.*, 2022) Documentation regarding the detection of gO-specific nAbs is hardly available. (Gerna *et al.*, 2016) The low detection rate of gO-specific nAbs is mostly explained by the high glycosylation pattern of the subunit. (Vigerust and Shepherd, 2007; Kschonsak *et al.*, 2021) Moreover, such nAbs would need to target highly conserved epitopes, in order to overcome the gO-related sequence variability and provide strain-overlapping protection. (Rasmussen *et al.*, 2002; Ai *et al.*, 2022; He *et al.*, 2022) Currently, there is only one detailed report describing a gO-specific nAb, the so-called elite neutralizer (CS2it1p2_F7K), that is predicted to prevent PDGFRα- as well as TGFßR3-binding and provides strain-overlapping protection for epithelial, endothelial and fibroblast cells (Figure 4B). (Zehner *et al.*, 2023) This leads to the conclusion, that the combination of trimer- (gH/gL/gO) and pentamer-specific (gH/gL/UL128-131A) nAbs, especially those targeting the receptor-accessory subunits and those that prevent receptor-binding, play an essential role in the protection from HCMV infection. (Vanarsdall *et al.*, 2019)

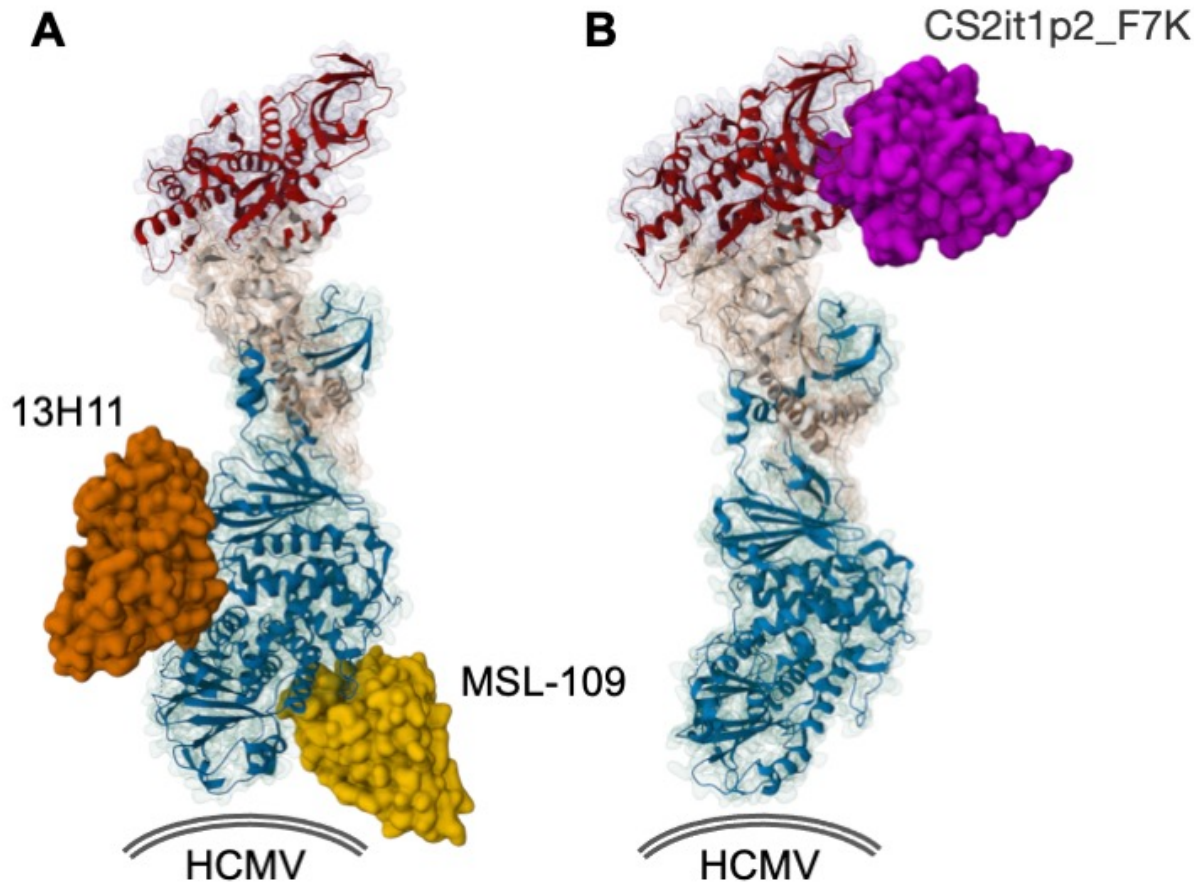

Figure 4: Electron-microscopic structure of the trimeric gH/gL/gO complex with reported nAbs. *Image from the RCSB PDB (RCSB.org) of PDB ID 7LBF* (Kschonsak *et al.*, 2021) *and 8TCO* (Zehner *et al.*, 2023) ***(A)*** *Front view of HCMV gH/gL/gO trimeric complex (shown in ribbon) bound to neutralizing Fabs 13H11 (orange) and MSL-109 (yellow).* ***(B)*** *Front view of HCMV gH/gL/gO Trimer complex (shown in ribbon) bound to neutralizing Fabs CS2it1p2_F7k (magenta).*

1.6 Role of IgG antibodies in diagnostics and treatment of HCMV primary infections

Due to the asymptomatic course in immunocompetent individuals, HCMV infections usually remain undetected. Especially during pregnancy, it is of major importance to detect and differentiate between recent and past HCMV infections in order to monitor the possibility of an in-utero transmission and prevent developmental damage of the fetus. Apart from the detection of viral DNA and IgM antibodies, which cannot distinguish between primary infection and reactivation, determination of the HCMV-specific IgG avidity index can be used as a diagnostic marker, to specifically differentiate between recent or past primary infection. (Bodéus, Feyder and Goubau, 1998; Prince and Lapé-Nixon, 2014; Abdullahi Nasir, Babayo and Shehu, 2016) Antibody avidity describes the overall strength of the antibody-antigen interaction, which for IgG antibodies usually increases in the course of antibody affinity maturation,

during first four to six months after primary infection. (Eisen and Siskind, 1964; Blank, Leslie and Clem, 1972) Thereby, the rate of avidity maturation differs between certain epitope-specific antibodies and can generally be slowed down upon immunosuppression. (Lutz, Ward and Gray, 1994; Lazzarotto *et al.*, 1998) Different studies show that IgG antibodies of high avidity provide higher neutralization efficiency than antibodies of low avidity. (Boppana and Britt, 1995; Furione *et al.*, 2013; Lilleri *et al.*, 2013)

Treatment of HCMV infection becomes necessary upon disease development or imminent risk of long-term complications, mainly concerning newborn infants and immunocompromised individuals. Antiviral drugs such as Ganciclovir (Valganciclovir) or Foscarnet expose patients to adverse side effects and bear the risk resistance development, attributing only a limited benefit for patients. (Bacigalupo *et al.*, 2012; Komatsu *et al.*, 2014) Moreover, there are no vaccines to HCMV approved at the moment. Those in development mainly target the envelope glycoprotein complexes gB and gH/gL/UL128-131A as templates, but fail to elicit antibody-mediated neutralization efficiency compared to those of a natural infection. (Cui *et al.*, 2008; Freed *et al.*, 2013) Another therapeutic approach is the passive immunization with standard intravenous immunoglobulins (IVIGs) or cytomegalovirus hyperimmune immunoglobulins (CMVIGs), like Cytotect®CP. (Miescher *et al.*, 2015) CMVIGs are highly concentrated antibody solutions purified from donor blood, chosen on the basis of high HCMV-specific antibody titers. (Snydman *et al.*, 1987; Bass *et al.*, 1993) Passive immunization with CMVIGs have been observed to reduce the risk of vertical HCMV transmission from mother to child and to improve survival in transplant patients. (Nigro *et al.*, 2005; Hsu and Safdar, 2011; Alsuliman *et al.*, 2018; Kagan *et al.*, 2021; Coste Mazeau *et al.*, 2023) Similar to human sera, CMVIGs also provide higher neutralization (48-fold) against viral entry into epithelial cells than fibroblasts. (Cui *et al.*, 2008) Followingly, there is uncertainty if the increased neutralization efficiency correlates with the concentration of the overall HCMV-specific IgG titer or depends on the subclass and individual efficiency of certain antibodies, respectively. (Chehimi, Peppard and Emanuel, 1987; Planitzer *et al.*, 2011; Miescher *et al.*, 2015; Germer, Herbener and Schüttrumpf, 2016)

2 Aim of the thesis

The detection and characterization of so-called elite neutralizers, providing broad and strain-overlapping neutralizing efficiency in endothelial, epithelial and fibroblast cells represents a new outlook against HCMV infection. (Falk *et al.*, 2018; Harnois *et al.*, 2022) The high neutralizing efficiency of endothelial- and epithelial cell-specific nAbs targeting the pentameric UL128-131 subunits as well as the equivalent functional role of the trimeric gH/gL/gO complex for cell entry, give reason to believe that iAbs targeting conserved gO epitopes and specifically inhibit receptor-binding could also represent highly potent and strain-overlapping nAbs. (Manuel *et al.*, 2009; Day *et al.*, 2020; He *et al.*, 2022)

The work of this thesis is dedicated to the production of soluble gH/gL/gO utilizing different gO genotypes and to the establishment of a gH/gL/gO-specific PDGFRα-binding assay based on the principle of the recently described surrogate virus neutralization test (sVNT) (Figure 5). With this assay we aim to compare the trimer-specific antibody-mediated neutralization in regards to different gO variants and, in further instance, promote the detection of trimer-specific nAbs with potential of being strain-overlapping neutralizers. (Tan *et al.*, 2020)

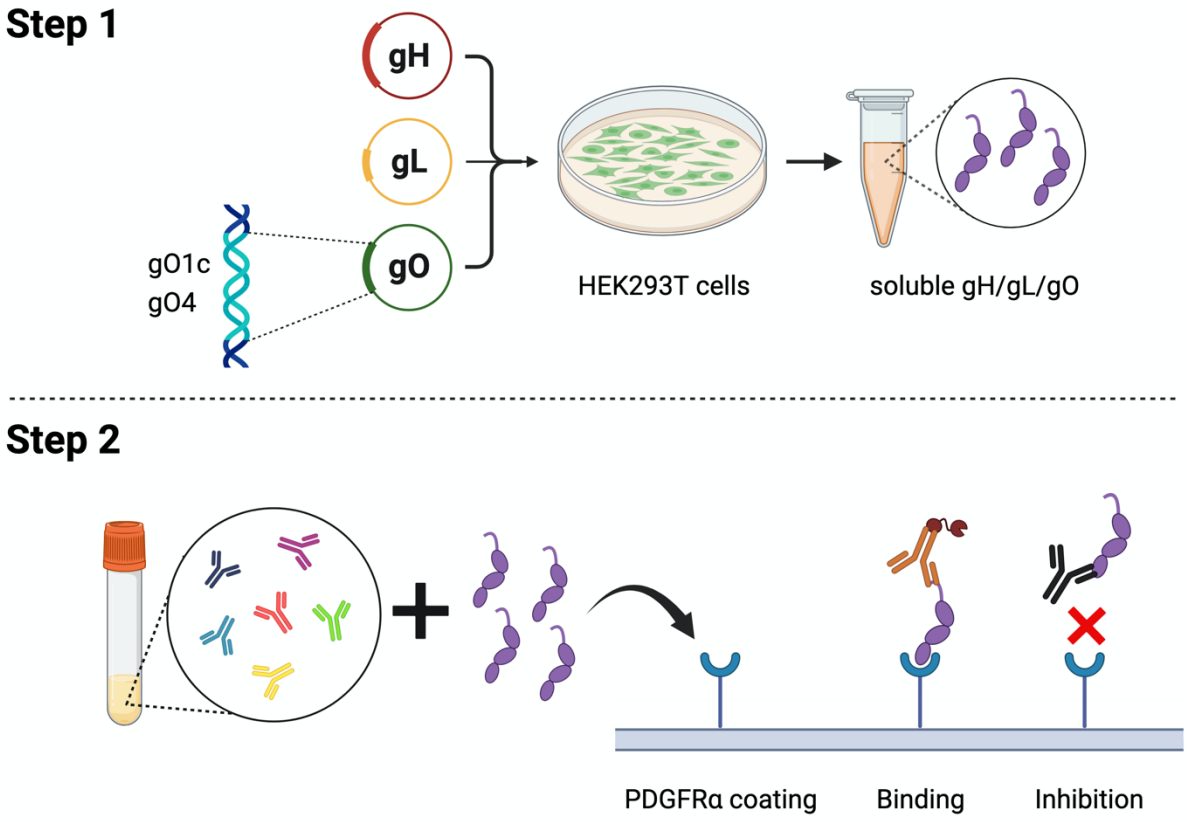

Figure 5: Graphical illustration of the workflow established in the course of this master thesis. *(Step 1) Production of recombinant and soluble gH/gL/gO utilizing different gO variants using HEK293T cells. (Step 2) Establishment of a PDGFRα-binding assay and analysis of serum-antibody mediated inhibition using priorly produced gH/gL/gO.*

3 Material and Methods

3.1 Materials

3.1.1 Expression vectors

Table 1: Description of the gene inserts and properties of the expression vector backbones used for transformation of E.coli cells and transfection of HEK293T cells.

Insert	Properties	Backbone
HCMV TB40/E, glycoprotein gH [UL75/ NCBI KF297339]	IL-2 signal peptide ΔTM-domain ΔCytoplasmic tail	pMT7 [Cytiva LifeSciences, US]
HCMV TB40/E, glycoprotein gL [UL115/ NCBI KF297339]	IL-2 signal peptide	pMT1 [Cytiva LifeSciences, US]
HCMV TB40/E, glycoprotein gO (gO1c) [UL74/ NCBI KF297339]	IL-2 signal peptide	pMT1 [Cytiva LifeSciences, US]
HCMV Towne, glycoprotein gO (gO4) [UL74/ NCBI FJ616285]	IL-2 signal peptide	pMT1 [Cytiva LifeSciences, US]

3.1.2 Cell lines

Table 2: Bacterial and human cell lines used for DNA amplification, transfection and virus neutralization assays.

Cells	Type	Source
DH5α-T1^R	Escherichia Coli (Enterobacteria)	Thermo Fisher, US [cat.nr. 12297-016]
HEK293T	Human embryonic kidney 293 (human, immortalized)	ATCC, US [cat.nr. CRL-3216]
HFF	Foreskin fibroblast (human)	Center for Virology, MUW, AT

3.1.3 Virus

Table 3: BAC-derived HCMV strain used for the infection of HFF cells during virus neutralization assay.

Virus/ Strain	Properties	Source
HCMV TB40 strain (TB40-BAC4-luc)	BAC-derived clone containing luciferase reporter gene (Scrivano *et al.*, 2011)	Görzer Irene, MUW, AT

3.1.4 Primary Western Blot antibodies

Table 4: Properties and dilutions of primary western blot detection antibodies.

Specificity	Isotype	Species	Source	Properties	Dilution
HCMV gH (AP86, SA4)	IgG	Mouse	Mach Michael, FAU Erlangen-Nürnberg, DE (Urban, Britt and Mach, 1992)	monoclonal (N-terminal, aa 34 – 42)	1:2 (supernatant)
HCMV gO.02	IgG	Mouse	Adler Barbara, LMU Munich, DE (Kalser *et al.*, 2017)	monoclonal	1:500
6x his-tag (HIS.H8)	IgG2b	Mouse	Abcam, UK [cat.nr. ab18184]	monoclonal	1:5.000

3.1.5 Secondary Western Blot antibodies

Table 5: Properties and dilutions of secondary western blot detection antibodies.

Specificity	Isotype	Species	Source	Properties	Dilution
Mouse IgG	IgG	Sheep	Cytiva, US [cat.nr. NA931]	HRP-conjugated	1 : 6.000
Rabbit IgG	IgG	Donkey	Cytiva, US [cat.nr. NA934]	HRP-conjugated	1 : 5.000

3.1.6 ELISA antibodies

Table 6: Properties and dilution of ELISA detection antibody used during receptor-binding assay.

Specificity	Isotype	Species	Source	Properties	Dilution
6x his-tag (AD1.1.10)	IgG1	Mouse	Abcam, UK [cat.nr. 15149]	HRP-conjugated	1:250

3.1.7 Media for bacterial culture

LB medium

10 g peptone, 5 g yeast extract and 10 g NaCl and 0.1 g NaOH dissolved in double-distilled water (ddH2O), filled up to 1L and autoclaved (pH 7.5)

LB agar

10 g peptone, 5 g yeast extract, 10 g NaCl and 20 g Bacto-agar dissolved in double-distilled water (ddH2O), filled up to 1L and autoclaved (pH 7.5)

LB-Amp medium/ LB-Amp agar

LB medium and LB agar supplemented with ampicillin to a final concentration of 100µg/mL, prior to inoculation with bacterial cells or pouring of the agar plates (pH 7.5)

3.1.8 Media for cell culture

Table 7: Basic medium used for the cultivation and transfection of HEK293T and HFF cells.

Name	Source
Gibco™ DMEM	Thermo Fisher, AT [cat.nr. 41965-039]
Gibco™ Opti-MEM™ | Reduced Serum Medium	Thermo Fisher, AT [cat.nr. 31985-070]
Gibco™ OptiPRO SFM	Thermo Fisher, AT [cat.nr. 12309-019]
MEM with Earle's Salts (with L-Glutamine)	Capricorn, DE [cat.nr. MEM-A]

DMEMc medium

DMEM medium supplemented with 10% FBS, 10 mM HEPES, 500 U/mL Penicillin and 500 µg/mL Streptomycin (pH 7.0)

MEM +/+ medium

Minimum essential medium supplemented with 10% FBS, 1% non-essential amino acid solution, 50 µg/mL neomycin

3.1.9 Buffers

Phosphate buffered saline (PBS)

137 mM NaCl, 8.1 mM $Na_2HPO_4 \bullet 2H_2O$, 2.7 mM KCl and 1.5 mM KH_2PO_4 in ddH_2O (pH 7.4)

Phosphate buffered saline-Tween (PBS-T)

Phosphate buffered saline supplemented with 0.05% Tween®20 (pH 7.4)

Tris buffered saline (TBS)

20 mM Tris and 150 mM NaCl in ddH_2O (pH 7.5 adjusted with HCl)

Tris buffered saline-Tween (TBS-T)

Tris buffered saline supplemented with 0.05% Tween®20 (pH 7.5)

FPLC sample buffer

50 mM $NaH_2PO_4 \bullet H_2O$, 150 mM NaCl and 10 mM Imidazole (pH 8.0)

FPLC wash buffer

50 mM $NaH_2PO_4 \bullet H_2O$, 300 mM NaCl, 0.05% Tween®20 and 20 mM imidazole (pH 8.0)

FPLC elution buffer

50 mM $NaH_2PO_4 \bullet H_2O$, 300 mM NaCl, 0.05% Tween®20 and 250 mM imidazole (pH 8.0)

2x Sample buffer/ protein loading dye (non-reducing)

5% SDS, 125 mM Tris (pH 6.8), 10% glycerol and 0.004% bromophenol blue

2x Sample buffer/ protein loading dye (reducing)

5% SDS, 125 mM Tris-HCl (pH 6.8), 10% glycerol, 0.04% bromophenol blue and 10% 2-mercaptoethanol

Laemmli running buffer for SDS-PAGE

50 mM Tris and 384 mM glycine in ddH2O supplemented with 0.1% SDS before use

Western Blot blocking buffer

Tris buffered saline supplemented with 0.05% Tween®20 and 5% BSA (pH 7.5)

Western Blot washing buffer

Tris buffered saline supplemented with 0.05% Tween®20 (pH 7.5)

0.05 M Carbonate/ bicarbonate buffer

15 mM Na_2CO_3 and 35 mM $NaHCO_3$ in ddH_2O (pH 9.6)

ELISA washing buffer

Phosphate buffered saline supplemented with 0.05% Tween®20 (pH 7.4)

ELISA blocking solution

Phosphate buffered saline supplemented with 2% BSA and 2% Tween®20 (pH 7.4)

ELISA dilution buffer

Phosphate buffered saline supplemented with 1% BSA and 2% Tween®20 (pH 7.4)

3.1.10 Reagents, chemicals and supplementation

Table 8: Reagents, chemicals, supplements and proteins used for the generation of buffers, cell medium or assay testing.

Description	Stock conc.	Source
1-Step™ Ultra TMB substrate	1x	Thermo Fisher Scientific, US [cat.nr. 34028]
Ampicillin sodium salt	10 mg/mL	Sigma-Aldrich, US [cat.nr. A0166]
BD Bacto-Agar	-	Becton Dickinson [cat.nr. 214010]
Bovine Serum Albumin	1x	Serva, DE [cat.nr. 119-26-04]
Bromophenol Blue	-	Bio-Rad, UK [cat.nr. 1610404]
Ethanol absolute (EtOH)	96%	ITW Reagents, IT [cat.nr. A3678]
Fetal Bovine Serum (FBS)	1x	Capricorn, DE [cat.nr. FBS-12A]
Glycerol	≥99%	Sigma-Aldrich, US [cat.nr. G5516]
Glycine	≥98.5%	Sigma-Aldrich, US [cat.nr. 410225]
H2SO4 (sulfuric acid)	95 – 97%	Merck, DE [cat.nr. 100731]
HCl (hydrochloric acid)	5 M	Merck, DE [cat.nr. 109911]
HEPES (in ddH2O)	1 M	Serva, DE [cat.nr. 25245]
Imidazole	≥99%	Sigma-Aldrich, US [cat.nr. I2399]
KCl (potassium chloride)	99-100%	Sigma-Aldrich, US [cat.nr. P3911]
KH2PO4 (potassium phosphate monobasic)	≥99%	Sigma-Aldrich, US [cat.nr. P0662]
Lipofectamine® 2000	1x	Thermo Fisher, US [cat.nr. 11668019]
Na2CO3 (sodium carbonate)	≥99.5%	Sigma-Aldrich, US [cat.nr. 223530]
Na2HPO4•2H2O (sodium phosphate dibasic dihydrate)	-	Sigma-Aldrich, US [cat.nr. 1.06580]

NaCl (sodium chloride)	≥99%	Sigma-Aldrich, US [cat.nr. S9888]
NaH2PO4•H2O (sodium phosphate monobasic monohydrate	≥98%	Sigma-Aldrich, US [cat.nr. S9638]
NaHCO3 (Sodium hydrogen carbonate)	-	Sigma-Aldrich, US [cat.nr. 1.06329]
NaOH (sodium hydroxide pellets)	-	Merck, DE [cat.nr. 106462]
NaOH (sodium hydroxide solution)	10 M	Merck, DE [cat.nr. 480648]
Neomycin	10 mg/mL	Sigma-Aldrich, US [cat.nr. N1142]
Non-essential amino acids	100x	Sigma-Aldrich, US [cat.nr.M7145]
Penicillin	10.000 U/mL	Sigma-Aldrich, US [cat.nr. P4333]
Peptone	-	Sigma-Aldrich, US [cat.nr. P6838]
Rec. hPDGFRα/ CD140a	250 µg/mL	Szabo-Scandic, AT [ELA-PKSH031527]
SDS (sodium dodecyl sulfate)	≥99%	Sigma-Aldrich, US [cat.nr. 436143]
Streptomycin	50 mg/mL	Sigma-Aldrich, US [cat.nr. P4333]
Tris(hydroxymethyl)-aminomethane	≥99.8%	Sigma-Aldrich, US [cat.nr. 252859]
Trypan blue solution	0.4%	Sigma-Aldrich, US [cat.nr. 93595]
Trypsin-EDTA (0.25%)	1x	Sigma-Aldrich, US [cat.nr. 59428C]
Tween®20	100%	Sigma-Aldrich, US [cat.nr. P1379]
Yeast extract	-	Sigma-Aldrich, US [cat.nr. 1.03753]

3.1.11 Hardware, Kits and Systems

Table 9: Test kits, hardware and devices used for experiments.

Product	Source
4 - 15% Mini-Protean® TGX™ precast gel	Bio-Rad, UK [cat.nr. 4561083S]
ÄKTA pure 25L chromatography system	Cytiva LifeSciences, US [cat.nr. 29018224]
ÄKTA Superloop, 1/16" fittings 50 mL	Cytiva LifeSciences, US [cat.nr. 18111382]
BioTek® Synergy HTX multi-mode reader	Agilent Technologies
Cell culture flasks (surface treated, vented)	VWR, US [cat.nr. 734-2315P]
Cellometer® Auto T4	Nexcelom, US
Cytomegalovirus (CMV) avidity determination/	Euroimmun, DE [cat.nr. EI 2570-9601-1 G]

antigen-coated microplate wells	
Cytomegalovirus (CMV) IgG/ antigen-coated microplate wells	Euroimmun, DE [cat.nr. EI 2570-9601 G]
Cytomegalovirus (CMV) IgM/ antigen-coated microplate wells	Euroimmun, DE [cat.nr. EI 2570-9601 M]
Heraeus Multifuge X3 FR Centrifuge	Thermo Fisher, US
HisTrap FF crude 5 mL/ Ni-Sepharose fast flow column	Cytiva LifeSciences, US [cat.nr. 17528601]
Invitrogen® iBright™ 750CL imaging system	Thermo Fisher, US [cat.nr. A44116]
Leica DMi8 S inverted light microscope	Leica Microsystems, DE
Lonza™ Pro-Sieve™ quad color protein ladder	Thermo Fisher, US [cat.nr. BMA00193837]
MasterFlex® L/S EasyLoad® peristaltic pump	Cole Parmer Instruments, US
Micro BCA™ protein assay kit	Thermo Fisher, US [cat.nr. 23235]
Mini-Protean® Tetra vertical electrophoresis chamber	Bio-Rad, UK [cat.nr. 1658004]
NanoDrop® ND1000 spectrophotometer	peQlab Biotechnology, DE
Nunc™ 96-Well Polystyrene Round Bottom Microwell Plates	Thermo Fisher, US [cat.nr. 4912]
PageBlue™ staining solution	Thermo Fisher, US [cat.nr. 24620]
PureYield® Plasmid Midiprep kit	Promega, US [cat.nr. A2495]
Sample loop, 1/16” fittings 500 µL	Cytiva LifeSciences, US [cat.nr. 18111399]
SD100 Cellometer® counting chambers	Nexcelom, US [cat.nr. CHT4-SD100-002]
Sorvall LYNX 4000 Superspeed Centrifuge	Thermo Fisher, US [cat.nr. 75006580]
Steady-Glo® Luciferase assay system	Promega, US [cat.nr. E2510]
Superdex®200 Increase 10/300 GL	Cytiva LifeSciences, US [cat.nr. 28990944]
SuperSignal® West Pico plus substrate	Thermo Fisher, US [cat.nr. 34577]
Trans-Blot Turbo Mini 0.2 µm PVDF Transfer Pack	Bio-Rad, UK [cat.nr. 1704156]
Trans-Blot® Turbo™ Transfer System	Bio-Rad, UK [cat.nr. 1704150]
Vac-Man® Laboratory Vacuum Manifold	Promega, US [cat.nr. A7231]
Vivoflow®200 PES (100.000 MWCO)	Sartorius [cat.nr. VF20P4]
Vivospin®20 PES (100.000 MWCO)	Sartorius [cat.nr. VS2042]

3.1.12 Human sera and HCMV hyperimmune immunoglobulin used for test establishment

In the course of the establishment of the gH/gL/gO receptor-binding assay, residual human serum samples were characterized for HCMV-specific serodiagnostic markers prior to assigning them to cohorts. Human sera were received from the biobank of the Center for Virology of the Medical University of Vienna. Approval was obtained from the local ethics committee of the Medical University of Vienna (ethics approval number: 2156/2019). Tested sera were further categorized into cohorts according to parameters regarding HCMV serostatus defined by HCMV-specific IgG titer, HCMV IgG-specific avidity and medical history. Detection and concentration determination of HCMV-specific IgG and IgM antibodies was performed under the use of Euroimmun Cytomegalovirus ELISA-test kits (EI 2570-9601 G/ EI 2570-9601 M). HCMV-specific IgG avidity was determined under the use of Euroimmun Cytomegalovirus avidity determination ELISA-test kit (EI 2570-9601-1 G). As positive control for binding inhibition in the gH/gL/gO neutralization assay Cytotect®CP (50 mg/mL IgG) CMV hyperimmunoglobulin solution was used.

3.2 Methods

3.2.1 Designing of gH, gL and gO expression vectors

The expression vectors carrying the genetic information of the individual subunits of the HCMV gH/gL/gO complex were designed and ordered under the use of the online gene synthesis tool of Synbio Technologies LLC. The insert nucleotide sequences, coding for the subunits gH (UL75) and gL (UL115) were obtained from the HCMV TB40 strain (NCBI refseq KF297339), whereas for the gO subunit (UL74) two different genotypes were accessed, the HCMV TB40/E strain-derived gO1c genotype (NCBI refseq KF297339) and the HCMV Towne strain-derived gO4 genotype (NCBI refseq FJ616285). For the insert sequences of the regarding gH (aa 24 - 718), gL (aa 31 – 278), gO1c (aa 30-464) and gO4 (aa 30 – 457), the first 23, 30 and 29 amino acid residues (aa) of the wild type signal sequences were replaced with the 20 aa interleukin-2 (IL-2) signal peptide sequence, respectively. The gH insert sequence was further adapted by the deletion of the transmembrane domain (aa 719 - 737) and the cytoplasmic tail (aa 742 – 743). Insert sequences for gL, gO1c and gO4 were not further adapted. For the expression in human cells, the sequences for the gL and gO subunits and the gH subunit were optimized to human codon bias and cloned into the mammalian expression vectors pMT1 and pMT7, respectively (Synbio Technologies LLC) (Supplementary Figure S1 - Supplementary **Figure S4**). Both of the vector backbones contained a bacterial origin of replication and an ampicillin resistance gene. For the enhanced

protein expression in mammalian cells, the vectors provided the multiple cloning site (MCS) located downstream to a CMV promoter and upstream to a woodchuck hepatitis virus post-transcriptional regulatory element (WPRE). Additionally to that, the backbones contained an SV40 origin of replication, which allows for plasmid DNA replication and prolonged protein expression in cell lines that were stably transfected with the SV40 large T-antigen. The pMT7 vector additionally carried a cleavable C-terminal ten-fold histidine tag (10x his-tag) downstream to the MCS and an EF-1α-promoter-regulated GFP reporter gene for the control of the transfection efficiency. The insert sequences for the gL, gO1c and gO4 subunits were each cloned into a respective pMT1 vector in between the restriction sites EcoRI and AgeI. The adapted gH insert sequence was cloned into the pMT7 vector using the restriction sites EcoRI and ApaI, leading to a 13 aa insertion between the ApaI restriction site and the 10x his-tag. This insertion contains the TEV-cleavage sequence for the histidine tag, which is flanked by 3 aa on each side (G-S-S-TEV-K-S-S).

3.2.2 Transformation of E. Coli cells

DNA amplification was achieved through the transformation and cultivation of chemically competent One-Shot™ MAX Efficiency™ DH5α-T1^R cells, an adapted *Escherichia Coli* (E.Coli) strain that is resistant to infection with bacteriophage T1 and T5. If not mentioned otherwise, bacterial cells were cultivated upon antibiotic selection in Luria-Broth medium with 100 µg/mL ampicillin (LB-Amp) and incubated at 37°C shaking with 220 rotations per minute (rpm). The expression vectors, coding for gH1, gL, gO1c and gO4, were individually introduced into One-Shot™ MAX Efficiency™ DH5α-T1^R cells. According to manufacturer's instructions, aliquots DH5α cells were thawed on ice and further incubated with 20 – 40 ng plasmid DNA. During heat shock, the cells were exposed to 42°C for 30 seconds, put back on ice and resuspended in pre-warmed super optimal broth (SOC) medium. After that, cells were incubated for one hour at 37°C and 220 rpm. For the selection of successfully transfected cells, ten-fold and hundred-fold dilutions of the cultures were spread onto Luria broth (LB) agar supplemented with 100 µg/mL ampicillin (LB-Amp). The agar plates were incubated overnight at 37°C and checked the following day for well-spread colony growth. Picked colonies were used to inoculate mini cultures (4 mL) in fresh LB-Amp medium, which were incubated for 16 – 20 hours at 37°C and 220 rpm. The agar plates were sealed and stored at 4°C.

3.2.3 Plasmid DNA amplification

Amplification of plasmid DNA was achieved through cultivation of transformed DH5α-T1^R cells at larger scale. Therefore, incubated mini cultures with an optical density (OD) between two to four were used for 1:500 inoculation of midi cultures (200 mL) in LB-Amp medium. Midi cultures were also incubated for 16 – 20 hours at 37°C and 220 rpm. Extraction and purification of amplified plasmid DNA was performed under the use of the PureYield® Plasmid Midiprep system. To do so, midi cultures were centrifuged for ten minutes at 4°C and 5.000 relative centrifugal force (rcf). The cleared cell supernatant was discarded and according to manufacturers' instructions and upon application of the provided buffer systems, the cells were resuspended and lysed. The lysates were centrifuged for 15 minutes at room temperature and 15.000 rcf and later on filtered through a kit-supplied column stack, consisting of a clearing column and a DNA binding column. Upon the application of vacuum, the lysate was passed through both columns and the membrane-bound DNA was further washed with endotoxin-removal- and column wash solution. For removal of the solution-derived ethanol, the binding membrane was dried upon further application of vacuum and short incubation on a heat block at 50°C. The DNA binding column was transferred into a 50 mL conical tube and incubated for two minutes with pre-warmed nuclease-free water. The conical tubes were centrifuged for five minutes at room temperature and 2.000 rcf and the eluted DNA was transferred into sterile microcentrifuge tubes. DNA concentration was determined in duplicates through NanoDrop™ measurement.

3.2.4 Cell Culture

For the expression and testing of the trimeric gH/gL/gO complex, human embryonic kidney cells 293T (HEK293T) and human foreskin fibroblasts (HFF) were kept in culture. If not mentioned otherwise, HEK293T cells were cultivated within Gibco™ Dulbecco's minimum essential medium (DMEM) supplemented with 10% fetal bovine serum (FBS), 500 U/mL Penicillin, 500 µg/mL Streptomycin and 10 mM HEPES (DMEMc) and HFF cells were cultivated in minimum essential medium (MEM) supplemented with 10% FBS, 1% non-essential amino acids and 50 µg/mL Neomycin. The cells were incubated in a humidified atmosphere upon 37°C and 5% CO^2 air volume. HEK293T cells were thawed at the 7th passage, used for transfection experiments from the 10th passage and kept in culture until reaching the 30th passage. HFF were thawed at the 2nd passage, used for experiments from the 6th passage and were discarded after passing the 20th passage. Handling of cells was strictly carried out upon aseptic conditions.

3.2.5 Thawing of HEK293T cells and HFF

Frozen cell aliquots were recovered from liquid nitrogen and placed in a water bath at 37°C. Aliquots were thawed until almost no ice crystals remained and were then carefully transferred into a T25 cell culture dish pre-filled with 9 mL fresh medium. The cryo-tube was washed with 1 mL medium, which was later added to the culture. After 24 hours incubation, a complete medium exchange was done. In the first passage, cells were completely transferred to a T75 cell culture dish. After that, cells were passaged as described.

3.2.6 Passaging of HEK293T cells

HEK293T cells were frequently passaged twice a week, upon reaching a confluence of approximately 80%. Split rates of 1:10 and 1:20 were used for incubation periods of either three or four days. For passaging, the cell monolayer was washed once with PBS and once with 0.25% Trypsin-EDTA. Upon incubation with fresh 0.25% Trypsin-EDTA, cells detached from the treated surface and were then thoroughly resuspended in DMEMc medium. According to the split rate, a certain volume of the resuspended cells was transferred into a new cell culture dish pre-filled with fresh DMEMc medium. Scale switching was performed upon adaption of the transfer volume in consideration to the factorial change of the cultivation area.

3.2.7 Passaging of HFF

HFF cells were frequently passaged once a week with a split rate of 1:4. Additionally, half medium change was performed three days after passaging. During passaging, HFF were washed twice with PBS and once 1xTrypsin. Cell detachment was achieved upon incubation with fresh 1xTrypsin for five to seven minutes at 37°C. The detached cells were thoroughly resuspended within fresh MEM+/+ medium and transferred into a new cell culture flask with fresh medium. Scale switching was performed upon adaption of the transfer volume in consideration to the factorial change of the cultivation area.

3.2.8 Freezing of HEK293T cells and HFF

For storage in liquid nitrogen, cells were resuspended in fresh medium and live cell concentration was determined via cell counter. After five minutes of centrifugation at 4°C and 250 rcf, the pelleted cells were resuspended in freezing medium to a specific concentration. HEK293T cells were resuspended to a total concentration of 1×10^7 cells/mL in pre-cooled DMEMc supplemented with 10% DMSO. HFF cells were resuspended to a total concentration of 1×10^6 cells/mL in MEM+/+ supplemented with 10% DMSO. Aliquots of 1 mL were

transferred into cryotubes, then stored at -80°C for 24 - 72 hours and later transferred to a liquid nitrogen tank.

3.2.9 Transient transfection of HEK293T cells

Resuspended cells were counted via cell counter, seeded with a density of 1.6 - 1.7 x 10^5 cells/cm^2 and incubated overnight upon 37°C and 5% CO_2. The following day, monolayer confluence (70 – 80%) was controlled via light microscopy, supernatant was discarded and cells were covered with Gibco™ Opti-MEM medium. For liposomal-based transient cell transfection, plasmid DNA and Lipofectamine®2000 transfection reagent were separately prepared and incubated for 5 minutes at room temperature. Depending on the cultivation area, an amount of 0.33 µg/cm^2 DNA was diluted in a volume of 2.75 µL/cm^2 Gibco™ Opti-MEM medium. For the expression of the trimeric complex, this corresponded to a 1:1:1 ratio of 0.11 µg/cm^2 of the respective expression vectors gH, gL and gO. The Lipofectamine®2000 transfection reagent was prepared as 30% solution in the same volume using Gibco™ Opti-MEM medium. Both, the DNA and transfection reagent, were then carefully mixed and again incubated for 15 minutes at room temperature. The transfection mix was added dropwise, upon gentle swirling and incubated onto the cells for four to six hours at 37°C and 5% CO_2. Cells were washed with DMEM medium and again incubated with Gibco® Opti-Pro medium. After 5 days incubation, the supernatant was transferred into 50 mL conical tubes and centrifuged for 20 minutes at 4°C with 4200 rcf. The cleared supernatant was transferred into fresh 50 mL tubes and stored at -20°C.

3.2.10 Fluorescence Microscopy

At intervals of 24 hours, transfected HEK293T cells were checked for EGFP expression under a Leica DMi8 S inverted light microscope running on the related LAS X software. Photos were taken at a 10-fold magnification using an exposure time of 3.10 ms at an intensity of 230 for capture of the phase contrast and an exposure time of 200 ms and a fluorescence intensity of 100% for capture of fluorescence.

3.2.11 Vivoflow® sample concentration and buffer adaption

To prevent protein degradation, samples and used buffers were kept on ice throughout the whole purification process. Frozen supernatant was thawed overnight at 4°C and sterile filtrated through a 0.2 µm polyether sulfone (PES) membrane filter the next day. In preparation for affinity chromatography, the supernatant was ultra-filtrated through a Vivoflow®200 PES tangential flow filtration cassette, with a molecular weight cutoff (MWCO) of 100 kDa. Flow

rates and pressure limits were monitored according to manufacturer's instructions. After equilibration of the cassette with 1x FPLC sample buffer, the supernatant was pumped through the cassette in a loop until reaching a volume of approximately 150 - 200 mL. The concentrated supernatant was placed on ice, rebuffered through addition of 10x FPLC sample buffer and controlled for pH-adjustment. For the additional recovery of membrane-bound protein, the ultrafiltration step was repeated with 50 – 70 mL 1x FPLC sample buffer, which was later added to the concentrated supernatant to achieve a final volume of approximately 250 mL.

3.2.12 Fast Protein Liquid Chromatography

FPLC affinity chromatography was performed against the gH-conjugated 10x his-tag using a 5 mL HisTrap FF crude/ Ni-Sepharose fast flow column, connected to an ÄKTA™ pure 25L system. The recommended maximum pressure of 0.52 MPa and flow rate of 2 mL/min were not exceeded throughout the chromatography run and monitored together with other system parameters and the UV absorbance. Prior to sample load, the column was equilibrated with five column volumes FPLC wash buffer. The concentrated supernatant was administrated under the multiple use of a 50 mL Superloop. During the sample load and the following washing step, the flow through was collected, stored at 4°C and later controlled via western blot. After sample load, the column was washed with ten column volumes (CVs) FPLC wash buffer. Protein elution was performed under the use of FPLC elution buffer and monitored through measurement of the UV absorbance at 280 nm. During elution, fractions of 0.5 mL were collected until the UV absorbance returned to baseline. The collected fractions were stored overnight at 4°C.

3.2.13 Vivaspin® sample concentration and buffer exchange

The collected fractions derived from the FPLC were pooled and further processed with a Vivaspin®20 100,000 MWCO PES concentrator, which allows for simultaneous buffer exchange and concentration of the sample volume. According to manufacturers' instructions, the centrifugation was performed with a swing bucket at 3,000 rcf and 4°C. After two-fold equilibration of the PES membrane with phosphate-buffered saline (PBS), the protein sample was transferred into the devices' headpiece, complemented with PBS to a volume of 20 mL and concentrated to a volume of 0.5 – 1 mL. This process was repeated four times for a complete buffer exchange. During the last concentration step, the sample was concentrated to a volume of approximately 400 µL. The sample was recovered from the headpiece and placed on ice. The flow through from the respective centrifugation steps was collected and placed on ice for later control via western blot.

3.2.14 Size exclusion chromatography

Size exclusion chromatography was performed under the use of a Superdex®200 Increase 10/300 GL column connected to the ÄKTA™ pure 25L system. In order to not exceed the prescribed pressure limit of 3.5 MPa, flow rates were set between 0.5 – 0.75 mL/min depending on the used buffer system. Column equilibration was performed with two respective CVs of ddH_2O and PBS. The protein sample was applied under the use of a pre-equilibrated 500 µL sample loop, eluted upon a flow rate of 0.5 mL/min and collected in fractions of 0.5 mL. Protein elution was monitored via measurement of the UV-absorbance at 280 nm. Fraction collection was stopped after 1 CVs. The collected fractions were pooled according to UV-absorbance measurement and stored at 4°C.

3.2.15 Micro BCA™ protein concentration determination

Protein concentration was determined in a 96-well microplate format using the Micro BCA™ kit. Dilutions were prepared with PBS, using a four-fold serial dilution comprising factors from 1:5 to 1:40 for the unknown protein concentrations. Dilutions of the protein sample and the BSA reference were prepared with PBS and measured in duplicates. The respective protein samples, BSA references and blanks were analyzed using 100 µL per well, which were mixed with 100 µL of the kit-related working reagent. The samples were incubated for two hours at 37°C, equilibrated to room temperature and subsequently the colorimetric staining was measured at a wavelength of 562 nm and 630 nm. According to the BSA reference, concentrations were calculated for each dilution and upon exclusion of outlying values, average protein concentration was determined.

3.2.16 SDS-PAGE and Western Blot analysis

Protein samples for SDS-PAGE derived either directly from the cell supernatant of transfected HEK293T cells or from purified protein pools. For control via SDS-PAGE and Western Blot, recombinantly produced proteins from HEK293T-derived cell supernatant was precipitated via salt precipitation. Therefore, 1 mL cell supernatant was supplemented with 25 µL of a 5 M NaCl solution (end concentration of 62.5 mM) and mixed 1:1 with pure ethyl alcohol. After at least 24 hours incubation at 4°C, precipitated samples were centrifuged for ten minutes at 16.000 rcf and the supernatant was removed completely. The precipitated pellet was resuspended in 30 µL 2x sample buffer and dissolved for five minutes at 45°C shaking at 300 rpm. Samples derived from the purified protein pools were mixed 1:1 with 2x sample buffer. Protein expression of the trimeric complex was controlled with 4 – 15% gradient polyacrylamide gels. Prior to loading, reducing and non-reducing samples were incubated at ei-

ther 95°C or 70°C for five minutes and then centrifuged for one minute at 16.000 rcf. Electrophoresis ran for 30 minutes at 80 V and was later switched to 130 V until protein bands completely passed through the gel. For evaluation protein gels were either stained through incubation with PageBlue™ staining solution according to manufacturer's instructions or blotted onto a 0.2 µm polyvinylidene fluoride membrane (PVDF) under the use of the Trans-Blot® Turbo™ transfer system. Upon western blotting, the membranes were blocked for 1 hour with 5% bovine serum albumin (BSA) diluted in 0.05% TBS-T. Antibody dilutions were prepared as described with blocking buffer (see **Table 4** and **Table 5**). First, primary antibody was incubated overnight at 4°C. After five-fold washing for five minutes with TBS-T, the secondary antibody was incubated for 1 hour at room temperature and the membrane was washed again. Protein detection was performed upon incubation with SuperSignal® West Pico Plus chemiluminescence substrate and evaluation with the Invitrogen® iBright™ CL750 imaging system. Evaluated membranes were stored in TBS at 4°C.

3.2.17 Virus inhibition assay on HFF cells

HFF cells were seeded with 1 x 10^4 cells/well on 96-well microtiter assay plates (white, clear bottom) and incubated overnight at 37°C and 5% CO_2. Monolayer confluency was controlled via light microscopy the next day. Serial dilutions of soluble trimeric gH/gL/gO were prepared with Gibco™ Opti-MEM medium and incubated onto HFF cells with 50 µL/well for one hour at 4°C. Simultaneously, viral stocks of HCMV TB40-*BAC4-luc (GT1c)* with an multiplicity of infection (MOI) of 2.0 were prepared with MEM+/+ medium and incubated for one hour at 4°C. Cells were infected at a MOI of 1.0 by addition of 50 µL/well virus dilution. Virus incubation was done first for one hour at 4°C, followed by two hours incubation at 37°C and 5% CO_2. The supernatant was discarded, cells were washed twice with MEM+/+ medium and incubated with 100 µL/well MEM+/+ medium for 24 hours at 37°C and 5% CO_2. For cell lysis, 100 µL/well Steady-Glo® substrate buffer were added and incubated for five minutes at room temperature. Samples and controls were tested as duplicates. Controls were treated only with the respective medium used during each incubation step. HCMV infection and was determined via plate reader, measuring relative light units between wavelengths of 300 to 700 nm.

3.2.18 Enzyme-linked immunosorbent assay/ Inhibition assay

For competitive ELISA assays 100 ng of recombinant PDGFRα/CD140 diluted in carbonate-bicarbonate buffer was coated with 50 µL into each well of a 96-well polystyrene round bottom microwell plate and incubated overnight at 4°C. The next day, the plate was washed by

rinsing the wells four times with 200 µl ELISA wash buffer. Coated plates were blocked for one hour at 37°C with 200 µL ELISA blocking buffer per well. Parallel, serum samples were prepared as serial dilutions with 25 µL per dilution using ELISA dilution buffer. Each dilution was mixed with 25 µL of a 2 µg/mL soluble trimer solution also prepared with ELISA dilution buffer. The trimer-serum mix was incubated for one hour at 37°C, afterwards transferred onto the coated plate without prior washing and again incubated for one hour at 37°C. After trimer incubation, the plate was again washed and incubated for one hour at 37°C with 20 ng HRP-conjugated anti-6xHis antibody diluted in ELISA dilution buffer (**Table 6**). Plates were washed again and incubated for 25 minutes at room temperature with 50 µL 1-Step™ Ultra TMB-ELISA substrate solution per well. The substrate was inactivated with 50 µL 1M H_2SO_4 and absorbance was measured at 450 nm and 650 nm wavelength. The OD450 absorbance was reduced by the blank value and upon normalization to the average HCMV seronegative control, transformed into percent inhibition [Inhibition % = 1 – (blank OD sample/ blank OD average seronegative) x 100]. Serum samples were tested as duplicates together with corresponding controls. Using GraphPad Prism software, the dose-dependent binding inhibition was evaluated via non-linear regression analysis (log[inhibitor] vs. response – variable slope/ for parameters) with the serum dilution factor assigned as inhibitor.

4 Results

4.1 Production of soluble gH/gL/gO

4.1.1 Design of plasmid DNA

The trimeric glycoprotein complex gH/gL/gO is a membrane-anchored receptor binding protein that takes up an essential role during cell entry of HCMV. (Kaye, Gompels and Minson, 1992; Li, Nelson and Britt, 1997) It underlies a certain genetic diversity, mostly given by the highly polymorphic gO subunit, which has been described in eight different variants so far. (Paterson *et al.*, 2002; Rasmussen *et al.*, 2002)

For our investigation, we retrieved gene sequences for the gH1 (UL75, nt 109,603 – 111,834), gL (UL115, nt 165,366 – 166,202) and gO1c (UL74, nt 107,833 – 109,227) subunits derived from the TB40/E strain (NCBI refseq KF297339) and the gO4 subunit derived from the Towne strain (NCBI refseq FJ616285 nt 106,666 – 108,039), exhibiting sequence differences of approximately 22% at the amino acid level. (Kalser *et al.*, 2017) For the expression of soluble trimer, the mentioned sequences were adapted, so that the formed complex got secreted into the supernatant and could be harvested easily (Figure 6A). In the first instance, signal peptide sequences of the respective wild type genes were replaced with the 20 aa Interleukin-2 (IL-2) signal peptide sequence (MYRMQLLSCIALSLALVTNS) (Figure 6B). Thus, for the peptide sequences of the subunits gH1, gL, gO1c and gO4, the first 23, 30, 29 and 29 amino acid residues were replaced, respectively. To avoid the incorporation into the lipid membrane, the gH-associated transmembrane domain (aa 719 – 732) and the relatively short cytoplasmic tail (aa 742 -743) were removed (Figure 6C, red letters). Using an online gene synthesis tool, the adapted gene sequences were codon optimized to human codon bias and ordered in the form of fully cloned constructs for the later expression in Human embryonic kidney 293T cells (HEK293T).

The gH1 gene insert (IL-2_gH1 aa 24 - 718) was cloned into mammalian expression vector pMT7 (Synbio Technologies) using the restriction sites EcoRI and ApaI. Gene inserts for gL (IL-2_gL aa 31 – 278), gO1c (IL-2_gO1c aa 30 – 464) and gO4 (IL-2_gO4 aa 30 – 457) were each cloned into the mammalian expression vector pMT1 (Synbio Technologies) using the restriction sites EcoRI and AgeI (Supplementary Figure S1 - S4). Both expression vectors offer a CMV promoter and a woodchuck hepatitis virus posttranscriptional regulatory element (WPRE) located upstream and downstream of the multiple cloning site (MCS), respectively. For the selective DNA amplification in bacterial cells, the vectors provided a bacterial origin of replication and an ampicillin resistance. Additionally, a SV40 origin of replication allowed for plasmid DNA replication and prolonged protein expression in HEK293T cells, stably expressing the SV40 large T-antigen. In consideration to the protein expression and purification

the pMT7 vector further featured a separately expressed EGFP reporter gene for the control of the transfection efficiency and a C-terminal ten-fold histidine tag (his-tag) downstream to the MCS allowing. The 13 aa linker sequence between the ApaI restriction site and the C-terminal 10-fold his-tag additionally contained a Tobacco Etch Virus (TEV) cleavage site (ENLYFQS) for posttranslational removal of protein tags.

As the wildtype form of the trimeric complex is formed in the ER and transferred to the cell membrane via the secretory pathway, prior to virus shedding, we considered that these changes would lead to an increased expression of a soluble form of the trimeric complex, which was still formed and modified in the ER but finally secreted into the cell supernatant via the secretory pathway. (Huber and Compton, 1999)

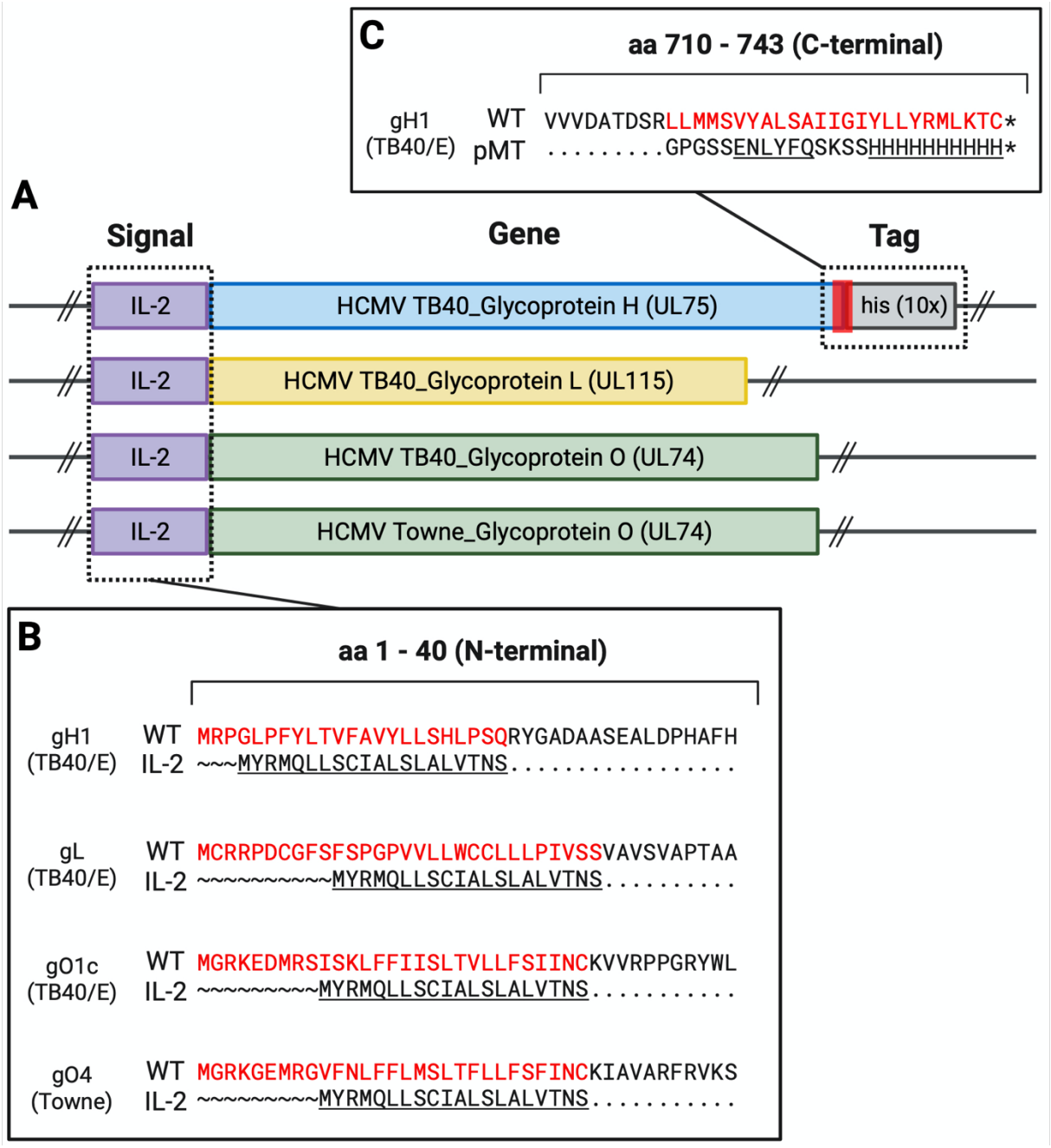

Figure 6: Gene structure of the subunits of the trimeric complex gH/gL/gO according to the described changes. (A) *Schematics representing the protein domains of the subunits gH1 (blue), gL (yellow), gO1c and gO4 (green).* ***(B)*** *The N-terminal aa sequences positions 1 – 40 are indicated for the respective subunits. The individual WT signal peptides (red) were replaced with the 20 aa IL-2 signal peptide (MYRMQLLSCIALSLALVTNS) to facilitate directed localization of the subunits and secretion of the formed trimeric complex.* ***(C)*** *The C-terminal transmembrane domain and cytoplasmic tail (aa 719 – 743) of the gH subunit were replaced with a TEV-containing linker sequence and a ten-fold histidine-tag to promote secretion and purification of the trimeric complex.*

4.1.2 Expression of soluble gH1/gL/gO1c and gH1/gL/gO4

Prior to high scale production and purification, we conducted transfection experiments to see if our DNA constructs would lead to the successful expression of the different variants of our soluble gH/gL/gO complex. Therefore, we cultivated HEK293T and transfected them with different plasmid combinations in order to produce gH1/gL/gO1c and gH1/gL/gO4, respectively. Additionally, we conducted a control expression lacking the gO subunit, using gH1/gL only, and a cell culture control. Transfection experiments were conducted in duplicates in at least three independent transfection experiments.

Images were taken at intervals of 24 hours, to control the pMT7-mediated EGFP-expression over a time span of six days (144h) (Figure 7A). For all transfection experiments, except for the cell culture control (CC), EGFP expression was firstly controlled at 24 hours post transfection (hpt) and detectable up to 144 hpt. Visual comparison of the EGFP-signal showed similar intensity and transfection efficiency between the different plasmid combinations throughout the incubation period of 144 hours. The cell control (CC) received treatment with the transfection reagent only and showed no EGFP expression.

Due to the added IL-2 signal peptide and the deletion of the gH transmembrane domain, successfully assembled trimeric complex should be secreted into the supernatant. For this reason, we harvested the supernatant at 144 hpt and controlled protein secretion from precipitated supernatant samples via western blot using gH- and gO-specific antibodies (Figure 7B). Comparison of the gH- and gO-specific protein detection revealed clear protein bands for the detected subunits incorporated into the trimeric gH1/gL/gO1c and gH1/gL/gO4 complex at approximately 270 kDa. The supernatant derived from transfections with gH1/gL/gO4 exhibited an intense protein band for both, gH- and gO-specific detections. Transfections performed with gH1/gL/gO1c exhibited only weak protein bands for both detections, suggesting only little protein yields of gH1/gL/gO1c in the supernatant. Interestingly, gH1/gL transfections also led to the detection of a weak protein band migrating slightly below trimeric gH/gL/gO complexes, which only showed upon detection with the gH-, but not with the gO-specific antibody. For the cell control neither any gH- nor gO-related protein species was found. From these results, we concluded that transfection of HEK293T cells with our specifically designed DNA constructs enables the expression and secretion of soluble gH1/gL/gO4. Compared to that, the use the gO1c subunit showed hardly any presence of gH1/gL/gO1c within the supernatant, implying insufficient production or secretion of the complex. As for the gH1/gL-transfection, we conclude that due to the exclusive detection with the gH-specific mAb and the migration pattern similar to that of trimeric gH/gL/gO, the detected protein band represented the production and secretion of gH/gL-homodimer (gH/gL-gL/gH), which formed upon the absence of the gO subunit.

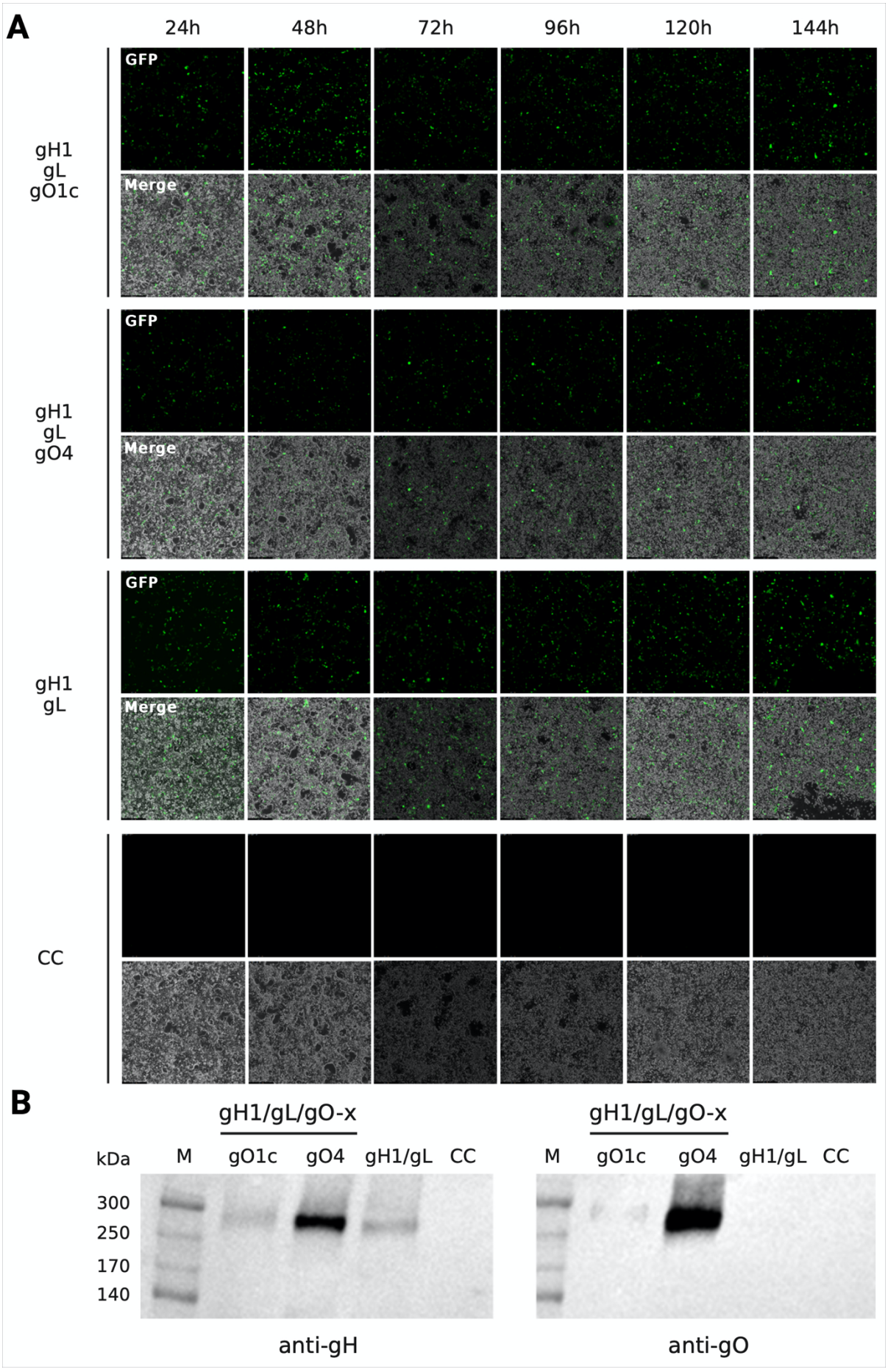
A
24h
48h
72h
96h
120h
144h
gH1
gL
gO1c
GFP
Merge
gH1
gL
gO4
GFP
Merge
gH1
gL
GFP
Merge
CC
B
gH1/gL/gO-x
gH1/gL/gO-x
kDa
M
gO1c
gO4
gH1/gL
CC
M
gO1c
gO4
gH1/gL
CC
300
250
170
140
anti-gH
anti-gO

Figure 7: Expression of soluble gH1/gL/gO1c and gH/gL/gO4. (A) *HEK293T cells were transfected with DNA constructs expressing gH1, gL (TB40/E) and different gO1c/ gO4 genotypes (TB40/E and Towne). The images represent a single transfection experiment displaying cells from the same wells in approximately the same spots captured at intervals of 24 hours until harvest after 144 hours. Cells are represented upon the fluorescence, phase contrast and the merge of both channels.* ***(B)*** *Western Blot analysis of precipitated supernatant samples (at 144h) using gH- and gO-specific mAbs upon non-reducing conditions. gO1c…subunit derived from HCMV TB40/E genotype, gO4 …subunit derived from HCMV Towne genotype, M, Marker; gH1/gL/gO-x, gO-genotype co-transfected with gH1 and gL; CC, Control culture treated with the transfection reagent only;*

4.1.3 Purification and characterization of soluble gH/gL/gO

From the results gained from test expression we decided to continue with the high-scale production of soluble gH1/gL/gO4 (hereinafter referred to as gH/gL/gO). Supernatant derived from seven independent transfection experiments was temporarily stored and controlled for trimer expression via western blot using anti-his mAb, detecting the his-tagged gH subunit at approximately 270 kDa (Supplementary Figure S5). Western blot analysis revealed that transfected cells that reached confluence at 24 hours after cell seed (T24, T27, T28, T29 and T30) produced more protein, than cells that reached confluence 48h after seeding (T23 and T25).

Making use of the properties of our soluble gH/gL/gO, we set up a two-step purification protocol starting with affinity chromatography for the gH his-tag, followed by size exclusion chromatography separating proteins by their molecular size. The collected volume of approximately 1.2 L cell supernatant was first concentrated and then applied to a Ni^{2+}-sepharose column, in order to sort out unspecific protein species within the supernatant. Absorbance measurement (280 nm) upon detachment from the column showed the elution his-tagged protein species between 1.5 – 10 mL. The measured peak reached a maximum absorbance of approximately 250 mAU between 4 – 5 mL (Figure 8A). In order to sort out possibly formed gH/gL-homodimer and other unspecific histidine-tagged or histidine-rich protein species, a further purification step was conducted.

Size exclusion chromatography (SEC) columns contain a dextran-agarose composite matrix utilizing small porous beads that can separate proteins according to their size. Whilst large proteins hardly diffuse through the pores, and thus elute early, smaller proteins diffuse easier through the pores and therefore take up more time for elution. (Cutler, 1996) Prior to protein purification, column calibration with a high molecular weight protein standard, allowed for approximation of an elution volume of 10.3 – 12.4 mL for proteins with a molecular mass between 440 – 158 kDa. (Supplementary Figure S6 and Supplementary Figure S7).

Fractions derived from His-affinity purification were pooled, concentrated and loaded onto a Superdex 200 Increase 10/300 GL column with a separation range of 600 – 10 kDa. Absorb-

ance measurement at 280 nm showed the detection of four sequential and overlapping peaks, eluting between 7 – 18 mL (Figure 8B and Figure 8C). The first peak reached a maximum absorbance of approximately 105 mAU at 8.5 mL and transitioned directly into the second peak with a maximum absorbance of approximately 60 mAU at approximately 10 mL. The third and fourth peak shared a similar maximum absorbance of approximately 35 mAU at 12 mL and 13.5 mL respectively. While the first and second peak were overlapping, the third and fourth peak showed slightly higher resolutions. The detected proteins were collected in fractions of 0.5 mL, which were further pooled according to the detected peaks (dashed frames 1 - 6; Figure 8C). The single fraction between peak 1 and peak 2 as well as peak 2 and peak 3 were not included into fraction pools since they cover the peak overlaps. Western Blot analysis, using his- and gO-specific mAbs, revealed broad elution of the trimeric complex between 7.5 – 12.5 mL. Hence, most of the trimeric complex eluted among pool one, pool two and the fraction in between, which comprise the first two peaks of the chromatogram. Surprisingly, smaller unspecific his-related proteins were not detected in the later fractions 4, 5 and 6 upon detection with his-specific mAb (Supplementary Figure S8). Due to the unclear separation of the trimeric complex on the chromatogram and the expected elution volume from the column calibration, purified gH/gL/gO derived from peak 2 was further investigated (red dashed frame/ pool 3; Figure 8C).

The purified fraction of the trimeric complex was characterized by determination of the protein concentration and analysis via SDS-PAGE and western blot. Concentration determination yielded in a total protein mass of approximately 290 µg soluble gH/gL/gO obtained from 1.2 L supernatant. Further SDS-PAGE and western blot analysis using his-, gH- and gO-specific mAbs revealed the trimer-specific protein band at approximately 270 kDa upon non-reducing conditions. Upon reducing conditions, the gH subunit migrated at approximately 100 kDa. The gO subunit migrated slightly above gH subunit at approximately 140 kDa (Figure 8D). The polyacrylamide gel upon reducing conditions, exhibited the gH and gO subunits and further the gL subunit at 30 kDa (red frames; Figure 8D). Weak protein bands of unspecific protein species were found upon non-reducing conditions at approximately 170, 60, and 40 kDa as well as 60, 45 and 40 kDa upon reducing conditions. Protein bands at the same height as the individual subunits of the trimeric complex were assumed to be products of protein degradation.

Studies have already demonstrated the trimer-mediated inhibition of HCMV entry into HFF, ARPE and also HUVEC cells. (Liu *et al.*, 2018) Since we were able to produce and purify soluble gH/gL/gO, functional testing by successful binding to PDGFRα and inhibition of HCMV infection marked the next step. Due to the restricted amount of purified trimer and the essential role of the trimeric complex for fibroblast infection, the virus neutralization was sole-

ly performed on HFF cells. Therefore, we first incubated HFF cells with serially diluted gH/gL/gO, starting at concentrations of 20 µg/mL, and followingly infected them with a BAC-derived HCMV TB40/E clone at an MOI of 1.0. Through a virus-incorporated luciferase reporter gene, expressed upon activation of the immediate early (IE) gene cascade, HFF infection could be measured. In order to exclude any buffer-related inhibition effects, an infection control using PBS dilutions of the corresponding protein dilutions (starting at a 7.3-fold dilution), was simultaneously tested on HFF cells. Similar to published data, soluble gH/gL/gO caused dose-dependent inhibition of HCMV infection in HFF cells, showing almost complete inhibition at concentrations of 10 µg /mL. (Liu *et al.*, 2018) Inhibitory concentrations of 50% (IC50) and 90% (IC90) were determined with 261 ng/mL and 4.59 µg/mL, respectively. PBS dilutions exhibited an average luciferase signal similar to the infection control (tick on y-axis; Figure 8E). This supported that purified soluble gH/gL/gO could successfully inhibit HCMV infection by functional binding and occupation of cellular PDGFRα.

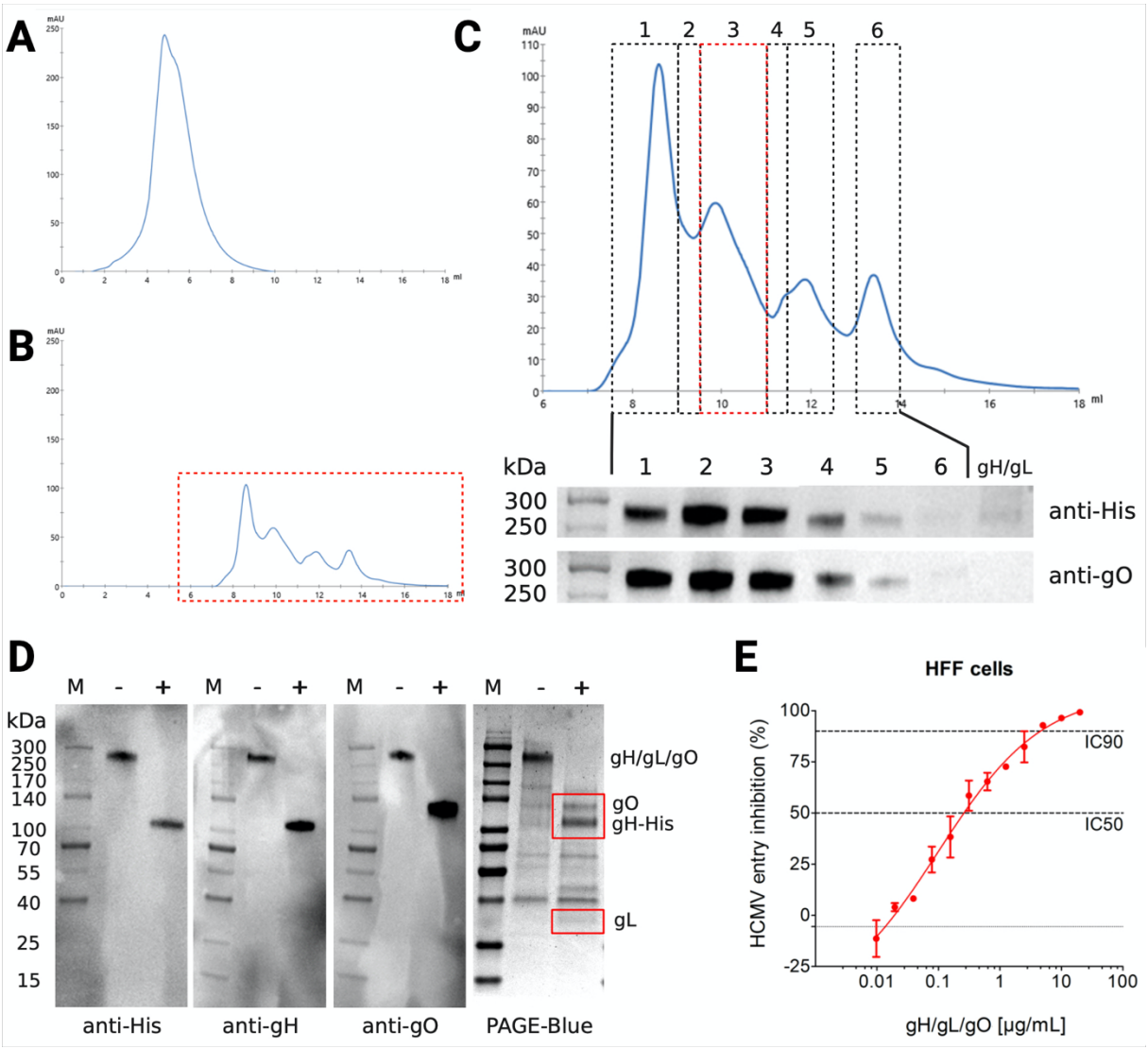

Figure 8: Purification and characterization of soluble trimeric gH/gL/gO. (A) *His-affinity purification of concentrated supernatant using a Ni2+ Sepharose matrix. Protein elution was monitored via UV-absorbance measurement at 280 nm. Fractions of 0.5 mL were collected and pooled according to the measured peak.* ***(B)*** *His-purified protein was again concentrated and separated through size exclusion chromatography. Protein elution was monitored via UV-absorbance measurement at 280 nm.* ***(C)*** *Magnification of SEC chromatogram (red dashed frame; Fig. 4B). Single fractions and pools, according to the dashed frames, were controlled via western blot using his- and gO-specific mAbs. Precipitated SN of a gH/gL-transfection was loaded as control for gO-mAb specificity.* ***(D)*** *Purified gH/gL/gO derived from SEC peak 2 (red dashed frame; Fig. 4C) was further characterized via Micro BCA assay, SDS-PAGE and western blot using anti-His, anti-gH and anti-gO mAbs. Subunits of the trimeric gH/gL/gO complex are marked in the SDS-PAGE (red frames; Fig. 4D).* ***(E)*** *HCMV inhibition assay. HFF cells treated with soluble gH/gL/gO (starting with 20 µg/mL) were infected with BAC-derived HCMV TB40/E (luciferase clone) at MOI of 1.0. Luciferase activity was measured 24 hpi. The grey line marks the buffer control of the inhibition assay. M, protein marker; +/-, reducing/ non-reducing conditions of sample buffer; IC, Inhibitory concentration of a certain percentage of inhibition;*

4.2 Detection of inhibitory antibodies against gH/gL/gO in human serum

4.2.1 Establishment of a PDGFRα receptor-binding assay

Treatment of HCMV virions with soluble PDGFRα as well as treatment of target cells with soluble gH/gL/gO, was shown to inhibit the infection of fibroblasts, endothelial and epithelial cells, highlighting the essential role of the trimeric complex for infection. (Stegmann *et al.*, 2017) Particularly for fibroblasts, PDFGRα was shown to be the interacting ligand for the trimeric complex. (Kabanova *et al.*, 2016; Wu *et al.*, 2017; Kschonsak *et al.*, 2021) Taking a closer look at this interaction, we utilized our in-house generated trimer for the establishment of an ELISA-based receptor binding assay. In concept, recombinant human PDGFRα was immobilized to an untreated round-bottom polystyrene surface and soluble gH/gL/gO bound via its gO-located binding side. In the next step, receptor-bound trimer was detected via horseradish peroxidase-conjugated (HRP) mAb binding to the histidine-tagged gH subunit. Successful binding of the soluble trimer was quantified on the basis of the 3, 3', 5, 5'-Tetramethylbenzidine-mediated (TMB) colorimetric reaction catalyzed by the HRP. (Figure 9A).

To define the detection range of our receptor binding assay, we coated rec. hPDGFRα at amounts of 6.25, 12.5, 25 and 50 ng, tested them with a respective amount of 12.5, 25, 50 and 100 ng of soluble gH/gL/gO and detected bound trimer with HRP-conjugated anti-his mAb at an amount of 50 ng (yellow, red, purple and green dashed lines; Figure 9B). The absorbance (OD_{450}) steadily increased with the amount of PDGFRα coated. Independent from the amount of PDGFRα coated, the absorbance remained nearly constant upon an amount of at least 50 ng of soluble trimer. The highest absorbance was measured upon PDGFRα coating with 50 ng. In the next step, PDGFRα coating of 50, 100 and 150 ng was tested with equivalent amounts of soluble gH/gL/gO and detected with an adjusted amount of 10 ng HRP-conjugated his-specific mAb. (solid orange, blue and black line; Figure 9B) Upon reduced antibody concentrations, the combination of 50 ng PDGFRα coating with 50 and 100 ng soluble trimer, resulted in similar absorbance when detected upon increased mAb concentrations (solid orange and dashed green line; Figure 9B). Compared to coating with 50 ng PDGFRα, coating with 100 and 150 ng exhibited only slightly increased absorbance upon binding of 50 and 100 ng soluble trimer. For all of the tested amounts of PDGFRα coating (50, 100 and 150 ng) a respective amount of 150 ng soluble trimer led to a decreased absorbance than detected with the previous trimer concentration. Binding of soluble gH/gL/gO upon the lack of PDGFRα coating and detection with his-specific mAb at 50 and 10 ng, resulted in absorbance below the specificity threshold at any of the given trimer concentrations.

Due to the represented data and the following analysis of human sera, we set-up a standard protocol using excess amounts of the coating protein and the detection antibody. This protocol comprises coating of PDGFRα with 100 ng, binding of soluble gH/gL/gO with 50 ng and detection 20 ng HRP-conjugated his-specific mAb.

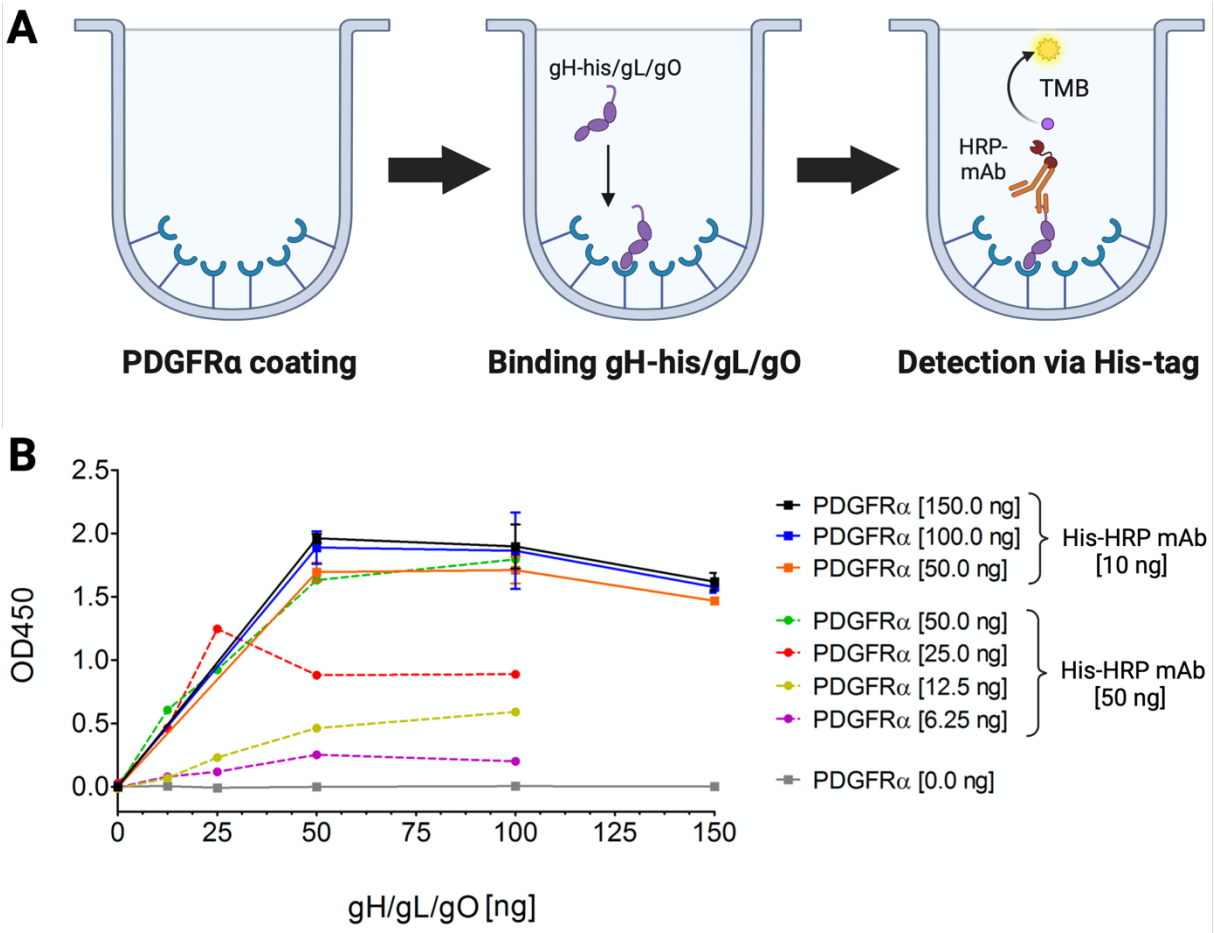

Figure 9: Establishment of a PDGFRα receptor-binding assay. (A) *Schematic representation of the developed PDGFRα-gH/gL/gO binding assay. Recombinant hPDGFRα was immobilized to an untreated polystyrene surface and later exposed to soluble gH/gL/gO. Bound gH/gL/gO was detected with HRP-conjugated anti-His mAb.* ***(B)*** *Different amounts of the coating and binding proteins, rec. hPDGFRα and soluble gH/gL/gO, were tested and detected upon the use of different concentrations of HRP-conjugated his-specific mAb, respectively. PDGFRα, Platelet-derived growth factor receptor alpha; HRP, horseradish peroxidase; TMB, 3, 3', 5, 5'-Tetramethylbenzidine; mAb, monoclonal antibody;*

4.2.2 Serum antibody-mediated inhibition of gH/gL/gO receptor binding

Viral envelope glycoproteins usually represent the primary and most effective docking site for neutralizing antibodies and therefore play an important role for the humoral immune response of the adaptive immune system. Despite the essential role of the trimeric gH/gL/gO complex for the infection of fibroblasts, epithelial cells and endothelial cells, there are only

few reports regarding the antibody-driven immune response against the whole trimer and the gO subunit in particular. (Wille *et al.*, 2010; Zhou, Lanchy and Ryckman, 2015; Gerna *et al.*, 2016; Liu *et al.*, 2018) A recently published study, reported about an gO-specific neutralizing antibody that is considered an elite neutralizer, since it serves as strain-overlapping inhibitor of HCMV infection in trimer-associated target cells. (Zehner *et al.*, 2023)

In 2020, Tan and Chia et al. were the first to describe a surrogate virus neutralization test (sVNT) based on SARS-CoV-2, that specifically detected serum-derived neutralizing antibodies (nAbs) and in contrast to traditional neutralization tests, did not require the use of infectious pathogens and handling upon strict biosafety levels. (Tan *et al.*, 2020) In accordance to this simplified neutralization assay, we adapted the protocol of our in-house generated receptor binding assay by a preceding step, during which soluble gH/gL/gO is preincubated with serially diluted human serum prior to addition to immobilized PDGFRα. During this step, serum-derived inhibitory antibodies are able to bind the trimeric complex and inhibit receptor binding. Thus, the absence of the colorimetric reaction caused by detection of receptor-bound trimer indicates the presence of inhibitory antibodies (iAbs) (Figure 10).

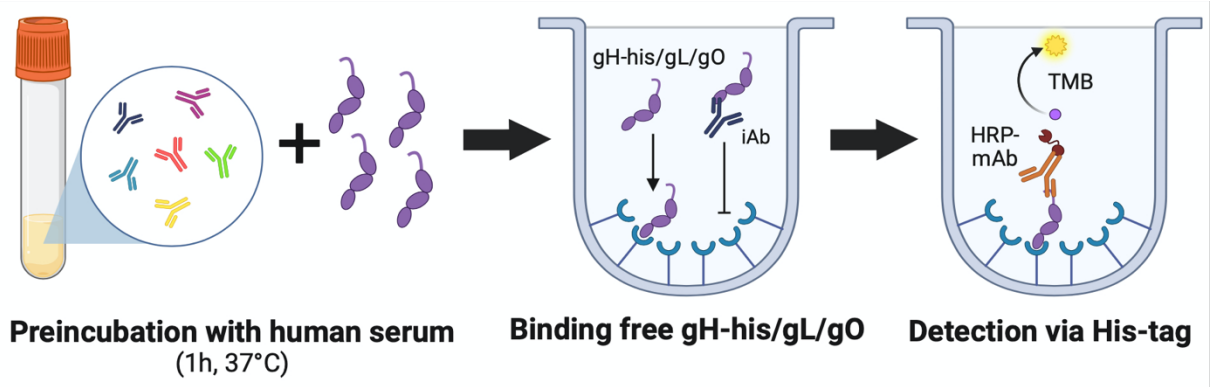

Figure 10: Serum antibody-mediated binding Inhibition of soluble gH/gL/gO to PDGFRα. *Prior to the addition to the PDGFRα-coated surface, serial dilutions of human sera were preincubated with soluble gH/gL/gO. Receptor-bound gH/gL/gO was detected with HRP-conjugated anti-His mAb, whereas iAb-bound gH/gL/gO would not be able to bind to the coated PDGFRα. PDGFRα, Platelet-derived growth factor receptor alpha; iAb, inhibitory antibody; HRP, horseradish peroxidase; TMB, 3, 3', 5, 5'-Tetramethylbenzidine; mAb, monoclonal antibody;*

In order to subject our receptor-binding assay and determine its specificity and sensitivity, we obtained sera derived from 21 healthy individuals, taken in the course of TBE- and HBV-specific antibody titer determination. The samples were retested for HCMV-specific IgG titers and thereby assigned into two groups.

HCMV seropositive individuals (n = 9) exhibited HCMV-specific IgG antibody concentrations above the assay-related detection limit (≥200 RU/mL; Figure 11A), indicating infection far back in time. HCMV-specific IgG antibody concentrations below the cutoff range of ≤20

RU/mL (grey area; Figure 11A) were assigned as HCMV seronegative individuals (1.99 – 4.74 RU/mL), which had not experienced a HCMV infection so far. As inhibition control, soluble gH/gL/gO was preincubated with Cytotect®CP (Biotest), an HCMV-specific IgG antibody preparation with a concentration of 50 mg/mL, which is used for the treatment and prevention of HCMV infection and reactivation. (Alsuliman *et al.*, 2018) HCMV seropositive sera and the Cytotect®CP control were tested in form of a two-fold serial dilution, ranging from four- to 512-fold dilutions. Due to the lack of HCMV-specific IgG antibodies, seronegative-defined sera were tested at higher serum concentrations only, using a range of four- to 32-fold dilutions. The Cytotect®CP inhibition-control and HCMV seropositive individuals, exhibited binding inhibition in a dose-dependent manner (Figure 11C). Thereby, not all individuals reached a total inhibition and showed different inhibition efficiencies, given by the varying inhibitory concentrations of 50% (IC50). The seronegative samples in contrast, showed no inhibition (Figure 11B). Compared to the IC50 of the Cytotect®CP control (52.5 -fold dilution), three seropositive samples exhibited higher IC50 values, indicated higher inhibition efficiency (Figure 11D).

With this initial analysis, we demonstrated the functionality of gH/gL/gO-inhibitory assay as well as the inhibitory effect, exclusively mediated by highly seropositive serum samples, which is most likely attributed to the presence of inhibitory antibodies in the human sera.

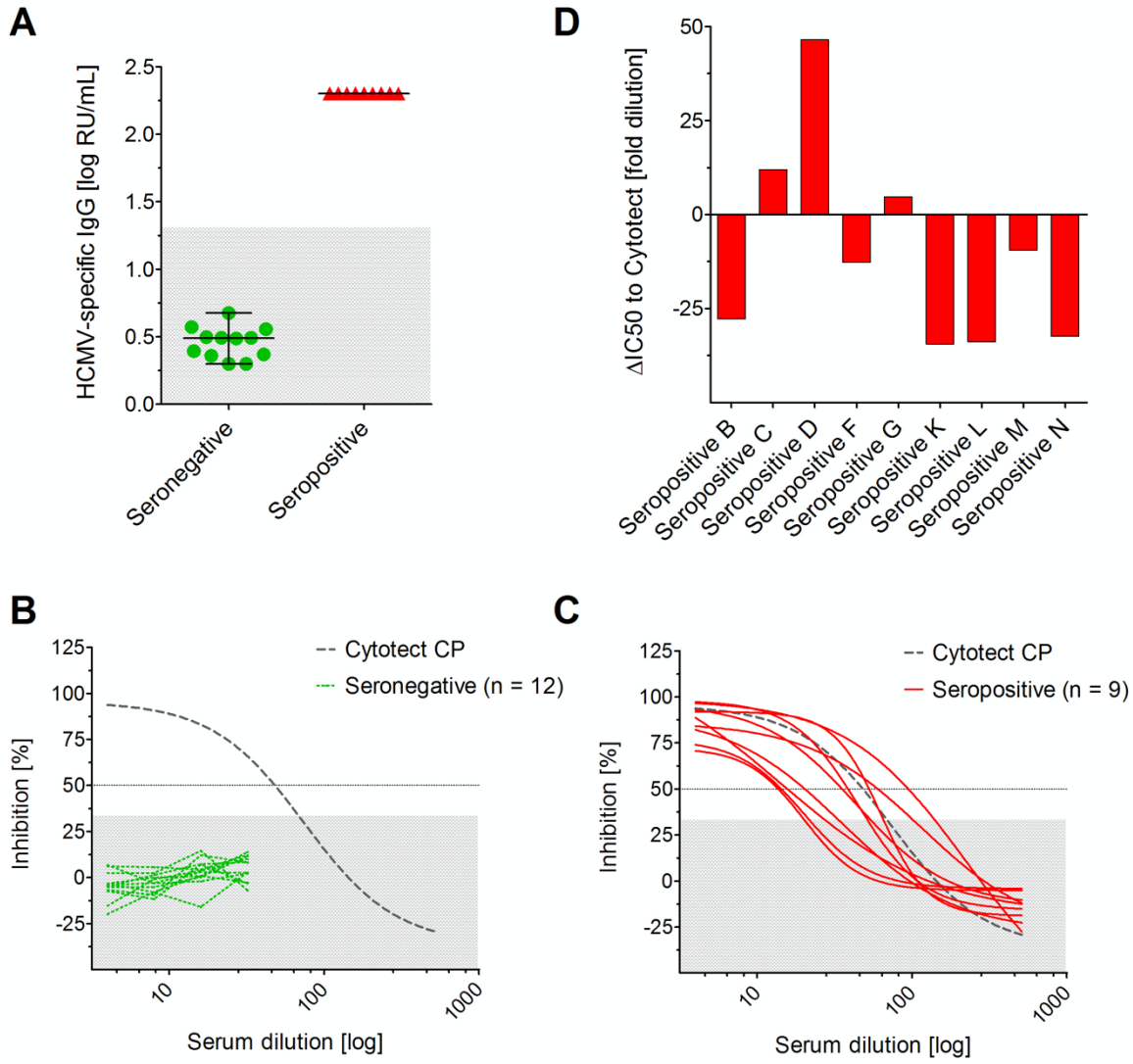

Figure 11: Comparison of serum antibody-mediated binding inhibition of gH/gL/gO to PDGFRα between HCMV seropositive and seronegative samples as well as Cytotect®CP. ***(A)*** *HCMV IgG antibody concentrations within serum samples were determined upon use of Euroimmun Cytomegalovirus IgG ELISA-test kit (EI 2570-9601 G). Comparison of the different serum samples showed that antibody concentrations in seronegative samples did not exceed the cutoff range (grey area), whereas seropositive samples (red) revealed antibody concentrations above the detection limit.* ***(B and C)*** *Serum antibody-mediated binding inhibition by seronegative samples (n = 12) as well as seropositive samples (n = 9) and Cytotect®CP (black dashed) were tested in form of two-fold serial dilutions, ranging from 4 – 32-fold and 4 – 512-fold dilutions, respectively. Serum samples that exhibited dose-dependent inhibition are represented in form of a dose-response curve (variable slope) generated via non-linear regression analysis using GraphPad Prism software. The inhibitory concentration of 50% (IC50; dashed line) and the inhibition cutoff (∅ seronegative + 3x SD) are indicated (grey area).* ***(D)*** *Delta of the IC50 of HCMV seropositive individuals in reference to the Cytotect®CP inhibition control.*

The early recognition of a primary HCMV infection plays an essential role for the treatment and monitoring, especially in the course of pregnancy. The current gold standard for the dif-

ferentiation between a recent and past HCMV infection relies on the determination of the HCMV-specific IgG antibody avidity, which usually matures in a course between three to six months after primary infection, but shows individual maturation-rates for HCMV-specific antibodies. Moreover, high IgG avidity has been shown to correlate with high neutralization efficiency. (Boppana and Britt, 1995).

Here we wanted to see, if our in-house generated gH/gL/gO inhibition assay was consistent with the literature and could detect differences in the inhibition efficiency between sera of high and low HCMV-specific IgG avidity. Therefore we tested a cohort comprising a total of 20 serum samples derived from healthy and HCMV seropositive individuals. Prior determination of the avidity index (AI) led to the further differentiation of the cohort into ten high avid and ten low avid serum samples. Comparison of the HCMV-specific IgG concentrations between low AI (66 – 190 RU/mL, Median 112) and high AI individuals (96 – 191 RU/mL, Median 147.5) showed no significant difference between the two groups. (Figure 12A). Serum samples assigned with high AI as well as samples assigned with low AI, and the Cytotect®CP control, were tested in two-fold serial dilution, ranging from four- to 512-fold dilutions. Similar to HCMV seropositive sera from prior observation, all HCMV seropositive individuals with high AI exhibited binding inhibition in a dose dependent manner. (Figure 12C) Similarly, the observed inhibition efficiency between individuals differed, as seen on the basis of the total inhibition and the compared IC50 (Figure 12D). The Cytotect®CP inhibition control, again revealed an inhibition efficiency between those of high avid individuals (Figure 12C).

With these results, we showed again that serum-mediated binding inhibition of the HCMV gH/gL/gO complex to PDGFRα receptor exists in HCMV infected individuals. Moreover, we observed that this inhibitory response depends on the IgG antibody avidity, implying that related iAbs arise in the course of antibody affinity maturation.

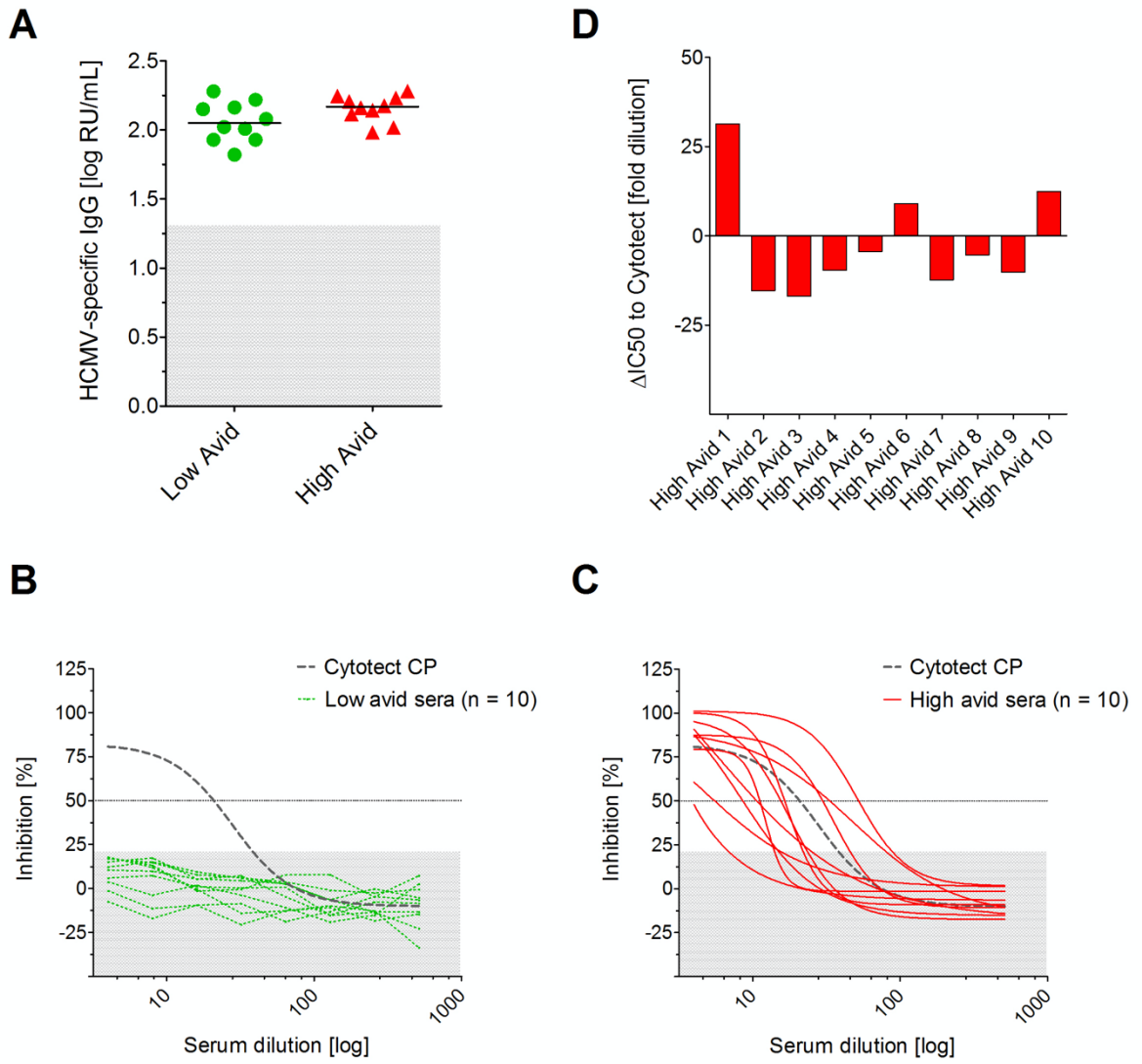

Figure 12: Comparison of serum antibody-mediated binding inhibition of gH/gL/gO to PDGFRα between HCMV seropositive individuals of low and high HCMV-specific IgG avidity index and Cytotect®CP. (A) *HCMV IgG antibody concentrations within serum samples were determined upon use of Euroimmun Cytomegalovirus IgG ELISA-test kit (EI 2570-9601 G). Comparison of the different serum samples showed that antibody concentrations in samples of low avidity (green) as well as high avidity (red) samples were similarly distributed above the cutoff range (grey area).* ***(B and C)*** *Serum antibody-mediated binding inhibition by low avid sera (n = 10), high avid sera (n = 10) and Cytotect®CP (black dashed) were tested in a two-fold serial dilution, ranging from 4 – 512-fold dilutions. Serum samples that exhibited dose-dependent inhibition are represented in form of a dose-response curve (variable slope) generated via non-linear regression analysis using GraphPad Prism software. The inhibitory concentration of 50% (IC50; dashed line) and the inhibition cutoff (∅ seronegative + 3x SD) are indicated (grey area).* ***(D)*** *Difference of the IC50 of HCMV IgG high avidity sera compared to Cytotect®CP.*

4.2.3 Retrospective detection of inhibitory antibodies upon IgG avidity maturation

Antibody avidity is the measurable overall binding strength of antibodies that individually increases in the course of antibody affinity maturation within the first four to six months after primary infection. (Eisen and Siskind, 1964; Blank, Leslie and Clem, 1972) Conventional assays distinguish between a low avidity index and a high avidity index, but leave out an undefined threshold range in between, which in the following is referred to as intermediate avidity. (Bodéus, Feyder and Goubau, 1998; Prince and Lapé-Nixon, 2014) Due to the correlation between high neutralization efficiency and high avidity, this threshold range remains elusive for the predictive protection from vertical transmission provided by maternal antibodies during pregnancy. (Boppana and Britt, 1995) Since our data indicates that gH/gL/gO-specific iAbs against receptor binding emerge late after primary infection, upon high IgG avidity, we wondered if our assay could further be utilized to track down the generation of those antibodies and narrow down the threshold range between the low and high avidity index.

For this pilot study, we retrospectively analyzed up to four sequential serum samples from six different patients that were assigned with either low (n = 4) or intermediate (n = 2) avidity index at a specific point in time (t_0). Patients were considered as healthy, since they did not suffer from any immunocompromising illness. Additionally to the sequential serum samples of each patient, a Cytotect®CP control was tested in a four- to 512-fold serial dilution. Of note, absorbance measurement onwards from the 32-fold dilutions of serum samples and Cytotect®CP exhibited higher signaling than the binding controls (HCMV seronegative control and binding control). Due to the insufficient signaling from the positive binding control, the calculated inhibition also covered values within the advanced negative range, which still allowed for a clear interpretation of true inhibition, but not for an exact comparison of the inhibition efficiency (Supplementary Figure S9 and Supplementary Figure S10).

Patients A – D provided sequential serum samples that allowed for a follow-up on IgG avidity maturation from low avidity to either intermediate or high avidity, covering an overall time span of 59 weeks (Figure 13). The results on the binding inhibition, gained from the individual serum samples, was further compared to data regarding HCMV-specific IgG avidity, IgM and IgG titers in order to identify certain factors involved into the generation of iAbs (Table 10).

Investigation of the IgG avidity maturation in patient A comprised a period of 55 weeks, with serum samples tested at three weeks prior as well as 36, 49 and 52 weeks after t_0. By week 36, the HCMV-specific IgG avidity index had shifted from low to high IgG avidity and the HCMV-specific IgM concentrations decreased below the detection point (Patient A; Figure 13 and Table 10). Tested serum samples from week 36 onwards revealed a dose-dependent

and similarly efficient inhibition of gH/gL/gO, with an average IC50 at a 17.6-fold dilution. (Patient A; Supplementary Figure S9).

For patient B the investigation period covered 48 weeks, whereby seven weeks prior to t_0 the patient had still been naïve to HCMV infection. Further serum samples tested for inhibition derived from six and 41 weeks after t_0. During this 41-week period, IgG avidity had shifted from low to intermediate avidity at week 6 and from intermediate to high avidity at week 41. HCMV-specific IgM antibodies were present from t_0 up to week 41. (Patient B; Figure 13 and Table 10) None of the tested serum samples exhibited gH/gL/gO-specific binding inhibition. (Patient B; Supplementary Figure S9)

Avidity maturation for patient C was observed for a period of 16 weeks with serum samples tested from one week before as well as two, three and 15 weeks after t_0. At week 15, the avidity index shifted from low to intermediate IgG avidity and HCMV-specific IgM antibodies were still detectable (Patient C; Figure 13 and Table 10). The tested serum samples of patient C showed no inhibition within the observed period (Patient C; Supplementary Figure S9).

Data regarding patient D comprised a period of 13 weeks, with sera tested for inhibition at one, twelve and 13 weeks after t_0. Avidity index shifted from low to intermediate IgG avidity at week 13. HCMV-specific IgM antibodies remained detectable throughout the whole period (Patient D; Figure 13 and Table 10). The tested sera from patient D did not exhibit binding inhibition (Patient D; Supplementary Figure S9).

The preliminary data suggested that after a recent primary infection, the development of iAbs against gH/gL/gO-receptor binding took up to several months in patient A, until a high IgG avidity had been established and no IgM antibodies were detectable anymore.

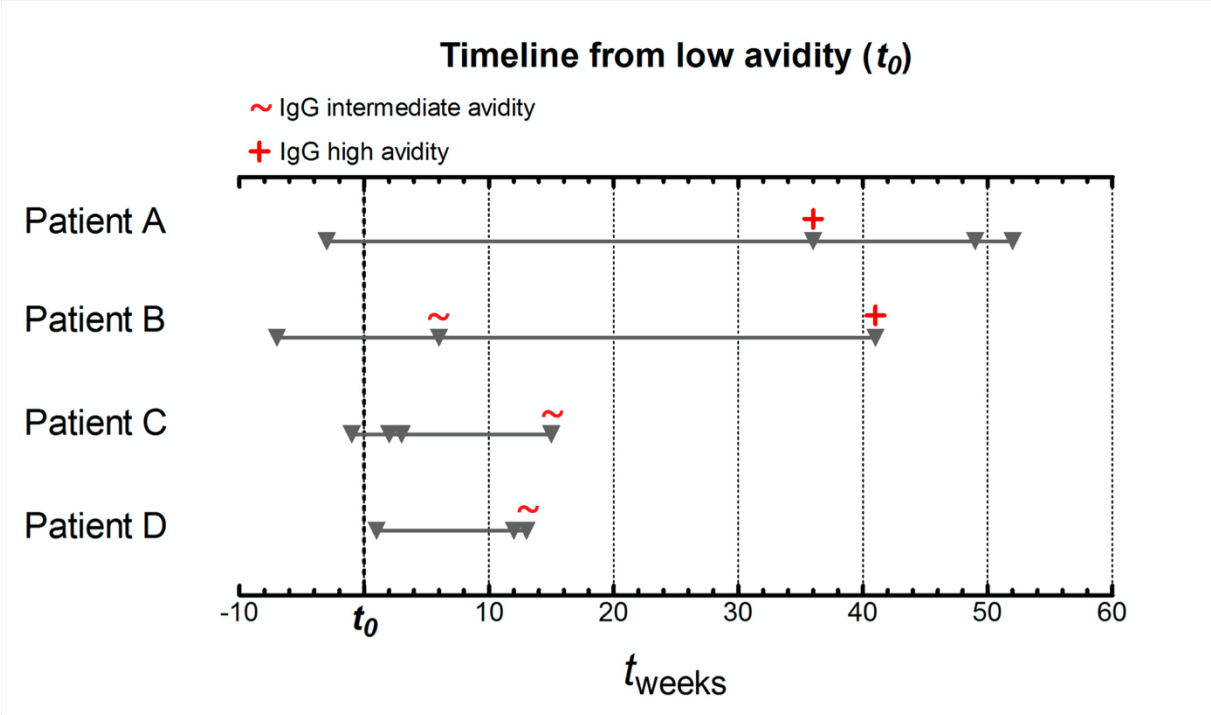

Figure 13: Retrospective analysis of sequentially taken serum samples of different patients upon avidity maturation. *The timeline represents the time passed after determination of low IgG avidity (t_0) for patients A - D in weeks. Serum antibody-mediated inhibition of gH/gL/gO was tested for available serum samples (grey triangles) from before and after low avidity determination. Changes in IgG avidity are indicated (red symbols). ~, intermediate IgG avidity; +, high IgG avidity;*

Table 10: Development of serum antibody-mediated inhibition against gH/gL/gO-PDGFRα binding in patients followed from HCMV-specific low IgG avidity (t_0). *The generation of iAbs within individual patients was investigated upon the course of IgG avidity maturation from low avidity. Serum analysis further provided information about the changes regarding the presence of IgG and IgM antibodies in the course of IgG avidity maturation.*

Patient ID	t (weeks)[a]	IgG AVT[b]	IgG[c]	IgM[d]	iAbs (IC50)[e]
A	-3	ND	ND	ND	- (-)
	t_0	Low	+	+	ND
	36	High	+	-	+ (19.1)
	49	High	+	ND	+ (17.7)
	52	High	+	ND	+ (15.9)
B	-7	ND	ND	ND	- (-)
	t_0	Low	+	+	ND
	6	Intermediate	+	+	- (-)
	41	High	+	+	- (-)
C	-1	ND	ND	ND	- (-)
	t_0	Low	+	+	ND
	2	Low	+	+	- (-)
	3	Low	+	+	- (-)
	15	Intermediate	ND	ND	- (-)
D	t_0	Low	+	+	ND
	1	Low	+	+	- (-)
	12	Low	+	+	- (-)
	13	Intermediate	+	+	- (-)

*Abbreviations: ID, identification; t, time (in weeks); iAbs, inhibitory antibodies; IC50, inhibitory concentration at 50%; IgG, Immunoglobulin G; AVT, avidity; IgM, Immunoglobulin M; t_0, time at primary low IgG avidity determination; ND, no data/ not determined; *, not tested for inhibition;*

[a] Weeks passed after primary low avidity determination

[b] HCMV-specific IgG avidity determined with the Euroimmun Cytomegalovirus (CMV) avidity determination ELISA-test kit (EI 2570-9601-1 G).

[c] Presence of HCMV-specific IgG antibodies was determined with the Euroimmun Cytomegalovirus (CMV) ELISA-test kit (EI 2570-9601 G)

[d] Presence of HCMV-specific IgM antibodies was determined with the Euroimmun Cytomegalovirus (CMV) ELISA-test kit (EI 2570-9601 M)

[e] Results gained from inhibition assay of individual serum samples from patients interpreted as presence of inhibitory antibodies and the determined IC50 value (fold dilution).

Patient E and patient F were followed from the primary detection of intermediate avidity, whereby the tested serum samples covered a total period of 30 weeks from t_0 away (Figure 14 and Table 11). Despite of several months passed, none of the patients revealed a shift in

the avidity index to high IgG avidity, allowing for the more detailed investigation of iAb generation within the intermediate avidity phase.

The investigation of the IgG avidity maturation within Patient E covered a period of 15 weeks, with serum samples tested at t_0 as well as one and 14 weeks after t_0 (Patient E; Figure 14 and Table 11). HCMV-specific IgM titers were not detected at any point since t_0. Although the tested sera from patient E showed no binding inhibition beyond the cutoff range, a trend towards inhibition was observed at increased serum concentrations at week 15. (Patient E; Supplementary Figure S10)

For patient F, the tested sera covered a period of 29 weeks, including samples from t_0 as well as three, ten and 29 weeks after t_0 (Patient F; Figure 14 and Table 11). HCMV-specific IgM antibody titers decreased to a threshold value in the course of three to ten weeks. Inhibition of gH/gL/gO receptor binding was not observed for any of the serum samples. (Patient F; Supplementary Figure S10)

Although patients E and F had prolonged phases of intermediate avidity, the generation of iAbs could not be observed. Overall, the collected data of all patients suggested that the generation of iAb effectively inhibiting gH/gL/gO-specific receptor binding takes place late after primary infection during the final stage of IgG avidity maturation.

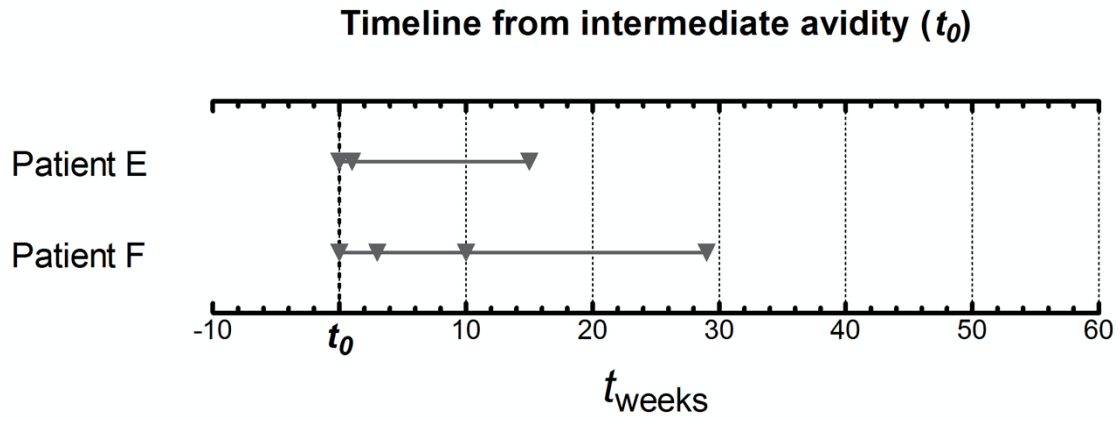

Figure 14: Retrospective analysis of sequentially taken serum samples upon avidity maturation. *The timeline represents the time passed after determination of intermediate IgG avidity (t_0) for patients E and F in weeks. Serum antibody-mediated inhibition of gH/gL/gO was tested for available serum samples (grey triangles) from before and after intermediate avidity determination.*

Table 11: Development of serum antibody-mediated inhibition against gH/gL/gO-PDGFRα binding in patients followed from HCMV-specific intermediate IgG avidity (t_0). *The generation of iAbs within individual patients was investigated upon the course of IgG avidity maturation from intermediate avidity. Serum analysis further provided information about the changes regarding the presence of IgG and IgM antibodies in the course of intermediate IgG avidity.*

Patient ID	t (weeks)[a]	IgG AVT[b]	IgG[c]	IgM[d]	iAbs (IC50)[e]
E	t_0	Intermediate	+	-	- (-)
	1	Intermediate	+	-	- (-)
	15	Intermediate	ND	ND	~ (-)
F	t_0	Intermediate	+	+	- (-)
	3	Intermediate	+	+	- (-)
	10	Intermediate	+	~	- (-)
	29	Intermediate	+	~	- (-)

Abbreviations: ID, identification; t, time (in weeks); iAbs, inhibitory antibodies; IC50, inhibitory concentration at 50%; IgG, Immunoglobulin G; AVT, avidity; IgM, Immunoglobulin M; t_0, time at primary low IgG avidity determination; ND, no data/ not determined;

[a] Weeks passed after primary intermediate avidity determination

[b] HCMV-specific IgG avidity determined with the Euroimmun Cytomegalovirus (CMV) avidity determination ELISA-test kit (EI 2570-9601-1 G).

[c] Presence of HCMV-specific IgG antibodies was determined with the Euroimmun Cytomegalovirus (CMV) ELISA-test kit (EI 2570-9601 G)

[d] Presence of HCMV-specific IgM antibodies was determined with the Euroimmun Cytomegalovirus (CMV) ELISA-test kit (EI 2570-9601 M)

[e] Results gained from inhibition assay of individual serum samples from patients interpreted as presence of inhibitory antibodies and the determined IC50 value (fold dilution).

Discussion

The important role of the trimeric gH/gL/gO glycoprotein complex, mediating viral entry into the majority of target cells, suggests it as an favorable target for the nAb response. (Ciferri, Chandramouli, Donnarumma, *et al.*, 2015) Similar to antibodies that bind the receptor-accessory subunits UL128-131A of the pentameric complex, antibodies targeting the gO-subunit or at least inhibit PDGFRα receptor-binding could be considered highly potent neutralizers, but need to overcome the gO-related sequence variability, in order to provide strain-overlapping immunity. (Rasmussen *et al.*, 2002; Ciferri, Chandramouli, Leitner, *et al.*, 2015; Cui *et al.*, 2017; Day *et al.*, 2020; He *et al.*, 2022) Here, we aimed at the generation of soluble gH/gL/gO using the gH1 as well as the distinct gO1c and gO4 genotypes from the HCMV strains TB40/E (gH1, gO1c) and Towne (gO4). Next, we applied soluble gH1gLgO4 in an ELISA-based assay to investigate the serum antibody-mediated inhibition of PDGFRα receptor binding.

Here we showed that expression of soluble gH/gL/gO and secretion into the supernatant can be achieved through the deletion of the TM-domain of the gH subunit and the use of a N-terminal IL-2 signal peptide within the individual subunits. Fluorescence emitted by EGFP-reporter gene within the pMT7 vector backbone, indicated the successful uptake of the DNA into HEK293T cells through transient transfection. While soluble trimeric gH/gL/gO utilizing the HCMV Towne-derived gO4 subunit was clearly detectable within the supernatant, the co-transfection of gH1 and gL with the TB40/E-derived gO1c subunit revealed only minimal production of trimer. Due to the successful generation of gH1/gL/gO4 as well as the detection of at least small amounts of gH1/gL/gO1c and gH/gL-homodimer in the supernatant, we had concluded that not the expression and formation of the gH/gL-core dimer nor the secretion of the complex, but rather the expression of the gO1c subunit or the assembly with the gH/gL-core dimer posed a problem during trimer production.

Expression of soluble trimeric complex was performed throughout multiple studies, recording different combinations of gH and gO genotypes. (Ciferri, Chandramouli, Donnarumma, *et al.*, 2015; Ciferri, Chandramouli, Leitner, *et al.*, 2015; Schultz *et al.*, 2016, 2021; Liu *et al.*, 2018; J. Liu *et al.*, 2021; Kschonsak *et al.*, 2021) In 2022, Ai *et al.* produced trimeric gH/gL/gO in a similar set-up using the gH1 and gO1c subunit derived from the HCMV VR1814 strain, which both share 99.9% and 100% sequence similarity with the gH1 and gO1c sequences of the TB40/E strain, respectively. For the secretion of the complex they used the wildtype sequences of gL, gO1c and a truncated version of the gH1 sequence, encoding only the extracellular domain (aa 1 - 715). (Ai *et al.*, 2022) Liu et al. additionally added a vascular endothelial growth factor (VEGF) signal peptide to each subunit in order to promote secretion of the

formed complex. (Liu *et al.*, 2018) For our approach, we also used a truncated version of the gH1 subunit (aa 24 - 718), lacking the transmembrane domain and the cytoplasmic tail and exchanged the wildtype signal peptide sequence of the individual subunits gH1, gL, gO1c and gO4 with the signal peptide of the secretory Interleukin-2 protein. (Robb *et al.*, 1984) For the TB40/E- and Towne-derived gO1c and gO4 subunits, the wildtype signal peptides (aa 1 – 29) exhibited a sequence similarity of 65.5%. Although the exchange of the signal peptide did not affect the expression of the trimeric complex upon the use of the gO4 genotype, it might have caused an alteration in the glycosylation pattern or misfolding of the gO1c genotype, which followingly may lead to the degradation of the subunit and explain the hampered formation as well as the low secretion of trimeric gH1/gL/gO1c.

The formation and initial glycosylation of the trimeric complex is described to take place within the ER, while the final modification of the gO subunit happens within the Golgi-apparatus on the way to the cell membrane through the secretory pathway. (Huber and Compton, 1999; Theiler and Compton, 2002) In 2015 and 2018 Li *et al.* and Nguyen *et al.* described gO as constitutive substrate of the endoplasmic reticulum associated degradation (ERAD) for the identification of the viral cofactor UL148, which supports trimer formation upon inhibition of ERAD-stimulating factor SEL1L. (Li *et al.*, 2015; Nguyen *et al.*, 2018) Further investigations discovered that UL116 acts as a chaperone for the gH subunit that is involved in the assembly and incorporation of the gH/gL-complexes into the virion. UL116 was also shown to interact with UL148 and protect gH from ERAD-associated degradation. (Siddiquey *et al.*, 2021; Vezzani *et al.*, 2021) This data further fits to the observed abundancies of gH/gL-complexes among HCMV strains expressing different gO isoforms. (Zhou *et al.*, 2013) Considering the difficulties we experienced upon the recombinant expression of gH1gLgO1c, but not gH1gLgO4, we speculated that trimer expression and formation using certain gO-genotypes, depends on the co-expression of specific cofactors, which are present upon natural infection.

Upon absence of the gO subunit, we observed the production and secretion of gH/gL-homodimeric complex. However, compared to the amounts of trimeric complex in form of gH1/gL/gO4, the gH/gL-homodimer was detected to a clearly lesser amount in the supernatant. Together with the data obtained by Wille *et al.* in 2010, our results supported the promoting role of the gO-subunit during the export of the assembled gH/gL-complex from the ER. (Wille *et al.*, 2010) Additionally, Vanarsdall *et al.* showed that co-expression of gH/gL together with gO, derived from the HCMV TR strain (gO1b), led do an increased transport of gH/gL into the cellular Golgi compartment, whereas absent of the gO subunit led to retention of gH/gL within the ER. (Vanarsdall, Chase and Johnson, 2011) This suggests that production of gH/gL-homodimeric complex upon the co-expression with the gO4 subunit, and hence

the generation of gH1gLgO4 trimeric complex, would remain at a minimum and if not completely absent and thus should not interfere with the trimer production.

In order to understand the dynamics of trimer expression and the role of the gO-genotypes for the assembly, further transfection-experiments investigating different combinations of gH- and gO-variants, as well as the co-expression with the viral cofactors UL148 and UL116, would need to be conducted.

Purification of the trimeric complex was achieved through two-step protocol, comprising affinity- and size exclusion-chromatography. Affinity chromatography through the histidine-tagged gH subunit allowed for the extraction of the trimeric complex from the supernatant as well as the detection of trimeric complex without interfering with the receptor-binding site. Although often described among the literature, affinity purification through a gO-associated protein-tag was not taken into consideration, since the occupation and thus the impact on receptor binding was unpredictable, especially upon the use of different gO-genotypes. (Ciferri, Chandramouli, Donnarumma, *et al.*, 2015; Liu *et al.*, 2018) Since gH-associated purification could not prevent the co-purification of an eventually produced gH/gL-homodimer, we introduced size exclusion chromatography as a second purification step. Although the protein standard tested upon size exclusion chromatography predicted an approximate elution volume between 10.3 – 12.4 mL, trimeric complex eluted prematurely, which could be caused by the steric size of the complex acquired by its high glycosylation level. (Huber and Compton, 1999; Kschonsak *et al.*, 2021) Moreover, the elution comprised the first two peaks of the chromatogram, which implied the presence of differently sized protein species, both containing trimeric gH/gL/gO. According to the protein standard, the second peak was assigned to contain proteins of the size of trimeric gH/gL/gO. Thus, we suggested that the first peak fraction contained a dimerized gH/gL/gO particles, like those observed by Kschonsak *et al.* (Kschonsak *et al.*, 2021) In order to further investigate this instance and to prevent complex dimerization, future purification experiments need to be performed upon buffer supplementation with detergent. The two-step chromatography allowed for the purification of a total amount of 290 µg of soluble trimer in the end. At this point it has to mentioned that not all transfection experiments worked to the fullest efficiency, leading to decreased production and hence decreased protein yield receivable from 1.2L supernatant.

Furthermore, we were able to use our in-house generated trimer to develop a PDGFRα receptor binding assay that specifically detected bound gH/gL/gO and generated hardly any background noise. Pre-incubation of gH/gL/gO with human sera further enabled the detection of inhibitory antibodies that could prevent PDGFRα binding. By comparing serum derived from seronegative and seropositive individuals as well as seropositive individuals of similar HCMV-specific IgG titers but different IgG avidity, we observed that inhibition of gH/gL/gO-

PDGFRα binding was exclusively found in HCMV seropositive individuals of high IgG avidity index, independently from the IgG titers. Interestingly, the Cytotect®CP control exhibited inhibition of PDGFRα binding in a dose-dependent manner similar to those of the seropositive samples, with an IC50 in between those of the different seropositive sera. Since the total IgG concentration is described with 50 mg/mL, our results indicate that only a small fraction of the Cytotect®CP-contained IgG antibodies provided inhibition against gH/gL/gO-PDGFRα binding. This again would correspond to the lower neutralization efficiency in fibroblasts, compared to endothelial and epithelial cells, provided by Cytotect®CP. (Cui *et al.*, 2008) The increased inhibition potential of some seropositive individuals compared to Cytotect®CP therefore suggests that these individuals could also exhibit increased viral neutralization. Still, it remains difficult to draw conclusions regarding the inhibition quality of antibodies from certain individuals, as on the one hand the IC50 values provide a good indicator, but total inhibition was not always achieved. Thus, our assay allows a clear prediction of the presence of inhibitory antibodies against gH/gL/gO-PDGFRα binding, but only an approximate indication of the quality of the present iAbs. However, upon possible correlation of the data received by our assay and in-vitro-determined neutralization titers, our assay may provide a quick and broad screening method for the detection of eventually potent neutralizers (elite neutralizers), without the time-intensive and careful operating with infectious HCMV particles in the cell culture.

The investigation of sequential serum samples revealed that trimer-specific iAbs appear late after primary infection in the course of avidity maturation, whereby only patients of high IgG avidity seemed to bring up an inhibitory response. Similar to our observation, highly potent nAbs targeting the receptor-accessory UL128-UL131A subunits also emerge late after primary infection. (Furione *et al.*, 2013; Lilleri *et al.*, 2013) Interestingly, one patient reaching the high IgG avidity index within a similar time frame, did not exhibit any inhibitory response. Additionally to this, no inhibitory response could be detected among patients with prolonged intermediate avidity phase. From this, we concluded that the development of iAbs that target the trimeric complex and hence potentially neutralize HCMV entry, arise in the course of antibody affinity and avidity maturation late after primary HCMV infection. The time required for antibody maturation to high IgG avidity in turn probably depends on several factors such as positive selection of antigen-specific B-cells through frequent pathogen exposure, the patient's state of health, immunoregulatory factors and, of course, individual genetic factors. (Lutz, Ward and Gray, 1994; Lazzarotto *et al.*, 1998)

Curiously, although we were not able to compare the mediated binding inhibition between the gO4 and the gO1c variants, it seemed that all of the tested individuals, except for one, generated inhibitory antibodies against gH1/gL/gO4 upon high avidity. The further investigation with other gO variants and the comparison between risk groups and healthy individuals could

provide information on whether a cross-protective immune response is acquired after HCMV infection regardless of the strain or whether a lack of these antibodies could play a role in the activation and transmission of HCMV.

5 References

Abdullahi Nasir, I., Babayo, A. and Shehu, M. (2016) 'Clinical Significance of IgG Avidity Testing and Other Considerations in the Diagnosis of Congenital Cytomegalovirus Infection: A Review Update', *Medical Sciences*, 4(1), p. 5. doi: 10.3390/medsci4010005.

Adler, B. *et al.* (2006) 'Role of human cytomegalovirus UL131A in cell type-specific virus entry and release', *Journal of General Virology*, 87(9), pp. 2451–2460. doi: 10.1099/vir.0.81921-0.

Adler, S. P. (1991) 'Cytomegalovirus and child day care: Risk factors for maternal infection', *Pediatric Infectious Disease Journal*, 10(8), pp. 590–594. doi: 10.1097/00006454-199108000-00008.

Ai, Y. *et al.* (2022) 'Neutralization Epitopes in Trimer and Pentamer Complexes Recognized by Potent Cytomegalovirus-Neutralizing Human Monoclonal Antibodies', *Microbiology Spectrum*, 10(6). doi: 10.1128/spectrum.01393-22.

Alsuliman, T. *et al.* (2018) 'Cytotect®CP as salvage therapy in patients with CMV infection following allogeneic hematopoietic cell transplantation: a multicenter retrospective study', *Bone Marrow Transplantation*, 53(10), pp. 1328–1335. doi: 10.1038/s41409-018-0166-9.

Alwine, J. C. (2012) 'The Human Cytomegalovirus Assembly Compartment: A Masterpiece of Viral Manipulation of Cellular Processes That Facilitates Assembly and Egress', *PLoS Pathogens*, 8(9). doi: 10.1371/journal.ppat.1002878.

Bacigalupo, A. *et al.* (2012) 'Foscarnet in the management of cytomegalovirus infections in hematopoietic stem cell transplant patients.', *Expert review of anti-infective therapy*, 10(11), pp. 1249–1264. doi: 10.1586/eri.12.115.

Bagdonaite, I. *et al.* (2016) 'Global mapping of o-glycosylation of varicella zoster virus, human cytomegalovirus, and Epstein-Barr virus', *Journal of Biological Chemistry*, 291(23), pp. 12014–12028. doi: 10.1074/jbc.M116.721746.

Baldick, C. J. and Shenk, T. (1996) 'Proteins associated with purified human cytomegalovirus particles', *Journal of Virology*, 70(9), pp. 6097–6105. doi: 10.1128/jvi.70.9.6097-6105.1996.

Bass, E. B. *et al.* (1993) 'Efficacy of immune globulin in preventing complications of bone marrow transplantation: A meta-analysis', *Bone Marrow Transplantation*, 12(3), pp. 273–282.

Blank, S. E., Leslie, G. A. and Clem, L. W. (1972) 'Antibody Affinity and Valence in Viral Neutralization', *The Journal of Immunology*, 108(3), pp. 665–673. doi: 10.4049/jimmunol.108.3.665.

Bodéus, M., Feyder, S. and Goubau, P. (1998) 'Avidity of IgG antibodies distinguishes primary from non-primary cytomegalovirus infection in pregnant women', *Clinical and Diagnostic Virology*, 9(1), pp. 9–16. doi: 10.1016/S0928-0197(97)10016-2.

Bogdanow, B. *et al.* (2023) 'Spatially resolved protein map of intact human cytomegalovirus virions', *Nature Microbiology*, 8(9), pp. 1732–1747. doi: 10.1038/s41564-023-01433-8.

Bogner, E. *et al.* (1992) 'Recognition of compartmentalized intracellular analogs of glycoprotein H of human cytomegalovirus', *Archives of Virology*, 126(1–4), pp. 67–80. doi: 10.1007/BF01309685.

Boppana, S. B. *et al.* (1992) 'Symptomatic congenital cytomegalovirus infection: Neonatal morbidity and mortality', *Pediatric Infectious Disease Journal*, 11(2), pp. 93–99. doi: 10.1097/00006454-199202000-00007.

Boppana, S. B. and Britt, W. J. (1995) 'Antiviral antibody responses and intrauterine transmission after primary maternal cytomegalovirus infection', *Journal of Infectious Diseases*, 171(5), pp. 1115–1121. doi: 10.1093/infdis/171.5.1115.

Bowden, R. A. (1995) 'Transfusion-transmitted cytomegalovirus infection', *Hematology/Oncology Clinics of North America*, 9(1), pp. 155–166. doi: 10.1016/s0889-8588(18)30114-x.

Britt, W. J. *et al.* (1990) 'Cell surface expression of human cytomegalovirus (HCMV) gp55-116 (gB): use of HCMV-recombinant vaccinia virus-infected cells in analysis of the human neutralizing antibody response', *Journal of Virology*, 64(3), pp. 1079–1085. doi: 10.1128/jvi.64.3.1079-1085.1990.

Cannon, M. J., Hyde, T. B. and Schmid, D. S. (2011) 'Review of cytomegalovirus shedding in bodily fluids and relevance to congenital cytomegalovirus infection', *Reviews in Medical Virology*, 21(4), pp. 240–255. doi: 10.1002/rmv.695.

Cannon, M. J., Schmid, D. S. and Hyde, T. B. (2010) 'Review of cytomegalovirus seroprevalence and demographic characteristics associated with infection', *Reviews in Medical Virology*, 20(4), pp. 202–213. doi: 10.1002/rmv.655.

Chehimi, J., Peppard, J. and Emanuel, D. (1987) 'Selection of an intravenous immune globulin for the immunoprophylaxis of cytomeglovirus infections: An in vitro comparison of currently available and previously effective immune globulins.', *Bone Marrow Transplantation*, 2(4), pp. 395–402.

Chen, D. H. *et al.* (1999) 'Three-dimensional visualization of tegument/capsid interactions in the intact human cytomegalovirus', *Virology*, 260(1), pp. 10–16. doi: 10.1006/viro.1999.9791.

Chou, S. (1992) 'Molecular epidemiology of envelope glycoprotein H of human cytomegalovirus', *Journal of Infectious Diseases*, 166(3), pp. 604–607. doi: 10.1093/infdis/166.3.604.

Chowdary, T. K. *et al.* (2010) 'Crystal structure of the conserved herpesvirus fusion regulator complex gH-gL', *Nature Structural and Molecular Biology*, 17(7), pp. 882–888. doi: 10.1038/nsmb.1837.

Ciferri, C., Chandramouli, S., Leitner, A., *et al.* (2015) 'Antigenic Characterization of the HCMV gH/gL/gO and Pentamer Cell Entry Complexes Reveals Binding Sites for Potently Neutralizing Human Antibodies', *PLoS Pathogens*, 11(10). doi: 10.1371/journal.ppat.1005230.

Ciferri, C., Chandramouli, S., Donnarumma, D., *et al.* (2015) 'Structural and biochemical studies of HCMV gH/gL/gO and Pentamer reveal mutually exclusive cell entry complexes', *Proceedings of the National Academy of Sciences of the United States of America*. 2015/01/26, 112(6), pp. 1767–1772. doi: 10.1073/pnas.1424818112.

Compton, T., Nepomuceno, R. R. and Nowlin, D. M. (1992) 'Human cytomegalovirus penetrates host cells by PH-independent fusion at the cell surface', *Virology*, 191(1), pp. 387–395. doi: 10.1016/0042-6822(92)90200-9.

Contreras, G. and Ho, D. (2022) 'Human cytomegalovirus: A survey of end-organ diseases and diagnostic challenges in solid organ transplant recipients', *Current Opinion in Organ Transplantation*, 27(4), pp. 243–249. doi: 10.1097/MOT.0000000000000992.

Coste Mazeau, P. *et al.* (2023) 'New therapeutic perspective in the prevention of congenital cytomegalovirus infection', *Antiviral Research*, 216. doi: 10.1016/j.antiviral.2023.105661.

Crough, T. and Khanna, R. (2009) 'Immimobiology of human cytomegalovirus: From bench to bedside', *Clinical Microbiology Reviews*, 22(1), pp. 76–98. doi: 10.1128/CMR.00034-08.

Cui, X. *et al.* (2008) 'Cytomegalovirus vaccines fail to induce epithelial entry neutralizing antibodies comparable to natural infection', *Vaccine*, 26(45), pp. 5760–5766. doi: 10.1016/j.vaccine.2008.07.092.

Cui, X. *et al.* (2017) 'Impact of Antibodies and Strain Polymorphisms on Cytomegalovirus Entry and Spread in Fibroblasts and Epithelial Cells', *Journal of Virology*, 91(13). doi: 10.1128/jvi.01650-16.

Cutler, P. (1996) 'Size-exclusion chromatography.', *Methods in molecular biology (Clifton, N.J.)*, 59, pp. 255–267. doi: 10.1385/0-89603-336-8:255.

Davison, A. J. *et al.* (2003) 'The human cytomegalovirus genome revisited: Comparison with the chimpanzee cytomegalovirus genome', *Journal of General Virology*, 84(1), pp. 17–28. doi: 10.1099/vir.0.18606-0.

Day, L. Z. *et al.* (2020) 'Polymorphisms in Human Cytomegalovirus Glycoprotein O (gO) Exert Epistatic Influences on Cell-Free and Cell-to-Cell Spread and Antibody Neutralization on gH Epitopes', *Journal of Virology*, 94(8). doi: 10.1128/jvi.02051-19.

Demarchi, J. M., Schmidt, C. A. and Kaplan, A. S. (1980) 'Patterns of Transcription of Human Cytomegalovirus in Permissively Infected Cells', *Journal of Virology*, 35(2), pp. 277–286. doi: 10.1128/jvi.35.2.277-286.1980.

Dolan, A. *et al.* (2004) 'Genetic content of wild-type human cytomegalovirus', *Journal of General Virology*, 85(5), pp. 1301–1312. doi: 10.1099/vir.0.79888-0.

Dollard, S. C., Grosse, S. D. and Ross, D. S. (2007) 'New estimates of the prevalence of neurological and sensory sequelae and mortality associated with congenital cytomegalovirus infection', *Reviews in Medical Virology*, 17(5), pp. 355–363. doi: 10.1002/rmv.544.

Eisen, H. N. and Siskind, G. W. (1964) 'Variations in Affinities of Antibodies during the Immune Response', *Biochemistry*, 3(7), pp. 996–1008. doi: 10.1021/bi00895a027.

Falk, J. J. *et al.* (2017) 'A two-step screening approach for the identification of blood donors with highly and broadly neutralizing capacities against human cytomegalovirus', *Transfusion*, 57(2), pp. 412–422. doi: 10.1111/trf.13906.

Falk, J. J. *et al.* (2018) 'Identification of elite neutralizers with broad and potent neutralizing activity against human cytomegalovirus (hcmv) in a population of hcmv-seropositive blood donors', *Journal of Infectious Diseases*, 218(6), pp. 876–885. doi: 10.1093/infdis/jiy229.

Fish, K. N. *et al.* (1996) 'Cytomegalovirus persistence in macrophages and endothelial cells', *Scandinavian Journal of Infectious Diseases, Supplement*, (99), pp. 34–40.

Fornara, C. *et al.* (2023) 'Fibroblast, Epithelial and Endothelial Cell-Derived Human Cytomegalovirus Strains Display Distinct Neutralizing Antibody Responses and Varying Levels of gH/gL Complexes', *International Journal of Molecular Sciences*, 24(5). doi: 10.3390/ijms24054417.

Fouts, A. E. *et al.* (2014) 'Mechanism for neutralizing activity by the anti-CMV gH/gL monoclonal antibody MSL-109', *Proceedings of the National Academy of Sciences of the United States of America*, 111(22), pp. 8209–8214. doi: 10.1073/pnas.1404653111.

Fowler, K. *et al.* (2022) 'A systematic literature review of the global seroprevalence of cytomegalovirus: possible implications for treatment, screening, and vaccine development', *BMC Public Health*, 22(1). doi: 10.1186/s12889-022-13971-7.

Fowler, K. B. and Boppana, S. B. (2006) 'Congenital cytomegalovirus (CMV) infection and hearing

deficit', *Journal of Clinical Virology*, 35(2), pp. 226–231. doi: 10.1016/j.jcv.2005.09.016.

Fowler, K. B. and Boppana, S. B. (2018) 'Congenital cytomegalovirus infection', *Seminars in Perinatology*, 42(3), pp. 149–154. doi: 10.1053/j.semperi.2018.02.002.

Fowler, K. B. and Pass, R. F. (2006) 'Risk factors for congenital cytomegalovirus infection in the offspring of young women: Exposure to young children and recent onset of sexual activity', *Pediatrics*, 118(2). doi: 10.1542/peds.2005-1142.

Freed, D. C. *et al.* (2013) 'Pentameric complex of viral glycoprotein H is the primary target for potent neutralization by a human cytomegalovirus vaccine', *Proceedings of the National Academy of Sciences of the United States of America*, 110(51). doi: 10.1073/pnas.1316517110.

Furione, M. *et al.* (2013) 'Slow increase in IgG avidity correlates with prevention of human cytomegalovirus transmission to the fetus', *Journal of Medical Virology*, 85(11), pp. 1960–1967. doi: 10.1002/jmv.23691.

Germer, M., Herbener, P. and Schüttrumpf, J. (2016) 'Functional properties of human cytomegalovirus hyperimmunoglobulin and standard immunoglobulin preparations', *Annals of Transplantation*, 21, pp. 558–564. doi: 10.12659/AOT.898050.

Gerna, G. *et al.* (2016) 'Monoclonal Antibodies to Different Components of the Human Cytomegalovirus (HCMV) Pentamer gH/gL/pUL128L and Trimer gH/gL/gO as well as Antibodies Elicited during Primary HCMV Infection Prevent Epithelial Cell Syncytium Formation', *Journal of Virology*, 90(14), pp. 6216–6223. doi: 10.1128/jvi.00121-16.

Gonzalez-Del Pino, G. L. and Heldwein, E. E. (2022) 'Well Put Together—A Guide to Accessorizing with the Herpesvirus gH/gL Complexes', *Viruses*, 14(2). doi: 10.3390/v14020296.

Grefte, A. *et al.* (1993) 'Circulating Cytomegalovirus (CMV)-Infected Endothelial Cells in Patients with an Active CMV Infection', *Journal of Infectious Diseases*, 167(2), pp. 270–277. doi: 10.1093/infdis/167.2.270.

Griffiths, P. (2020) 'The direct and indirect consequences of cytomegalovirus infection and potential benefits of vaccination', *Antiviral Research*, 176. doi: 10.1016/j.antiviral.2020.104732.

Hamirally, S. *et al.* (2009) 'Viral mimicry of Cdc2/cyclin-dependent kinase 1 mediates disruption of nuclear lamina during human cytomegalovirus nuclear egress', *PLoS Pathogens*, 5(1). doi: 10.1371/journal.ppat.1000275.

Harnois, M. J. *et al.* (2022) 'Characterization of Plasma Immunoglobulin G Responses in Elite Neutralizers of Human Cytomegalovirus', *Journal of Infectious Diseases*, 226(9), pp. 1667–1677. doi: 10.1093/infdis/jiac341.

Haspot, F. *et al.* (2012) 'Human cytomegalovirus entry into dendritic cells occurs via a macropinocytosis-like pathway in a ph-independent and cholesterol-dependent manner', *PLoS ONE*, 7(4). doi: 10.1371/journal.pone.0034795.

He, L. *et al.* (2022) 'Polymorphic Forms of Human Cytomegalovirus Glycoprotein O Protect against Neutralization of Fibroblast Entry by Antibodies Targeting Epitopes Defined by Glycoproteins H and L', *Viruses*, 14(7). doi: 10.3390/v14071508.

Herbein, G. (2022) 'High-Risk Oncogenic Human Cytomegalovirus', *Viruses*, 14(11). doi: 10.3390/v14112462.

Hetzenecker, S., Helenius, A. and Krzyzaniak, M. A. (2016) 'HCMV Induces Macropinocytosis for Host Cell Entry in Fibroblasts', *Traffic*, 17(4), pp. 351–368. doi: 10.1111/tra.12355.

Hsu, J. L. and Safdar, N. (2011) 'Polyclonal Immunoglobulins and Hyperimmune Globulins in Prevention and Management of Infectious Diseases', *Infectious Disease Clinics of North America*, 25(4), pp. 773–788. doi: 10.1016/j.idc.2011.07.005.

Huber, M. T. and Compton, T. (1997) 'Characterization of a novel third member of the human cytomegalovirus glycoprotein H-glycoprotein L complex', *Journal of Virology*, 71(7), pp. 5391–5398. doi: 10.1128/jvi.71.7.5391-5398.1997.

Huber, M. T. and Compton, T. (1999) 'Intracellular Formation and Processing of the Heterotrimeric gH-gL-gO (gCIII) Glycoprotein Envelope Complex of Human Cytomegalovirus', *Journal of Virology*, 73(5), pp. 3886–3892. doi: 10.1128/jvi.73.5.3886-3892.1999.

Jarvis, M. A. and Nelson, J. A. (2002a) 'Human cytomegalovirus persistence and latency in endothelial cells and macrophages', *Current Opinion in Microbiology*, 5(4), pp. 403–407. doi: 10.1016/S1369-5274(02)00334-X.

Jarvis, M. A. and Nelson, J. A. (2002b) 'Mechanisms of human cytomegalovirus persistence and latency.', *Frontiers in bioscience : a journal and virtual library*, 7. doi: 10.2741/jarvis.

Jiang, X. J. *et al.* (2011) 'UL74 of human cytomegalovirus reduces the inhibitory effect of gH-specific and gB-specific antibodies', *Archives of Virology*, 156(12), pp. 2145–2155. doi: 10.1007/s00705-011-1105-x.

Jonjić, S. *et al.* (1994) 'Antibodies are not essential for the resolution of primary cytomegalovirus infection but limit dissemination of recurrent virus', *Journal of Experimental Medicine*, 179(5), pp. 1713–1717. doi: 10.1084/jem.179.5.1713.

Kabani, N. *et al.* (2023) 'Urine and Saliva Viral Load in Children with Congenital Cytomegalovirus Infection', *Journal of the Pediatric Infectious Diseases Society*, 12(4), pp. 230–233. doi: 10.1093/jpids/piad013.

Kabanova, A. *et al.* (2016) 'Platelet-derived growth factor-α receptor is the cellular receptor for human cytomegalovirus gHgLgO trimer', *Nature Microbiology*, 1(8). doi: 10.1038/nmicrobiol.2016.82.

Kagan, K. O. *et al.* (2021) 'Outcome of pregnancies with recent primary cytomegalovirus infection in first trimester treated with hyperimmunoglobulin: observational study', *Ultrasound in Obstetrics and Gynecology*, 57(4), pp. 560–567. doi: 10.1002/uog.23596.

Kalejta, R. F. (2008) 'Tegument Proteins of Human Cytomegalovirus', *Microbiology and Molecular Biology Reviews*, 72(2), pp. 249–265. doi: 10.1128/mmbr.00040-07.

Kalser, J. *et al.* (2017) 'Differences in growth properties among two human cytomegalovirus glycoprotein O genotypes', *Frontiers in Microbiology*, 8(AUG). doi: 10.3389/fmicb.2017.01609.

Kari, B. *et al.* (1990) 'Structure and composition of a family of human cytomegalovirus glycoprotein complexes designated gC-I (gB)', *Journal of General Virology*, 71(11), pp. 2673–2680. doi: 10.1099/0022-1317-71-11-2673.

Kari, B. and Gehrz, R. (1992) 'A human cytomegalovirus glycoprotein complex designated gC-II is a major heparin-binding component of the envelope', *Journal of Virology*, 66(3), pp. 1761–1764. doi: 10.1128/jvi.66.3.1761-1764.1992.

Kari, B. and Gehrz, R. (1993) ‘Structure, composition and heparin binding properties of a human cytomegalovirus glycoprotein complex designated gC-II’, *Journal of General Virology*, 74(2), pp. 255–264. doi: 10.1099/0022-1317-74-2-255.

Kaye, J. F., Gompels, U. A. and Minson, A. C. (1992) ‘Glycoprotein H of human cytomegalovirus (HCMV) forms a stable complex with the HCMV UL115 gene product’, *Journal of General Virology*, 73(10), pp. 2693–2698. doi: 10.1099/0022-1317-73-10-2693.

Kenneson, A. and Cannon, M. J. (2007) ‘Review and meta-analysis of the epidemiology of congenital cytomegalovirus (CMV) infection’, *Reviews in Medical Virology*, 17(4), pp. 253–276. doi: 10.1002/rmv.535.

Klein, M. *et al.* (1999) ‘Strain-Specific Neutralization of Human Cytomegalovirus Isolates by Human Sera’, *Journal of Virology*, 73(2), pp. 878–886. doi: 10.1128/jvi.73.2.878-886.1999.

Komatsu, T. E. *et al.* (2014) ‘Resistance of human cytomegalovirus to ganciclovir/valganciclovir: A comprehensive review of putative resistance pathways’, *Antiviral Research*, 101(1), pp. 12–25. doi: 10.1016/j.antiviral.2013.10.011.

Krech, U. (1973) ‘Complement fixing antibodies against cytomegalovirus in different parts of the world’, *Bulletin of the World Health Organization*, 49(1), pp. 103–106.

Kschonsak, M. *et al.* (2021) ‘Structures of HCMV Trimer reveal the basis for receptor recognition and cell entry’, *Cell*, 184(5), pp. 1232-1244.e16. doi: 10.1016/j.cell.2021.01.036.

Külekci, B. *et al.* (2022) ‘Human cytomegalovirus strain diversity and dynamics reveal the donor lung as a major contributor after transplantation’, *Virus Evolution*, 8(2). doi: 10.1093/ve/veac076.

Von Laer, D. *et al.* (1995) ‘Detection of cytomegalovirus DNA in CD34+ cells from blood and bone marrow’, *Blood*, 86(11), pp. 4086–4090. doi: 10.1182/blood.v86.11.4086.bloodjournal86114086.

Lamberson, H. V. and Dock, N. L. (1992) ‘Prevention of transfusion-transmitted cytomegalovirus infection’, *Transfusion*, 32(3), pp. 196–198. doi: 10.1046/j.1537-2995.1992.32392213798.x.

Lauron, E. J. *et al.* (2014) ‘Human Cytomegalovirus Infection of Langerhans-Type Dendritic Cells Does Not Require the Presence of the gH/gL/UL128-131A Complex and Is Blocked after Nuclear Deposition of Viral Genomes in Immature Cells’, *Journal of Virology*, 88(1), pp. 403–416. doi: 10.1128/jvi.03062-13.

Lazzarotto, T. *et al.* (1998) ‘Delayed acquisition of high-avidity anti-cytomegalovirus antibody is correlated with prolonged antigenemia in solid organ transplant recipients’, *Journal of Infectious Diseases*, 178(4), pp. 1145–1149. doi: 10.1086/515671.

Lemmermann, N. A. W. *et al.* (2015) ‘Non-redundant and Redundant Roles of Cytomegalovirus gH/gL Complexes in Host Organ Entry and Intra-tissue Spread’, *PLoS Pathogens*, 11(2). doi: 10.1371/journal.ppat.1004640.

Lemmon, M. A. and Schlessinger, J. (2010) ‘Cell signaling by receptor tyrosine kinases’, *Cell*, 141(7), pp. 1117–1134. doi: 10.1016/j.cell.2010.06.011.

Li, G. *et al.* (2015) ‘A viral regulator of glycoprotein complexes contributes to human cytomegalovirus cell tropism’, *Proceedings of the National Academy of Sciences of the United States of America*, 112(14), pp. 4471–4476. doi: 10.1073/pnas.1419875112.

Li, L., Nelson, J. A. and Britt, W. J. (1997) ‘Glycoprotein H-related complexes of human

cytomegalovirus: identification of a third protein in the gCIII complex', *Journal of Virology*, 71(4), pp. 3090–3097. doi: 10.1128/jvi.71.4.3090-3097.1997.

Lilleri, D. *et al.* (2013) 'Fetal Human Cytomegalovirus Transmission Correlates with Delayed Maternal Antibodies to gH/gL/pUL128-130-131 Complex during Primary Infection', *PLoS ONE*, 8(3). doi: 10.1371/journal.pone.0059863.

Liu, J. *et al.* (2018) 'The Human Cytomegalovirus Trimer and Pentamer Promote Sequential Steps in Entry into Epithelial and Endothelial Cells at Cell Surfaces and Endosomes', *Journal of Virology*, 92(21). doi: 10.1128/jvi.01336-18.

Liu, J. *et al.* (2021) 'Cryo-Electron Microscopy Structure and Interactions of the Human Cytomegalovirus gHgLgO Trimer with Platelet-Derived Growth Factor Receptor Alpha', *mBio*, 12(5). doi: 10.1128/mBio.02625-21.

Liu, Y. *et al.* (2021) 'Prefusion structure of human cytomegalovirus glycoprotein B and structural basis for membrane fusion', *Science Advances*, 7(10). doi: 10.1126/sciadv.abf3178.

Lu, L. L. *et al.* (2018) 'Beyond binding: Antibody effector functions in infectious diseases', *Nature Reviews Immunology*, 18(1), pp. 46–61. doi: 10.1038/nri.2017.106.

Lutz, E., Ward, K. N. and Gray, J. J. (1994) 'Maturation of antibody avidity after primary human cytomegalovirus infection is delayed in immunosuppressed solid organ transplant patients', *Journal of Medical Virology*, 44(4), pp. 317–322. doi: 10.1002/jmv.1890440402.

Macagno, A. *et al.* (2010) 'Isolation of Human Monoclonal Antibodies That Potently Neutralize Human Cytomegalovirus Infection by Targeting Different Epitopes on the gH/gL/UL128-131A Complex', *Journal of Virology*, 84(2), pp. 1005–1013. doi: 10.1128/jvi.01809-09.

Mach, M. *et al.* (2000) 'Complex Formation by Human Cytomegalovirus Glycoproteins M (gpUL100) and N (gpUL73)', *Journal of Virology*, 74(24), pp. 11881–11892. doi: 10.1128/jvi.74.24.11881-11892.2000.

Mach, M. *et al.* (2005) 'Complex Formation by Glycoproteins M and N of Human Cytomegalovirus: Structural and Functional Aspects', *Journal of Virology*, 79(4), pp. 2160–2170. doi: 10.1128/jvi.79.4.2160-2170.2005.

Maciejewski, J. P. *et al.* (1992) 'Infection of hematopoietic progenitor cells by human cytomegalovirus', *Blood*, 80(1), pp. 170–178. doi: 10.1182/blood.v80.1.170.bloodjournal801170.

Manuel, O. *et al.* (2009) 'Impact of genetic polymorphisms in cytomegalovirus glycoprotein b on outcomes in solid-organ transplant recipients with cytomegalovirus disease', *Clinical Infectious Diseases*, 49(8), pp. 1160–1166. doi: 10.1086/605633.

Marshall, G. S. *et al.* (1992) 'Antibodies to recombinant-derived glycoprotein b after natural human cytomegalovirus infection correlate with neutralizing activity', *Journal of Infectious Diseases*, 165(2), pp. 381–384. doi: 10.1093/infdis/165.2.381.

Martí-Carreras, J. and Maes, P. (2019) 'Human cytomegalovirus genomics and transcriptomics through the lens of next-generation sequencing: revision and future challenges', *Virus Genes*, 55(2), pp. 138–164. doi: 10.1007/s11262-018-1627-3.

Martinez-Martin, N. *et al.* (2018) 'An Unbiased Screen for Human Cytomegalovirus Identifies Neuropilin-2 as a Central Viral Receptor', *Cell*, 174(5), pp. 1158-1171.e19. doi:

10.1016/j.cell.2018.06.028.
Mattick, C. *et al.* (2004) 'Linkage of human cytomegalovirus glycoprotein gO variant groups identified from worldwide clinical isolates with gN genotypes, implications for disease associations and evidence for N-terminal sites of positive selection', *Virology*, 318(2), pp. 582–597. doi: 10.1016/j.virol.2003.09.036.
Mendelson, M. *et al.* (1996) 'Detection of endogenous human cytomegalovirus in CD34+ bone marrow progenitors', *Journal of General Virology*, 77(12), pp. 3099–3102. doi: 10.1099/0022-1317-77-12-3099.
Mettenleiter, T. C. (2002) 'Herpesvirus Assembly and Egress', *Journal of Virology*, 76(4), pp. 1537–1547. doi: 10.1128/jvi.76.4.1537-1547.2002.
Meyer-König, U. *et al.* (1998) 'Simultaneous infection of healthy people with multiple human cytomegalovirus strains', *Lancet*, 352(9136), pp. 1280–1281. doi: 10.1016/S0140-6736(05)70487-6.
Miescher, S. M. *et al.* (2015) 'In vitro evaluation of cytomegalovirus-specific hyperimmune globulins vs. standard intravenous immunoglobulins', *Vox Sanguinis*, 109(1), pp. 71–78. doi: 10.1111/vox.12246.
Moorman, N. J. *et al.* (2010) 'A targeted spatial-temporal proteomics approach implicates multiple cellular trafficking pathways in human cytomegalovirus virion maturation', *Molecular and Cellular Proteomics*, 9(5), pp. 851–860. doi: 10.1074/mcp.M900485-MCP200.
Murphy, E. *et al.* (2003) 'Reevaluation of human cytomegalovirus coding potential', *Proceedings of the National Academy of Sciences of the United States of America*, 100(23), pp. 13585–13590. doi: 10.1073/pnas.1735466100.
Murphy, E. and Shenk, T. E. (2008) 'Human cytomegalovirus genome', *Current Topics in Microbiology and Immunology*, 325, pp. 1–19. doi: 10.1007/978-3-540-77349-8_1.
Murrell, I. *et al.* (2017) 'The pentameric complex drives immunologically covert cell-cell transmission of wild-type human cytomegalovirus', *Proceedings of the National Academy of Sciences of the United States of America*, 114(23), pp. 6104–6109. doi: 10.1073/pnas.1704809114.
Newcomb, W. W. *et al.* (1996) 'Assembly of the herpes simplex virus capsid: Characterization of intermediates observed during cell-free capsid formation', *Journal of Molecular Biology*, 263(3), pp. 432–446. doi: 10.1006/jmbi.1996.0587.
Nguyen, C. C. *et al.* (2018) 'Human Cytomegalovirus Tropism Modulator UL148 Interacts with SEL1L, a Cellular Factor That Governs Endoplasmic Reticulum-Associated Degradation of the Viral Envelope Glycoprotein gO', *Journal of Virology*, 92(18). doi: 10.1128/jvi.00688-18.
Nguyen, C. C. and Kamil, J. P. (2018) 'Pathogen at the gates: Human cytomegalovirus entry and cell tropism', *Viruses*, 10(12). doi: 10.3390/v10120704.
Nicola, A. V. (2016) 'Herpesvirus Entry into Host Cells Mediated by Endosomal Low pH', *Traffic*, 17(9), pp. 965–975. doi: 10.1111/tra.12408.
Nigro, G. *et al.* (2005) 'Passive Immunization during Pregnancy for Congenital Cytomegalovirus Infection', *New England Journal of Medicine*, 353(13), pp. 1350–1362. doi: 10.1056/nejmoa043337.
Nogalski, M. T. *et al.* (2013) 'The HCMV gH/gL/UL128-131 Complex Triggers the Specific Cellular Activation Required for Efficient Viral Internalization into Target Monocytes', *PLoS Pathogens*, 9(7). doi: 10.1371/journal.ppat.1003463.

Ogawa-Goto, K. *et al.* (2003) 'Microtubule Network Facilitates Nuclear Targeting of Human Cytomegalovirus Capsid', *Journal of Virology*, 77(15), pp. 8541–8547. doi: 10.1128/jvi.77.15.8541-8547.2003.

Paterson, D. A. *et al.* (2002) 'A role for human cytomegalovirus glycoprotein O (gO) in cell fusion and a new hypervariable locus', *Virology*, 293(2), pp. 281–294. doi: 10.1006/viro.2001.1274.

Patrone, M. *et al.* (2007) 'Cytomegalovirus UL131-128 Products Promote gB Conformational Transition and gB-gH Interaction during Entry into Endothelial Cells', *Journal of Virology*, 81(20), pp. 11479–11488. doi: 10.1128/jvi.00788-07.

Pignatelli, S. *et al.* (2004) 'Genetic polymorphisms among human cytomegalovirus (HCMV) wild-type strains', *Reviews in Medical Virology*, 14(6), pp. 383–410. doi: 10.1002/rmv.438.

Plachter, B., Sinzger, C. and Jahn, G. (1996) 'Cell types involved in replication and distribution of human cytomegalovirus', *Advances in Virus Research*, 46, pp. 195–261. doi: 10.1016/s0065-3527(08)60073-1.

Planitzer, C. B. *et al.* (2011) 'Cytomegalovirus neutralization by hyperimmune and standard intravenous immunoglobulin preparations', *Transplantation*, 92(3), pp. 267–270. doi: 10.1097/TP.0b013e318224115e.

Podlech, J. *et al.* (2015) 'Principles for studying in vivo attenuation of virus mutants: defining the role of the cytomegalovirus gH/gL/gO complex as a paradigm', *Medical Microbiology and Immunology*, 204(3), pp. 295–305. doi: 10.1007/s00430-015-0405-2.

Pötzsch, S. *et al.* (2011) 'B cell repertoire analysis identifies new antigenic domains on glycoprotein b of human cytomegalovirus which are target of neutralizing antibodies', *PLoS Pathogens*, 7(8). doi: 10.1371/journal.ppat.1002172.

Prichard, M. N. *et al.* (2001) 'A review of genetic differences between limited and extensively passaged human cytomegalovirus strains', *Reviews in Medical Virology*, 11(3), pp. 191–200. doi: 10.1002/rmv.315.

Prince, H. E. and Lapé-Nixon, M. (2014) 'Role of cytomegalovirus (CMV) IgG avidity testing in diagnosing primary CMV infection during pregnancy', *Clinical and Vaccine Immunology*, 21(10), pp. 1377–1384. doi: 10.1128/CVI.00487-14.

Puchhammer-Stöckl, E. *et al.* (2006) 'Emergence of multiple cytomegalovirus strains in blood and lung of lung transplant recipients', *Transplantation*, 81(2), pp. 187–194. doi: 10.1097/01.tp.0000194858.50812.cb.

Rasmussen, L. *et al.* (1991) 'Antibody response to human cytomegalovirus glycoproteins gB and gH after natural infection in humans', *Journal of Infectious Diseases*, 164(5), pp. 835–842. doi: 10.1093/infdis/164.5.835.

Rasmussen, L. *et al.* (2002) 'The Genes Encoding the gCIII Complex of Human Cytomegalovirus Exist in Highly Diverse Combinations in Clinical Isolates', *Journal of Virology*, 76(21), pp. 10841–10848. doi: 10.1128/jvi.76.21.10841-10848.2002.

Robb, R. J. *et al.* (1984) 'Amino acid sequence and post-translational modification of human interleukin 2', *Proceedings of the National Academy of Sciences of the United States of America*, 81(20 I), pp. 6486–6490. doi: 10.1073/pnas.81.20.6486.

Roby, C. and Gibson, W. (1986) 'Characterization of phosphoproteins and protein kinase activity of virions, noninfectious enveloped particles, and dense bodies of human cytomegalovirus', *Journal of Virology*, 59(3), pp. 714–727. doi: 10.1128/jvi.59.3.714-727.1986.

Roizman, B. *et al.* (1981) 'Herpesviridae: Definition, provisional nomenclature, and taxonomy', *Intervirology*, 16(4), pp. 201–217. doi: 10.1159/000149269.

Roizman, B., Knipe, D. M. and Whitley, R. J. (2001) 'Fields virology. Vol. 2'. Raven press Philadelphia:

Rozman, B. *et al.* (2022) 'Temporal dynamics of HCMV gene expression in lytic and latent infections', *Cell Reports*, 39(2). doi: 10.1016/j.celrep.2022.110653.

Ryckman, B. J. *et al.* (2006) 'Human Cytomegalovirus Entry into Epithelial and Endothelial Cells Depends on Genes UL128 to UL150 and Occurs by Endocytosis and Low-pH Fusion', *Journal of Virology*, 80(2), pp. 710–722. doi: 10.1128/jvi.80.2.710-722.2006.

Ryckman, B. J. *et al.* (2008) 'Characterization of the Human Cytomegalovirus gH/gL/UL128-131 Complex That Mediates Entry into Epithelial and Endothelial Cells', *Journal of Virology*, 82(1), pp. 60–70. doi: 10.1128/jvi.01910-07.

Ryckman, B. J., Chase, M. C. and Johnson, D. C. (2008) 'HCMV gH/gL/UL128-131 interferes with virus entry into epithelial cells: Evidence for cell type-specific receptors', *Proceedings of the National Academy of Sciences of the United States of America*, 105(37), pp. 14118–14123. doi: 10.1073/pnas.0804365105.

Sampaio, K. L. *et al.* (2016) 'The contribution of pUL74 to growth of human cytomegalovirus is masked in the presence of RL13 and UL128 expression', *Journal of General Virology*, 97(8), pp. 1917–1927. doi: 10.1099/jgv.0.000475.

Sathiyamoorthy, K. *et al.* (2017) 'The COMPLEXity in herpesvirus entry', *Current Opinion in Virology*, 24, pp. 97–104. doi: 10.1016/j.coviro.2017.04.006.

Schrier, R. D., Nelson, J. A. and Oldstone, M. B. A. (1985) 'Detection of human cytomegalovirus in peripheral blood lymphocytes in a natural infection', *Science*, 230(4729), pp. 1048–1051. doi: 10.1126/science.2997930.

Schultz, E. P. *et al.* (2016) 'Scanning Mutagenesis of Human Cytomegalovirus Glycoprotein gH/gL', *Journal of Virology*, 90(5), pp. 2294–2305. doi: 10.1128/jvi.01875-15.

Schultz, E. P. *et al.* (2021) 'Mutagenesis of Human Cytomegalovirus Glycoprotein L Disproportionately Disrupts gH/gL/gO over gH/gL/pUL128-131', *Journal of Virology*, 95(17). doi: 10.1128/jvi.00612-21.

Scrivano, L. *et al.* (2011) 'HCMV spread and cell tropism are determined by distinct virus populations', *PLoS Pathogens*, 7(1). doi: 10.1371/journal.ppat.1001256.

Sénéchal, B. *et al.* (2004) 'Infection of mature monocyte-derived dendritic cells with human cytomegalovirus inhibits stimulation of T-cell proliferation via the release of soluble CD83', *Blood*, 103(11), pp. 4207–4215. doi: 10.1182/blood-2003-12-4350.

Siddiquey, M. N. A. *et al.* (2021) 'The Human Cytomegalovirus Protein UL116 Interacts with the Viral Endoplasmic-Reticulum-Resident Glycoprotein UL148 and Promotes the Incorporation of gH/gL Complexes into Virions', *Journal of Virology*, 95(15). doi: 10.1128/jvi.02207-20.

Sijmons, S. *et al.* (2015) 'High-Throughput Analysis of Human Cytomegalovirus Genome Diversity Highlights the Widespread Occurrence of Gene-Disrupting Mutations and Pervasive Recombination',

Journal of Virology, 89(15), pp. 7673–7695. doi: 10.1128/jvi.00578-15.

Sijmons, S., Van Ranst, M. and Maes, P. (2014) 'Genomic and functional characteristics of human cytomegalovirus revealed by next-generation sequencing', *Viruses*, 6(3), pp. 1049–1072. doi: 10.3390/v6031049.

Sinclair, J. and Sissons, P. (2006) 'Latency and reactivation of human cytomegalovirus', *Journal of General Virology*, 87(7), pp. 1763–1779. doi: 10.1099/vir.0.81891-0.

Sinzger, C. *et al.* (1995) 'Fibroblasts, epithelial cells, endothelial cells and smooth muscle cells are major targets of human cytomegalovirus infection in lung and gastrointestinal tissues', *Journal of General Virology*, 76(4), pp. 741–750. doi: 10.1099/0022-1317-76-4-741.

Sinzger, C. *et al.* (1999) 'Modification of human cytomegalovirus tropism through propagation in vitro is associated with changes in the viral genome', *Journal of General Virology*, 80(11), pp. 2867–2877. doi: 10.1099/0022-1317-80-11-2867.

Snydman, D. R. *et al.* (1987) 'Use of Cytomegalovirus Immune Globulin to Prevent Cytomegalovirus Disease in Renal-Transplant Recipients', *New England Journal of Medicine*, 317(17), pp. 1049–1054. doi: 10.1056/nejm198710223171703.

Sohn, Y. M. *et al.* (1991) 'Cytomegalovirus infection in sexually active adolescents', *Journal of Infectious Diseases*, 163(3), pp. 460–463. doi: 10.1093/infdis/163.3.460.

Stampfer, S. D. and Heldwein, E. E. (2013) 'Stuck in the middle: Structural insights into the role of the gH/gL heterodimer in herpesvirus entry', *Current Opinion in Virology*, 3(1), pp. 13–19. doi: 10.1016/j.coviro.2012.10.005.

Stanton, R. *et al.* (2005) 'Stability of Human cytomegalovirus genotypes in persistently infected renal transplant recipients', *Journal of Medical Virology*, 75(1), pp. 42–46. doi: 10.1002/jmv.20235.

Stanton, R. J. *et al.* (2010) 'Reconstruction of the complete human cytomegalovirus genome in a BAC reveals RL13 to be a potent inhibitor of replication', *Journal of Clinical Investigation*, 120(9), pp. 3191–3208. doi: 10.1172/JCI42955.

Staras, S. A. S. *et al.* (2008) 'Influence of sexual activity on cytomegalovirus seroprevalence in the United States, 1988-1994', *Sexually Transmitted Diseases*, 35(5), pp. 472–479. doi: 10.1097/OLQ.0b013e3181644b70.

Stegmann, C. *et al.* (2017) 'A derivative of platelet-derived growth factor receptor alpha binds to the trimer of human cytomegalovirus and inhibits entry into fibroblasts and endothelial cells', *PLoS Pathogens*, 13(4). doi: 10.1371/journal.ppat.1006273.

Stegmann, C. *et al.* (2019) 'The N Terminus of Human Cytomegalovirus Glycoprotein O Is Important for Binding to the Cellular Receptor PDGFRα', *Journal of Virology*, 93(11). doi: 10.1128/jvi.00138-19.

Tan, C. W. *et al.* (2020) 'A SARS-CoV-2 surrogate virus neutralization test based on antibody-mediated blockage of ACE2–spike protein–protein interaction', *Nature Biotechnology*, 38(9), pp. 1073–1078. doi: 10.1038/s41587-020-0631-z.

Theiler, R. N. and Compton, T. (2002) 'Distinct Glycoprotein O Complexes Arise in a Post-Golgi Compartment of Cytomegalovirus-Infected Cells', *Journal of Virology*, 76(6), pp. 2890–2898. doi: 10.1128/jvi.76.6.2890-2898.2002.

Urban, M. *et al.* (1996) 'Glycoprotein H of human cytomegalovirus is a major antigen for the

neutralizing humoral immune response', *Journal of General Virology*, 77(7), pp. 1537–1547. doi: 10.1099/0022-1317-77-7-1537.

Urban, M., Britt, W. and Mach, M. (1992) 'The dominant linear neutralizing antibody-binding site of glycoprotein gp86 of human cytomegalovirus is strain specific', *Journal of Virology*, 66(3), pp. 1303–1311. doi: 10.1128/jvi.66.3.1303-1311.1992.

Vanarsdall, A. L. *et al.* (2016) 'Human Cytomegalovirus gH/gL Forms a Stable Complex with the Fusion Protein gB in Virions', *PLoS Pathogens*, 12(4). doi: 10.1371/journal.ppat.1005564.

Vanarsdall, A. L. *et al.* (2019) 'HCMV trimer- and pentamer-specific antibodies synergize for virus neutralization but do not correlate with congenital transmission', *Proceedings of the National Academy of Sciences of the United States of America*, 116(9), pp. 3728–3733. doi: 10.1073/pnas.1814835116.

Vanarsdall, A. L., Chase, M. C. and Johnson, D. C. (2011) 'Human Cytomegalovirus Glycoprotein gO Complexes with gH/gL, Promoting Interference with Viral Entry into Human Fibroblasts but Not Entry into Epithelial Cells', *Journal of Virology*, 85(22), pp. 11638–11645. doi: 10.1128/jvi.05659-11.

Vankova, O. E., Brusnigina, N. F. and Novikova, N. A. (2023) 'NGS Technology in Monitoring the Genetic Diversity of Cytomegalovirus Strains', *Sovremennye Tehnologii v Medicine*, 15(2), pp. 41–46. doi: 10.17691/stm2023.15.2.04.

Varnum, S. M. *et al.* (2004) 'Identification of Proteins in Human Cytomegalovirus (HCMV) Particles: the HCMV Proteome', *Journal of Virology*, 78(20), pp. 10960–10966. doi: 10.1128/jvi.78.20.10960-10966.2004.

Vezzani, G. *et al.* (2021) 'The Human Cytomegalovirus UL116 Glycoprotein Is a Chaperone to Control gH-Based Complexes Levels on Virions', *Frontiers in Microbiology*, 12. doi: 10.3389/fmicb.2021.630121.

Vigerust, D. J. and Shepherd, V. L. (2007) 'Virus glycosylation: role in virulence and immune interactions', *Trends in Microbiology*, 15(5), pp. 211–218. doi: 10.1016/j.tim.2007.03.003.

Wang, D. *et al.* (2011) 'Quantitative analysis of neutralizing antibody response to human cytomegalovirus in natural infection', *Vaccine*, 29(48), pp. 9075–9080. doi: 10.1016/j.vaccine.2011.09.056.

Wang, H. Y. *et al.* (2021) 'Common polymorphisms in the glycoproteins of human cytomegalovirus and associated strain-specific immunity', *Viruses*, 13(6). doi: 10.3390/v13061106.

Weststrate, M. W., Geelen, J. L. M. C. and Van Der Noordaa, J. (1980) 'Human cytomegalovirus DNA: Physical maps for the restriction endonucleases BglII, HindIII and XbaI', *Journal of General Virology*, 49(1), pp. 1–21. doi: 10.1099/0022-1317-49-1-1.

Wilkinson, G. W. G. *et al.* (2015) 'Human cytomegalovirus: taking the strain', *Medical Microbiology and Immunology*, 204(3), pp. 273–284. doi: 10.1007/s00430-015-0411-4.

Wille, P. T. *et al.* (2010) 'A Human Cytomegalovirus gO-Null Mutant Fails To Incorporate gH/gL into the Virion Envelope and Is Unable To Enter Fibroblasts and Epithelial and Endothelial Cells', *Journal of Virology*, 84(5), pp. 2585–2596. doi: 10.1128/jvi.02249-09.

Wille, P. T. *et al.* (2013) 'Human cytomegalovirus (HCMV) glycoprotein gB promotes virus entry in Trans acting as the viral fusion protein rather than as a receptor-binding protein', *mBio*, 4(3). doi: 10.1128/mBio.00332-13.

Wu, Y. *et al.* (2017) 'Human cytomegalovirus glycoprotein complex gH/gL/gO uses PDGFR-α as a key for entry', *PLoS Pathogens*, 13(4). doi: 10.1371/journal.ppat.1006281.

Yu, X. *et al.* (2011) 'Biochemical and structural characterization of the capsid-bound tegument proteins of human cytomegalovirus', *Journal of Structural Biology*, 174(3), pp. 451–460. doi: 10.1016/j.jsb.2011.03.006.

Yuan, S. *et al.* (2018) 'Cryo-EM structure of a herpesvirus capsid at 3.1 Å', *Science*, 360(6384). doi: 10.1126/science.aao7283.

Zehner, M. *et al.* (2023) 'Single-cell analysis of memory B cells from top neutralizers reveals multiple sites of vulnerability within HCMV Trimer and Pentamer', *Immunity*, pp. 2602-2620.e10. doi: 10.1016/j.immuni.2023.10.009.

Zhang, L. *et al.* (2018) 'Expression Levels of Glycoprotein O (gO) Vary between Strains of Human Cytomegalovirus, Influencing the Assembly of gH/gL Complexes and Virion Infectivity', *Journal of Virology*, 92(15). doi: 10.1128/jvi.00606-18.

Zhou, M. *et al.* (2013) 'Comparative Analysis of gO Isoforms Reveals that Strains of Human Cytomegalovirus Differ in the Ratio of gH/gL/gO and gH/gL/UL128-131 in the Virion Envelope', *Journal of Virology*, 87(17), pp. 9680–9690. doi: 10.1128/jvi.01167-13.

Zhou, M., Lanchy, J.-M. and Ryckman, B. J. (2015) 'Human Cytomegalovirus gH/gL/gO Promotes the Fusion Step of Entry into All Cell Types, whereas gH/gL/UL128-131 Broadens Virus Tropism through a Distinct Mechanism', *Journal of Virology*, 89(17), pp. 8999–9009. doi: 10.1128/jvi.01325-15.

Zhou, Z. H. *et al.* (2000) 'Seeing the herpesvirus capsid at 8.5 Å', *Science*, 288(5467), pp. 877–880. doi: 10.1126/science.288.5467.877.

Zuhair, M. *et al.* (2019) 'Estimation of the worldwide seroprevalence of cytomegalovirus: A systematic review and meta-analysis', *Reviews in Medical Virology*, 29(3). doi: 10.1002/rmv.2034.

van Zuylen, W. J. *et al.* (2017) 'Prevalence of cytomegalovirus carriage among childcare staff', *Journal of Paediatrics and Child Health*, 53(7), p. 724. doi: 10.1111/jpc.13600.

6 Table of Figures

7 Supplementary Material

7.1 Expression vectors used for transfection of HEK293T cells

For expression of the trimeric gH/gL/gO complex, HEK293T cells were transfected with plasmid DNA encoding the gH1 and gL subunits and either the gO1c or gO4 subunit. The coding sequences were adapted with a 30 aa IL-2 signal sequence, which was replaced by the first

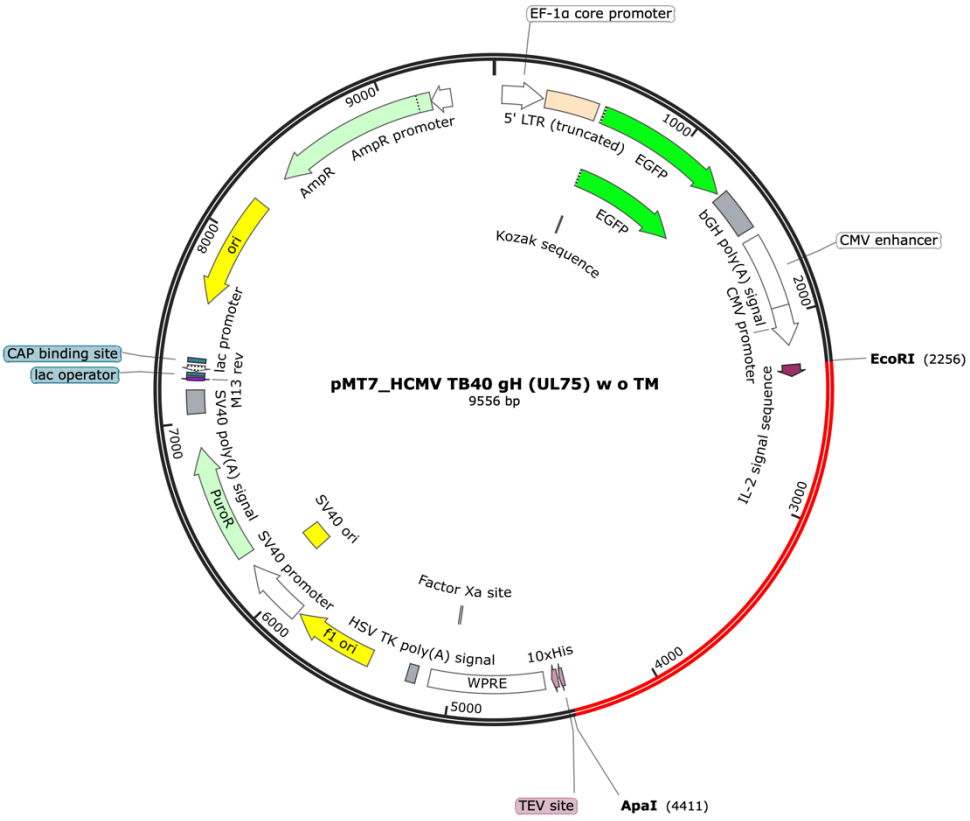

Supplementary Figure S1: Plasmid design for expression of the gH1 subunit. *Plasmid pMT7_HCMV TB40/E gH1 (UL75) w/o TM contains the codon optimized DNA sequence encoding the HCMV TB40/E UL75 gene carrying a deletion of the transmembrane domain and supplemented with an IL-2 signal sequence (red; 2.155 nts). The vector backbone consists of the pMT7 mammalian expression vector, which provided several displayed features. Restriction sites used for cloning are displayed.*

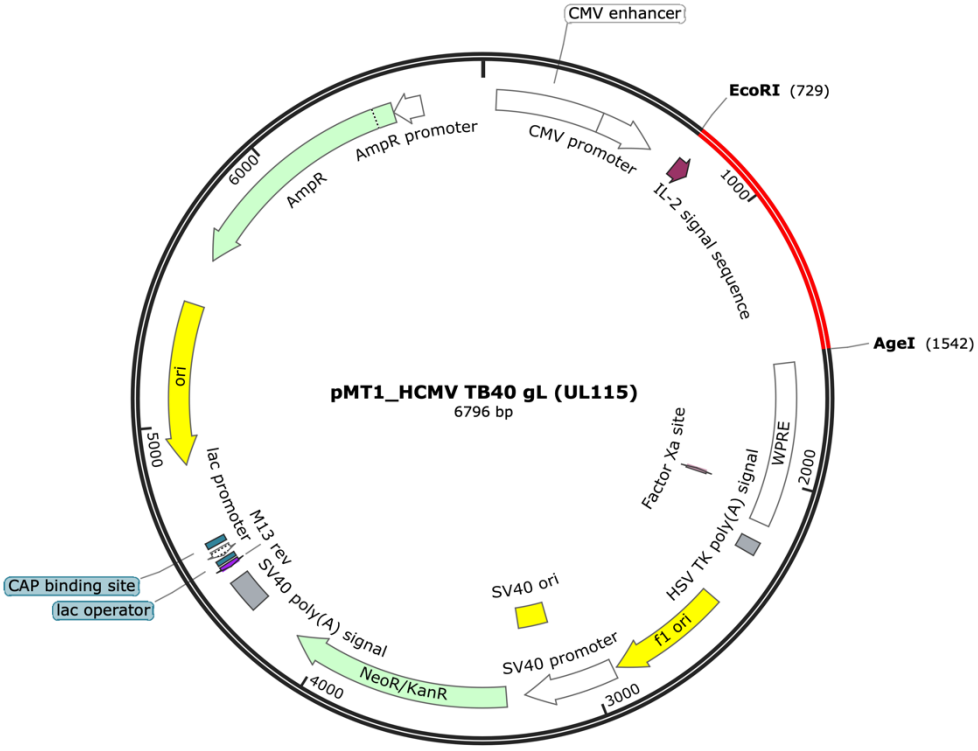

Supplementary Figure S2: Plasmid design for expression of the gL subunit. *Plasmid pMT1_HCMV TB40/E gL (UL115) contains the codon optimized DNA sequence encoding the HCMV TB40/E UL115 gene supplemented with an IL-2 signal sequence (red; 813 nts). The vector backbone consists of the pMT1 mammalian expression vector, which provided several displayed features. Restriction sites used for cloning are displayed.*

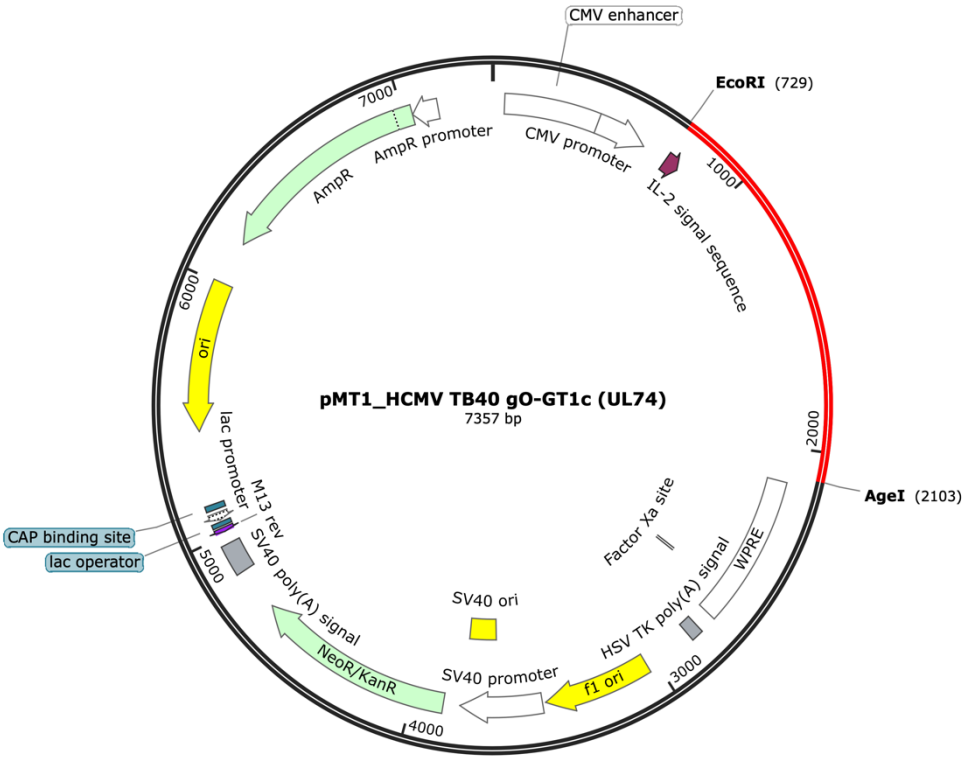

Supplementary Figure S3: Plasmid design for expression of the gO1c subunit. *Plasmid pMT1_HCMV TB40/E gO1c (UL74) contains the codon optimized DNA sequence encoding the HCMV TB40/E UL74 gene supplemented with an IL-2 signal sequence (red; 1.374 nts). The vector backbone consists of the pMT1 mammalian expression vector, which provided several displayed features. Restriction sites used for cloning are displayed.*

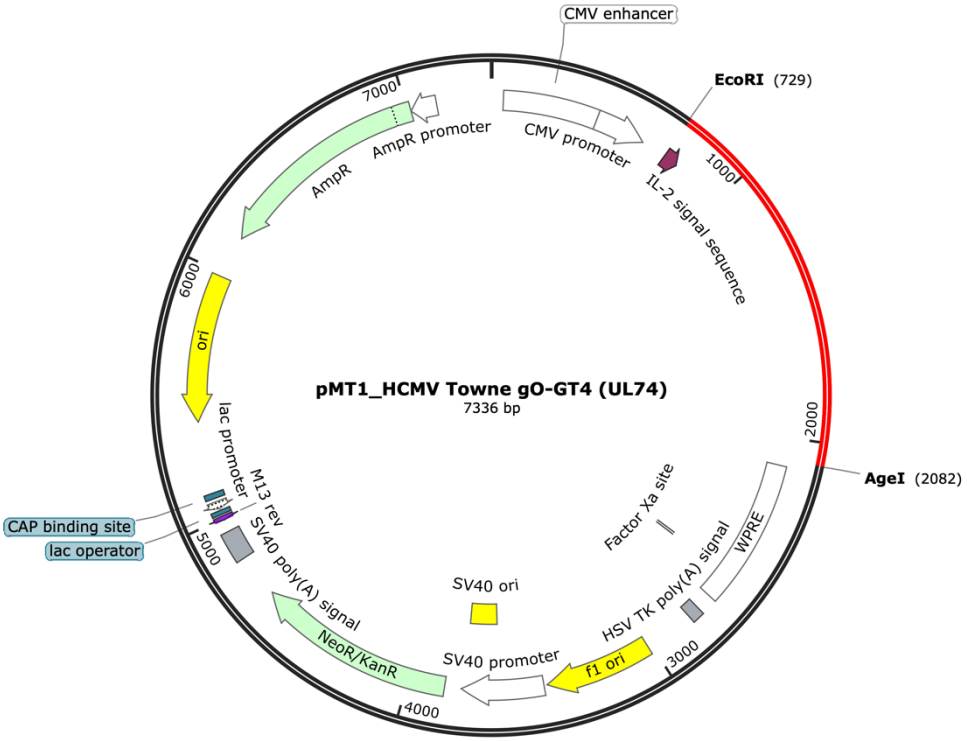

Supplementary Figure S4: Plasmid design for expression of the gO4 subunit. *Plasmid pMT1_HCMV Towne gO4 (UL74) contains the codon optimized DNA sequence encoding the HCMV Towne UL74 gene supplemented with an IL-2 signal sequence (red; 1.353 nts). The vector backbone consists of the pMT1 mammalian expression vector, which provided several displayed features. Restriction sites used for cloning are displayed.*

7.2 High scale production and purification

Western Blot of precipitated supernatant derived from transfections (T23-30) for high scale production of soluble gH1/gL/gO4 was performed in order to control successful expression of trimeric complex and the presence of the gH-associated 10x His-tag. T23 and T25 cells showed a confluency of approximately 50% 24h post cell seed and were therefor incubated for another 24h prior to transfection

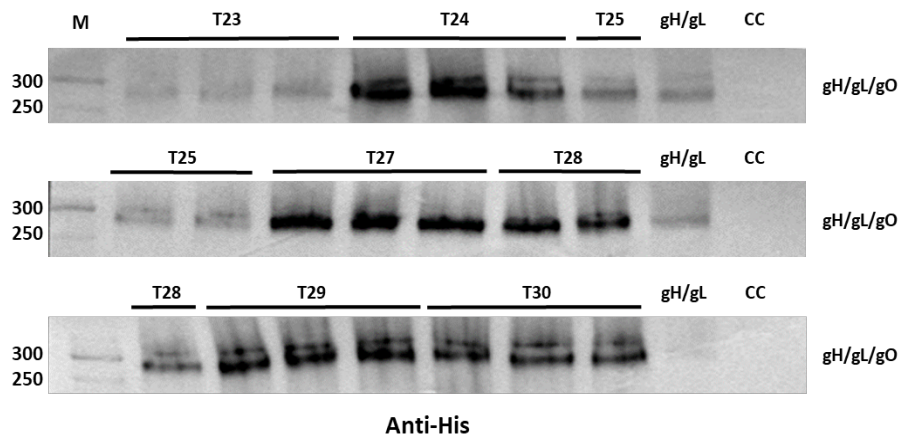

Supplementary Figure S5: High-scale production of soluble gH1/gL/gO4. *Western Blot of precipitated supernatant derived from transfections (T23-30) from high scale production of soluble gH/gL/gO using anti 6xhis-tag mAb. Samples were analyzed upon non-reducing conditions. T#… Transfection experiment, gH/gL… Control transfection using gH (TB40/E) and gL (TB40/E) DNA only, CC… Control culture treated with transfection reagent only.*

7.3 Calibration of SEC column

Prior to purification of trimeric gH/gL/gO, elution properties of the Superdex 200 Increase 10/300 GL column were determined using a high molecular weight protein standard. The column void volume (V_0) represented the earliest point of elution, applying to proteins of high molecular, which would pass by the porous bead matrix. V_0 was determined through loading of Dextran Blue with a molecular mass (M_r) of 2000 KDa. Dextran Blue eluted between 8 - 25 mL, with a maximum absorbance of approximately 45 mAU at 8.38 mL.

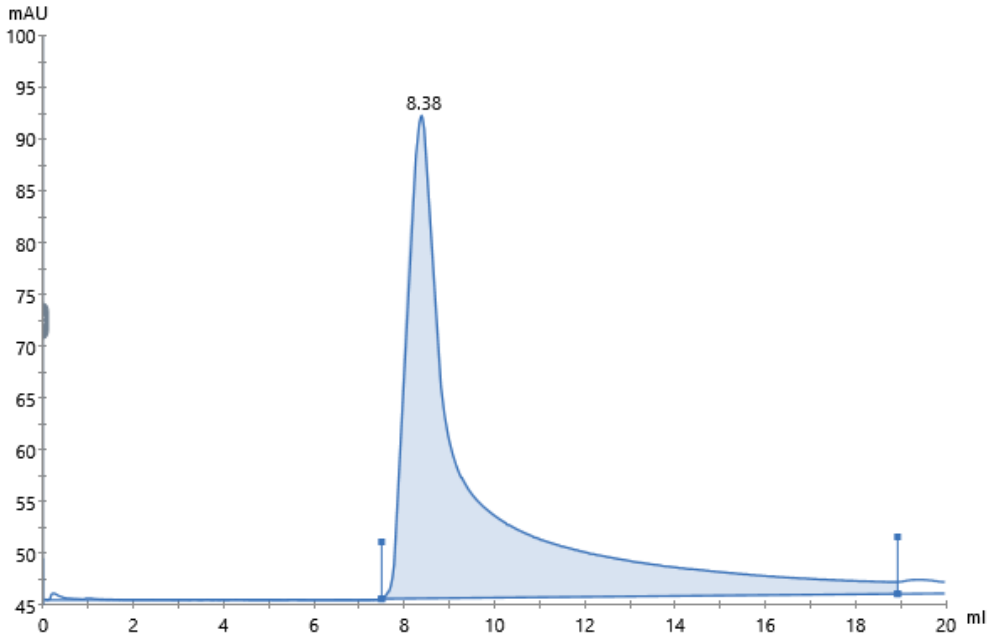

Supplementary Figure S6: Column calibration prior to purification of trimeric gH/gL/gO. *Loading of Dextran Blue allowed for the determination of the column void volume (V0), which represents the earliest point of elution for proteins of high molecular mass.*

Table 12: Protein-related data obtained from the column calibration. *Data regarding the relative molecular mass and elution volume of Dextran Blue.*

Peak	Protein	M_r (Dalton)	Retention (mL)
A	Dextran Blue	2.000.000	8.4

Calibration of the column was continued with a mix of five different standard proteins utilizing molecular mass range of 669 – 44 kDa. Loading of the standard led to the elution of 6 peaks between 8 – 17 mL. Thyroglobulin being the largest protein eluted in form of two peaks. According to the manuals instructuons the expected peak for thyroglubulin elution was the second one with a retention of 9.18 mL. The first peak with a retention of 8.61 mL was explained to be a consequence of dimerization of thyroglobulin, thus increasing its molecular mass, which in turn led to earlier elution. The other standard proteins ferritin, aldolase conalbumin and ovalbumin eluted at 10.3, 12.4, 13.8 and 14,9 mL, respectively. Since trimeric gH/gL/gO exhibited a molecular mass of approx 270 kDa (according to SDS-Page), we expect an elution between 10 – 12.5 mL.

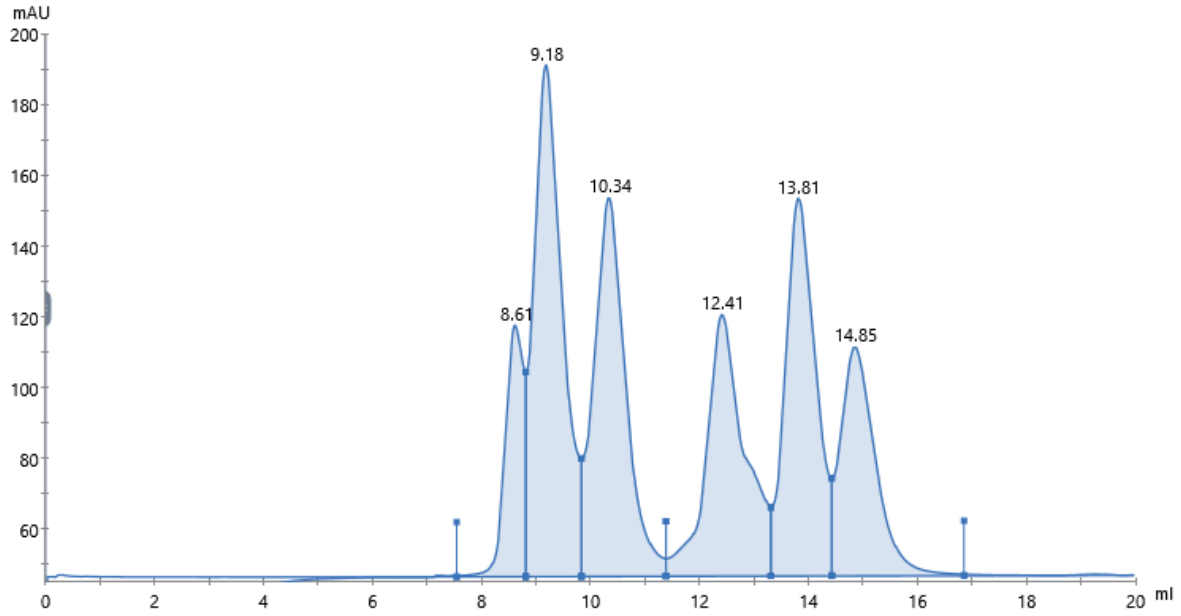

Supplementary Figure S7: Column calibration prior to purification of trimeric gH/gL/gO. *Loading a HMW-standard containing thyroglobulin, ferritin, aldolase, conalbumin and ovalbumin allowed for estimation of elution volumina of unknown proteins according to their size.*

Table 13: Protein-related data obtained from the column calibration. *Data regarding the relative molecular mass, elution volume and the corresponding fraction of the proteins comprised by the high molecular weight standard.*

Peak	Protein	M_r (Dalton)	Retention (mL)	Fractions
A	-	-	8.6	1.A.2 – 1.A.4
B	Thyroglobulin	669.000	9.2	1.A.4 – 1.A.6
C	Ferritin	440.000	10.3	1.A.6 – 1.B.1
D	Aldolase	158.000	12.4	1.B.1 – 1.B.5
E	Conalbumin	75.000	13.8	1.B.5 – 1.B.7
F	Ovalbumin	44.000	14.8	1.B.7 – 1.C.4

7.4 Distribution of soluble gH/gL/gO after size exclusion chromatography

In the course of size exclusion chromatography, the eluted proteins were collected in fractions of 0.5 mL. The collected fractions were pooled into six fractions according to the peak measurement of the chromatogram and further analyzed via western blot control using his- and gO-specific mAbs. Detection with both antibodies showed similar distribution patterns of soluble gH/gL/gO among the fractions one to six, while the majority of gH/gL/gO eluted within

fractions one to three. Since proteins elute according to their size it was interesting to observe, that no smaller histidine-specific protein species was detected upon western blot analysis.

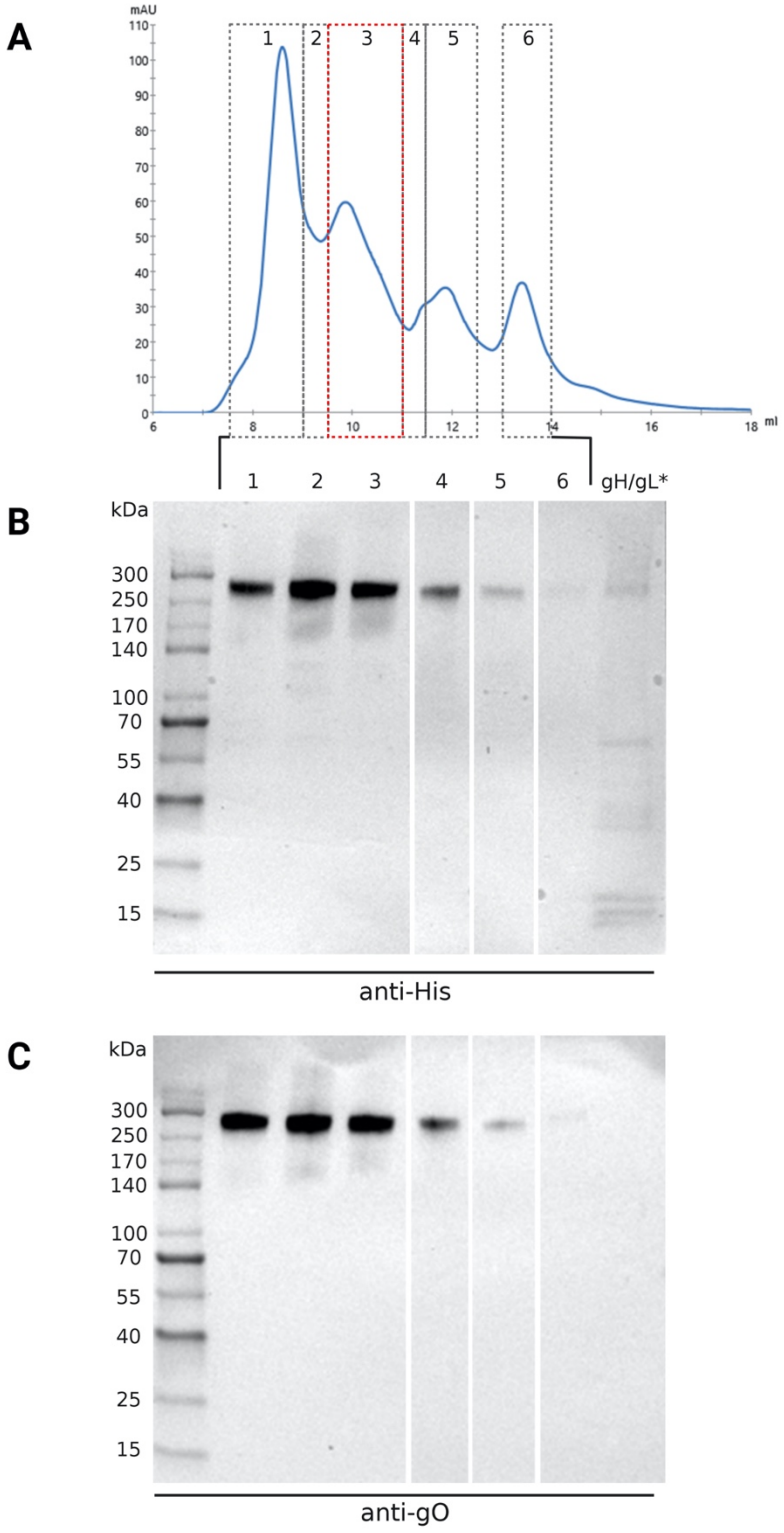

Supplementary Figure S8: Analysis of purified proteins after the size exclusion chromatography. (A)*Chromatogram derived by the size exclusion chromatography of His-purified concentrated protein sample containing gH/gL/gO. Fractions were either pooled according to peaks or kept as single*

fractions (dashed frames 1 – 6) ***(B and C)*** *Western Blot analysis of the fractions pools using His- and gO-specific mAbs revealing the elution of the majority of soluble gH/gL/gO among the first two peaks (fraction pools 1 – 3).*

7.5 Analysis of sequential sera for the generation of gH/gL/gO-specific inhibitory antibodies

In order to follow-up on the generation of iAbs targeting the gH/gL/gO, we tested sequential sera derived from patients that were diagnosed with low and intermediate HCMV-specific IgG avidity.

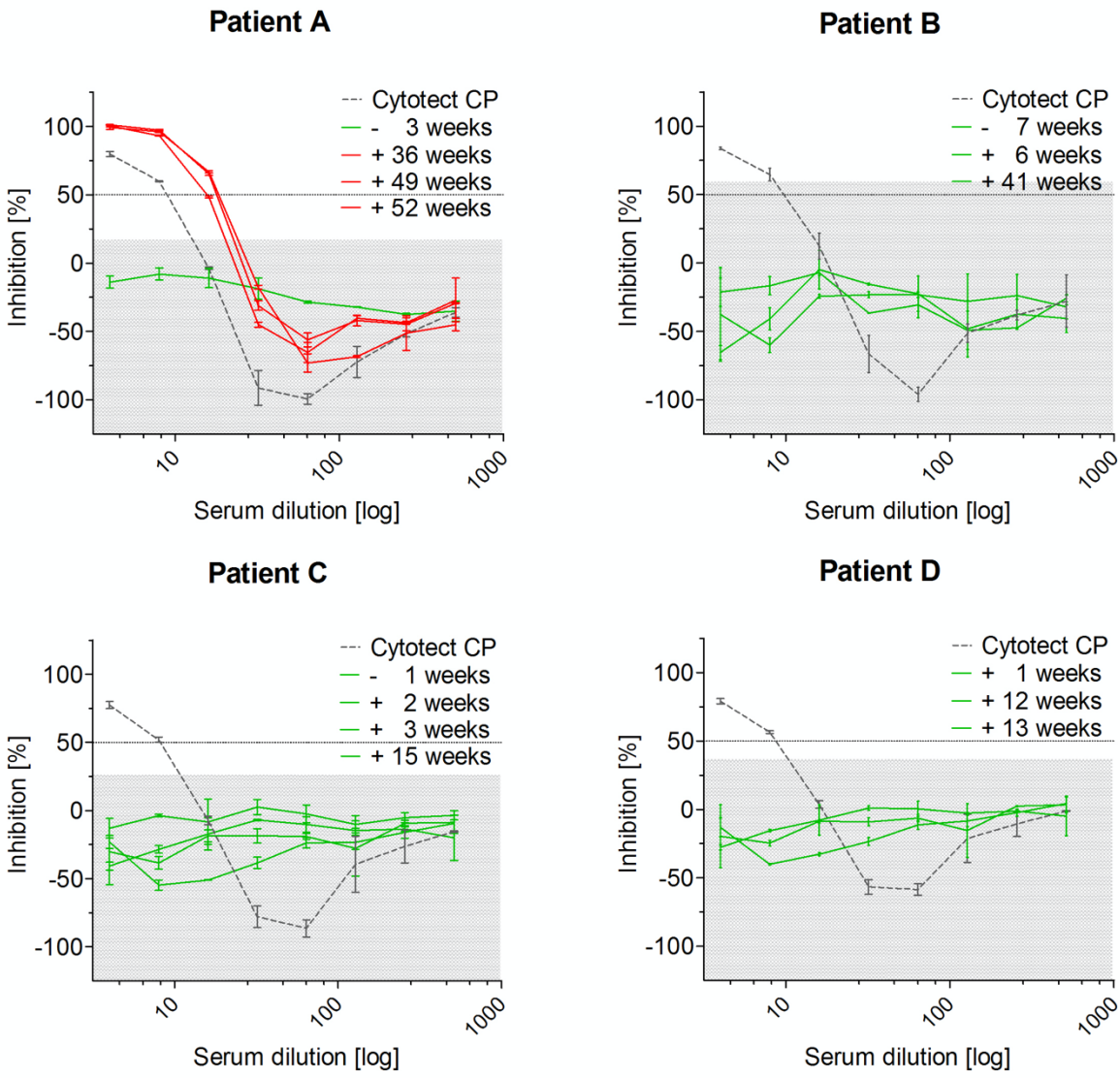

Supplementary Figure S9: Serum antibody-mediated inhibition of gH/gL/gO upon avidity maturation from low avidity. *Sequential serum samples derived from patients A – D as well as Cytotect®CP (black dashed) was tested in a two-fold serial dilution ranging from four- to 512-fold dilutions.*

Inhibitory and non-inhibitory sera were indicated in red and green respectively. The IC50 (dashed line) and inhibition cutoff (ØHCMV seronegative – 3x SD) are indicated (grey area).

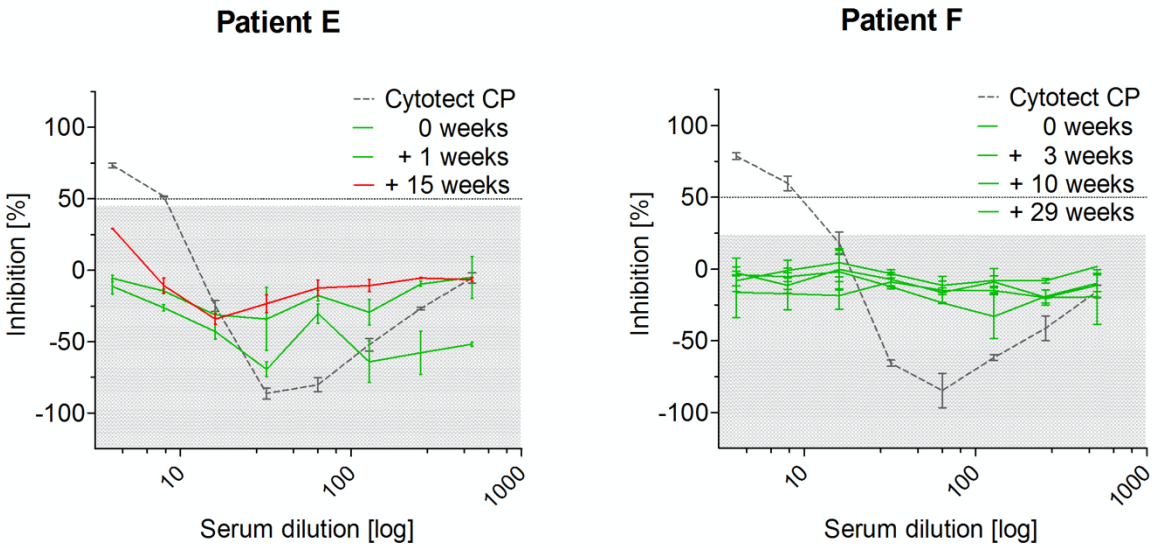

Supplementary Figure S10: Serum antibody-mediated inhibition of gH/gL/gO upon avidity maturation from intermediate avidity. *Sequential serum samples derived from patients E and F as well as Cytotect®CP (black dashed) was tested in a two-fold serial dilution ranging from four- to 512-fold dilutions. Inhibitory and non-inhibitory sera were indicated in red and green respectively. The IC50 (dashed line) and inhibition cutoff (ØHCMV seronegative – 3x SD) are indicated (grey area).*

Zusammenfassung

Der Zelleintritt des humanen Cytomegalovirus (HCMV) in Fibroblasten wird durch die Bindung des trimeren Glykoproteinkomplexes gH/gL/gO an den platelet-derived growth factor receptor alpha (PDGFRα) der Wirtszelle initiiert. Trotz ihrer wichtigen Rolle bei der Verhinderung der Virusausbreitung ist wenig über die humorale Immunantwort in Form von Serumantikörpern bekannt, die diese Interaktion im Besonderen hemmen, und über ihre Fähigkeit, eine stammübergreifende Immunität in Bezug auf die polymorphe gO-Untereinheit zu bieten. Um uns dieser Frage zu nähern, haben wir die Expression und Reinigung eines löslichen trimeren Komplexes unter Verwendung der Varianten gO1c (TB40/E) und gO4 (Towne) sowie die Entwicklung eines Rezeptorbindungstests angestrebt, um sowohl die Präsenz solch hemmender Antikörper nachzuweisen und ihr ungefähres Auftreten zu bestimmen. Im Gegensatz zur Expression von trimerem gH/gL/gO unter Verwendung der gO4-Untereinheit führte die Koexpression mit der gO1c-Untereinheit zu einer geringen Proteinausbeute, was auf einen subtilen Expressionsmechanismus mit Abhängigkeit von den gO-Genotypen und möglicherweise anderen Kofaktoren schließen lässt. Die Serumanalyse zeigte, dass HCMV-seropositive Personen mit hohem IgG-Titer und Cytotect®CP, ein Hyperimmunglobulinpräparat, die Rezeptorbindung dosisabhängig hemmen. Der Vergleich zwischen HCMV-seropositiven Personen mit unterschiedlicher IgG-Avidität und eine Nachverfolgung der IgG-Aviditätsreifung innerhalb einzelner Patienten ergab, dass hemmende Antikörper nur bei hoher IgG-Avidität vorhanden waren. Unsere aktuellen Daten deuten darauf hin, dass trimerspezifische IgG-Antikörper im Serum, welche die Bindung an den PDGFRα-Rezeptor blockieren, tatsächlich nach einer Primärinfektion gebildet werden, aber erst spät im Verlauf der IgG-Aviditätsreifung auftreten.

Humanes Cytomegalovirus; Glykoproteinkomplex; Thrombozytenwachstumsfaktor-Rezeptor; Humorale Immunantwort; IgG Avidität; Proteinreinigung; Enzyme-linked immunosorbent assay;

Abbreviations

BSA	Bovine serum albumin
DNA	Deoxyribonucleic acid
DMEM	Dulbecco's modified eagle medium
DMEMc	Dulbecco's modified eagle medium with supplements
EDTA	Ethylenediaminetetraacetic acid
ELISA	Enzyme-linked immunosorbent assay
E. Coli	Escherichia Coli
FBS	Fetal bovine serum
FPLC	Fast protein liquid chromatography
GFP	Green fluorescent protein
gH, gL, gO	Glycoprotein H/L/O
HCMV	Human Cytomegalovirus
HEK293	Human embryonic kidney cells 293
HEPES	4-(2-hydroxyethyl)-1-piperazineethanesulfonic acid
IgG	Immunoglobulin G
IgM	Immunglobulin M
IL-2	Interleukin-2
mAU	Milli-absorbance unit
MEM	Eagle's minimal essential medium
PBS	Phosphate buffered saline
PBS-T	Phosphate buffered saline-Tween20®
PDGFRα	Platelet-derived growth factor receptor alpha
Pen-Strep	Penicillin-Streptomycin
rcf	Relative centrifugal force
RNA	Ribonucleic acid
rpm	Rotations per minute
SEC	Size exclusion chromatography
TBS	Tris buffered saline
TBS-T	Tris buffered saline-Tween20®
UV	Ultraviolet
293T	SV40 large T antigen-transfected HEK293 cells
6x his-tag	6x histidine protein tag
TMB	3, 3', 5, 5'-Tetramethylbenzidine-mediated
iAb	inhibitory antibody

nAb	neutralizing antibody
CMVIG	Cytomegalovirus hyperimmune immunoglobulin
IVIG	intravenous immunoglobulin